UNIVERSITY OF CALIFORNIA
RIVERSIDE

Characterization of Binding Interactions Between Heparin, and Peptides and Peptidomimetics

A Dissertation submitted in partial satisfaction
of the requirements for the degree of

Doctor of Philosophy
in
Chemistry

by

Mark Hamza

June, 2010

Dissertation Committee:

Professor Dallas L. Rabenstein
Professor Cynthia K. Larive
Professor Quan J. Cheng

The Dissertation of Mark Hamza is approved:

_____

_____

_____

Committee Chairperson

University of California, Riverside

ACKNOWLEDGMENTS

There are many people who are to be thanked for their support and confidence in me. First, I would like to thank Dr. Dallas Rabenstein. His trust in me and guidance, allowed me to accomplish, the most challenging and satisfying endeavor, to date, of my life. I also want to thank Jennifer Zabzdyr, the love of my life! She has been my anchor to reality when my emotions get the best of me. Her continuous encouragement and faith in me helped me to realize that I will graduate when I thought it was in vain to continue. To my mother, Karen Hamza, thank you. Thank you for your love and for your unfailing support. I love you even though sometimes you think that I don't. I am also thankful for my children, Jacob, Ethan, and my newborn daughter, Lily. I love them so much. I also want to thank everyone who has had a positive impact in my life which has helped to contribute to the accomplishment of this goal.

ABSTRACT OF THE DISSERTATION

Characterization of Binding Interactions Between Heparin, and Peptides and Peptidomimetics

By

Mark Hamza

Doctor of Philosophy, Graduate Program in Chemistry
University of California, Riverside, June 2010
Dr. Dallas L. Rabenstein, Chairperson

The aim of this work is to determine the feasibility of peptides and/or peptidomimetics, such as peptoids and peptide/peptoid hybrids, as suitable replacements for Protamine, a drug used to inactivate heparin's anticoagulant activity. Heparin is administered to prevent blood coagulation during certain medical procedures, such as cardiopulmonary bypass. Heparin prevents coagulation by forming a complex with antithrombin, a serine protease inhibitor, thereby accelerating antithrombin's activity. Protamine is then used to restore the coagulation cascade by displacing heparin from antithrombin forming a heparin-Protamine complex. As Protamine has exhibited detrimental side-effects during its administration, this work has endeavored to design a safer alternative.

Several methods have been implemented to characterize the binding interaction between heparin, and the peptides and peptidomimetics developed in this work: (i) isothermal titration calorimetry was utilized to acquire a quantitative binding constant which demonstrated that some of the peptides and peptidomimetics exhibit a high heparin-binding affinity which is critical to displace heparin from antithrombin; (ii) heparin affinity chromatography was used to determine a relative heparin-binding affinity between peptides and peptidomimetics for which a quantitative binding constant could not be measured due to weak heparin-binding interactions; (iii) secondary structure of peptides and peptidomimetics was ascertained by circular dichroism. The compounds synthesized in this work were observed to conform to either a polyproline I-type or polyproline II-type helical secondary structure. Establishing secondary structure is a vital factor in the rational design of heparin-binding peptides and peptidomimetics.

The results of this work show that peptides and peptidomimetics can be rationally designed so as to bind heparin with high affinity. This is an important step in demonstrating that the peptides and peptidomimetics designed in this work have the potential to replace Protamine as an antagonist to heparin.

Table of Contents

List of Figures

List of Tables

Chapter 1

Introduction

1.1 Overview of Dissertation

The goal of the research presented in this dissertation is to develop new families of peptides and peptidomimetics, specifically peptoids and peptide/peptoid hybrids (hybrids) that bind to heparin. Such compounds might be a suitable replacement for the drug, Protamine, which is a drug that binds to heparin thereby neutralizing its anticoagulant activity. The reason it is of interest to find a replacement for Protamine will be discussed further below.

Heparin is a member of the glycosaminoglycan family of polysaccharides, which also includes the related compound heparan sulfate. The similarities in structure and biological activity between heparin and heparan sulfate are discussed below. Heparin can be used as a model for heparan sulfate; therefore, the binding interactions of heparin with peptides, peptoids, and hybrids studied in this research may also be correlated to their binding of heparan sulfate.

This study entails (i) the synthesis of three families of compounds, namely peptides, peptoids, and hybrids, Fig. 1.1, that will bind heparin with a high affinity and (ii) characterization of the binding by heparin by isothermal titration calorimetry, heparin affinity chromatography, and circular dichroism spectroscopy. Peptides were rationally designed so as to enhance their capacity to bind heparin by synthesizing

A.

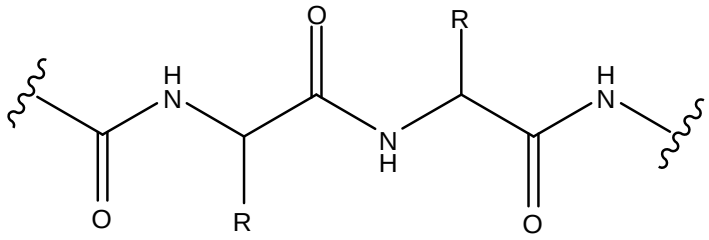

B.

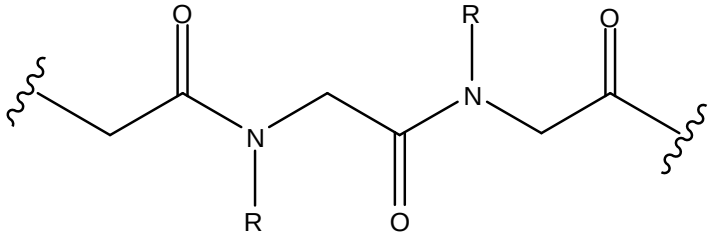

C.

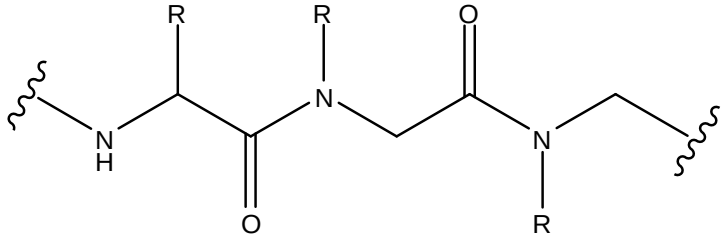

Fig. 1.1.A. Generic form of a peptide showing the side chains attached to the C_α carbon. **B.** A generic form of a peptoid showing the side chains located on the backbone amide nitrogen. **C.** A generic form of a hybrid in which there are both amino acid residues and peptoid monomer residues.

peptides with amino acid sequences that are similar to those that have been observed in the heparin-binding domain of a number of heparin-binding proteins. Heparin-binding peptoids and hybrids were designed by incorporating bulky chiral side chains and cationic residues and strategically placing them within the compound so as to form an amphipathic secondary structure. This particular arrangement of residues is predicted to enhance these compounds' capacity to bind heparin by orientating the cationic side chains of the peptoid or hybrid for optimal interaction with the anionic groups of heparin.

1.2 Overview of Glycosaminoglycans

The glycosaminoglycan family of polysaccharides, shown in Fig. 1.2 includes: hyaluronic acid, chondroitin sulfate, dermatan sulfate, keratan sulfate, and in Fig. 1.3 includes: heparin and heparan sulfate;[1] these compounds are linear polysaccharide chains composed of repeating disaccharide units of uronic acid (D-glucuronic acid or L-iduronic acid) and an amino sugar (D-galactosamine or D-glucosamine). The monosaccharides are bound to each other by a glycosidic bond from the anomeric carbon of one monosaccharide to an available hydroxyl group of another; this bond can be in either the α or β configuration. Except for hyaluronic acid, the glycosaminoglycans can be highly sulfated with sulfate groups located on the uronic acid and/or the amino sugar and they have a carboxylic acid group located on the uronic acid. At physiologic

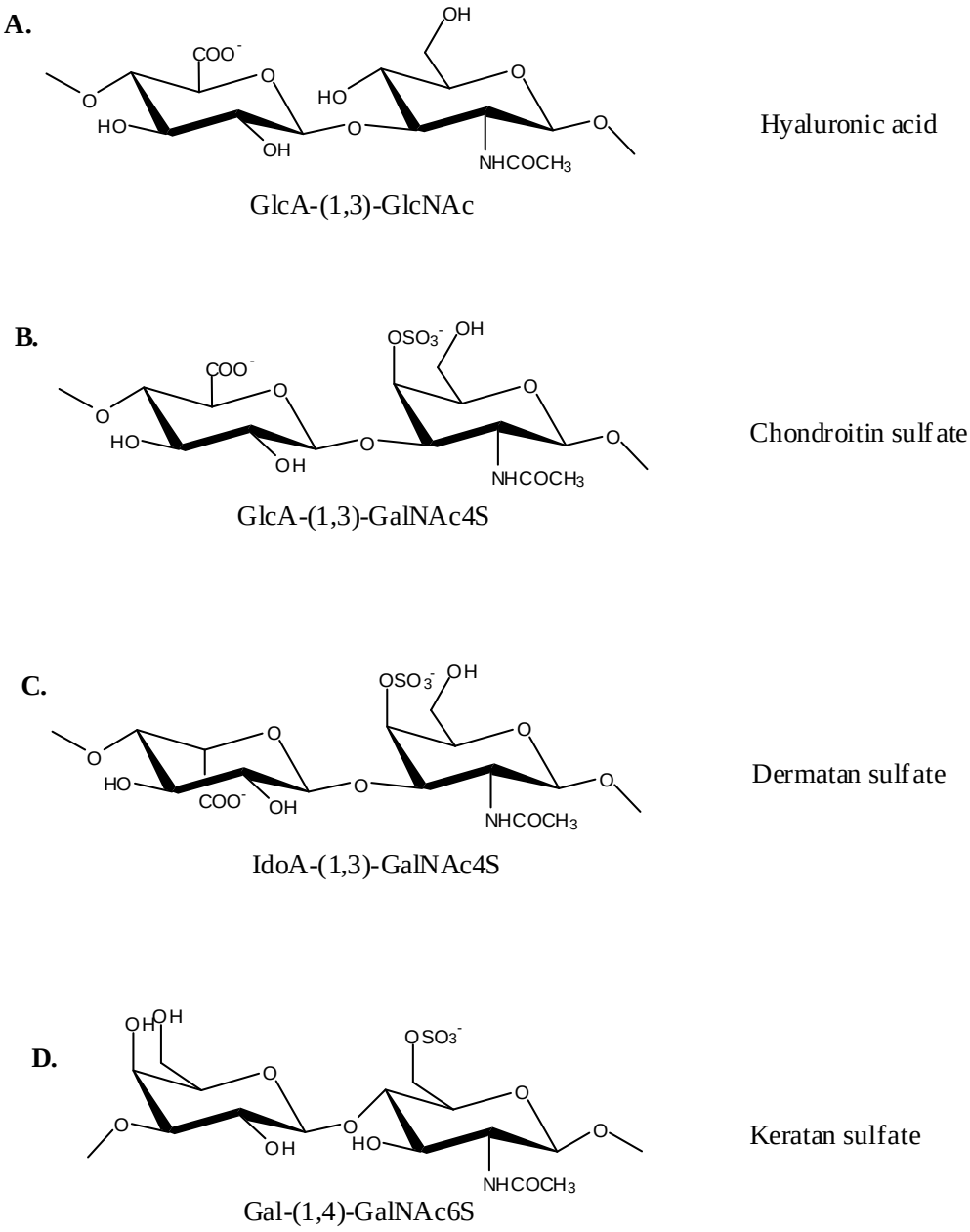

Fig. 1.2. The major repeat disaccharide sequences with their corresponding nomenclature below their structure: **A.** Hyaluronic acid: glucuronic acid (1,3) N-acetyl-glucosamine, **B.** Chondroitan sulfate: glucuronic acid (1,3) 4-sulfate-N-acetyl galactosamine, **C.** Dermatan sulfate: iduronic acid (1,3) 4-sulfate-N-acetylgalactosamine **D.** Keratan sulfate: galactose (1,4) 6-sulfate-N-acetyl-galactosamine.

A.

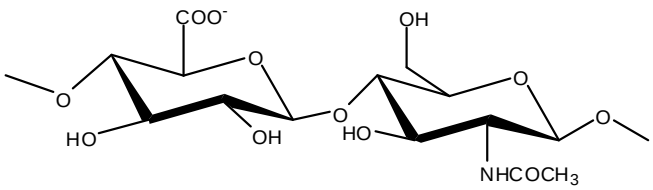

Heparan Sulfate

GlcA-(1,4)-GlcNAc

B.

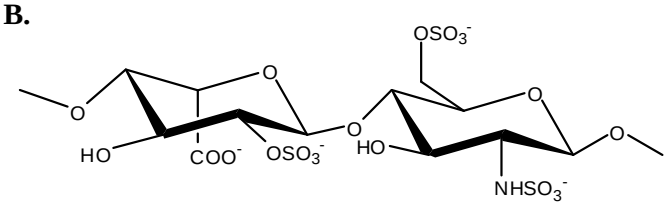

Heparin

IdoA2S-(1,4)-GlcNS6S

Fig. 1.3. The major repeat disaccharide sequences of heparan sulfate and heparin: **A.** Heparan sulfate: glucuronic acid (1,4) N-acetyl-glucosamine, **B.** Heparin: 2-Sulfate-iduronic acid (1,4) 6-sulfate-N-sulfate-glucosamine.

pH, the sulfate and carboxylic acid groups are fully deprotonated resulting in the polysaccharide chain having a high negative charge density.[2]

Glycosaminoglycans are produced within most mammalian cells, and with the exception of hyaluronic acid,[2] they are covalently bound to a core protein via a tetrasaccharide linker, from which they are synthesized. The tetrasaccharide linker is composed of a glucuronic acid, two galactose residues and one xylose residue which are attached to a serine residue of the protein core.[3] Keratan sulfate, however, has a galactose residue in place of a glucuronic acid in the linker.[4] The combination of a glycosaminoglycan and protein core is referred to as a proteoglycan. After synthesis they are excreted into the extracellular matrix, attached to the cell membrane, or stored in secretory granules.[2]

Glycosaminoglycans/proteoglycans play important roles in many biological processes.[5] Hyaluronic acid is necessary for the structure and assembly of various tissues and also binds to cell surface receptors to influence cell behavior.[6] Keratan sulfate helps to maintain stromal hydration which is critical for corneal transparency.[7] Dermatan sulfate has been found to bind to growth factors that stimulate cell growth and proliferation.[8] Aggrecan, a form of chondroitin sulfate, appears in high abundance in cartilage in which it participates in compressive resistance and resilience. It is also critical in the development of the skeleton.[7]

The naming of glycosaminoglycans is based on the sulfation pattern and a three to four letter code to represent each monosaccharide. Gal represents galactose,

GlcN represents glucosamine, and the uronic acid is represented by IdoA for iduronic acid and GlcA, for its C5 epimer, glucuronic acid. Acetyl groups are Ac. For example N-acetylglucosamine is GlcNAc. To define the location of sulfate groups, a number representing the carbon to which the sulfate group is attached and an S for sulfate is used. Numbers are also used to denote the carbon atoms that form the glycosidic bond. The code is read from the nonreducing end to the reducing end of the sequence.[2]

1.3 Heparan Sulfate

1.3.1 Biosynthesis and Structure

Heparan Sulfate (HS) is a member of the glycosaminoglycan family of complex, linear polysaccharides. HS is composed of a repeat 1,4-linked disaccharide sequence of a uronic acid and a D-glucosamine. In nature HS is covalently linked to a core protein, to form a proteoglycan. As a proteoglycan, HS resides on the surface of all eukaryotic cells, and in the extracellar matrix.[9, 10] Cell surface HS proteoglycans consist of two major families, the syndecans, and the glypicans. Syndecans are held to the cell surface by a transmembrane protein core, and the glypicans are attached to the cell membrane by a glycosylphosphatidylinositol anchor.[11] Three major familes of HS proteoglycans reside in the extracellular matrix, they are perlecan, agrin, and collagen XVIII. These proteoglycans are actually linked to the cell membrane via integrins and possibly other proteins which link the cell to its immediate surroundings. This linkage renders the cell

sensitive to changes in its pericellular microenvironment, thus acting as a biological sensor and actuation system for the cell. [9, 12]

Biosynthesis of heparan sulfate begins in the Golgi apparatus and consists of three phases: chain initiation, chain polymerization, and chain modification. The chain initiation phase begins with the covalent attachment of a tetrasaccharide linker (-GlcA-Gal-Gal-Xyl-) to a serine residue located on a core protein. During chain polymerization, two glycosyl transferases alternately add an N-acetyl glucosamine (GlcNAc) and a glucuronic acid (GlcA) to the tetrasaccharide linker, to from the repeating disaccharide sequence shown as the top structure in Fig. 1.4. After chain elongation, the chain is modified beginning with deacetylation and N-sulfation of glucosamine by N-deacetylase and N-sulfotransferase, respectively, which converts GlcNAc to GlcNS. Subsequently, D-glucuronic acid is empimerized to L-iduronic acid (IdoA) by C-5 empimerase. After epimerization, GlcA or IdoA can be sulfated by 2-O-sulfotransferase (Ido2S) and the glucosamine residue can be sulfated by 3-O and 6-O-sulfotransferases (GlcNS(3S(6S)).[13, 14] Fig. 1.4 shows this process.

Modification of the polysaccharide chain is, however, incomplete, and not all monosaccharides are sulfated or epimerized. This incomplete modification results in regions of highly sulfated domains of IdoA(2S)-(1,4)-GlcNS(6S) and unsulfated domains of GlcA-(1,4)-GlcNAc separated by transition regions which are comprised of both highly sulfated and unsulfated disaccharides. HS chains have an average molecular weight of

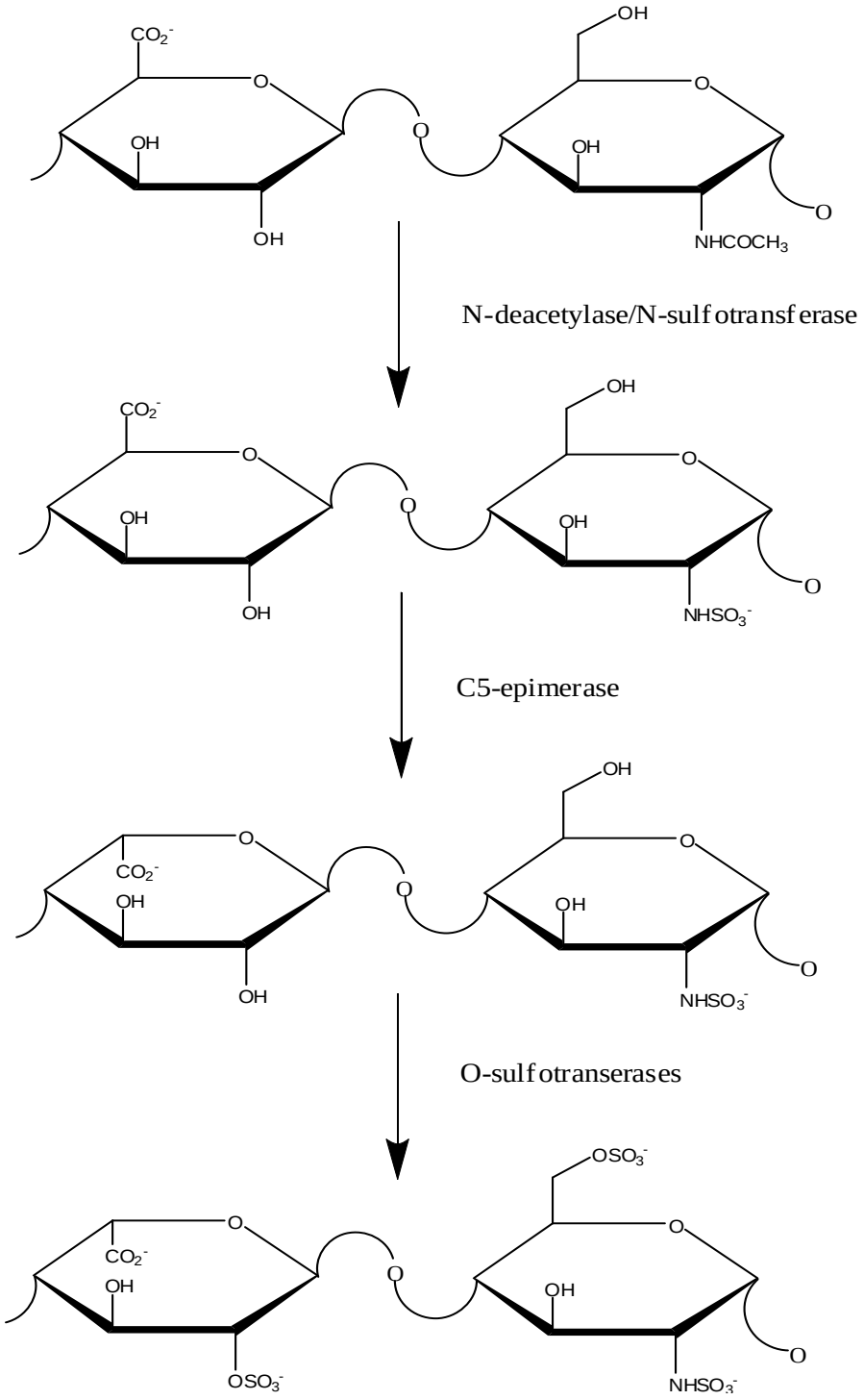

Fig. 1.4. Modification of the initial GlcA-(1,4)-GlcNAc dissacharide sequence of heparan sulfate by various enzymes to produce a trisulfated disaccharide.

about 30kD.[14] Due to the variation in sulfation patterns, HS can be composed of up to twenty-four different disaccharide subunits making it the most complex of the glycosaminoglycans, Fig. 1.5. This high density of information allows for a wide range of biological functions. Indeed, heparan sulfate glycosaminoglycan structure differs not only from cell-type to cell-type, but also depends on the stage of cell growth and development, and pathological state. [9, 14]

1.3.2 Heparan Sulfate and Biological Processes

Heparan sulfate has been implicated in a variety of biological and pathological processes. Heparan sulfate proteoglycans secreted by cells into the extracelluar matrix have been shown to be important in cell differentiation and growth.[15-19] In viral infection, binding interactions between proteins on the surface of the virus and cell surface heparan sulfate proteoglycans appear to play an important role in mediating entry of viruses such as HIV,[20-22] hepatitis B,[23] and herpes simplex virus type 1.[24-26] In fact, glycoprotein C, located on the viral coat of herpes simplex virus type 1, is the major attachment site for cell surface heparan sulfate on the host cell.[26] Lindahl et al. have determined the minimal binding site for Glycoprotein C (gC) to cell surface heparan sulfate.[25] By incubating African green monkey kidney cells (GMK) with whole virus HSV-1, a dodecamer-sized heparin oligosaccharide was found to inhibit infection by greater than 50%. Dodecamer-sized heparin also bound effectively to gC protein alone in solution and in gC affinity chromatography. Unfortunately, the detailed structure of the

A.

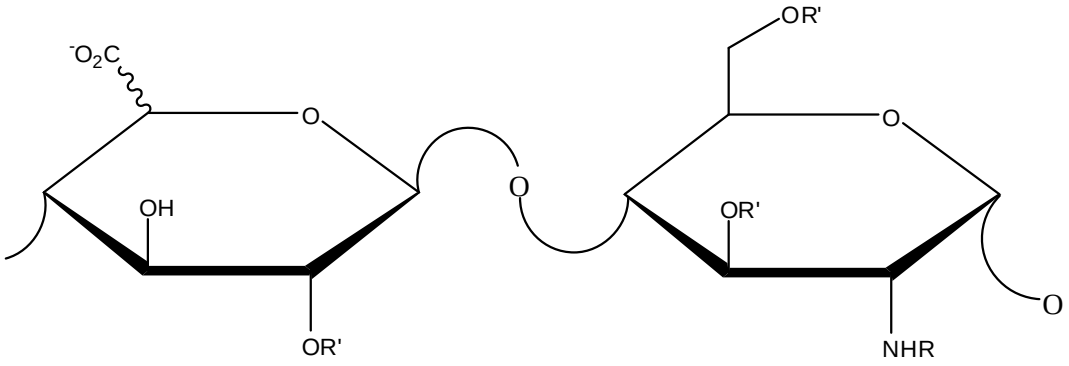

R' = H or SO_3^-

R = SO_3^- or $COCH_3$

B.

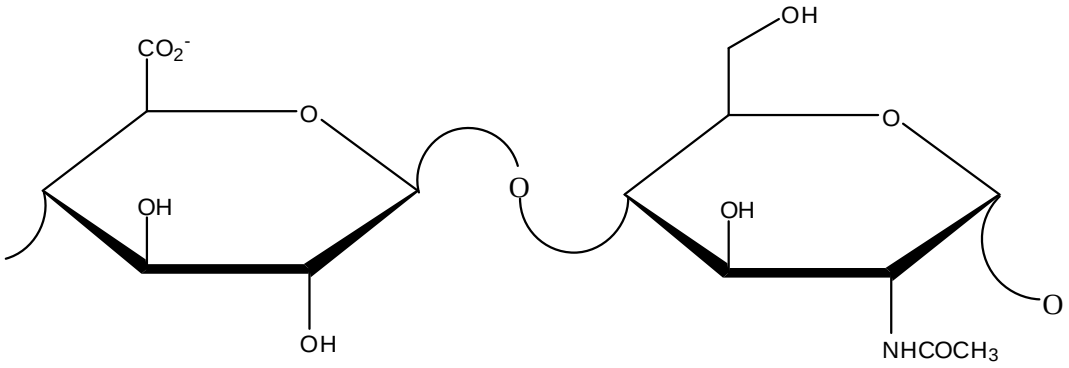

Fig. 1.5.A. The possible dissacharide sequences for heparan sulfate. **B.** The major repeating dissacharide sequence of heparan sulfate.

dodecamer could not be identified due to lack of appropriate sequencing technology. These results not only indicate that heparan sulfate on the surface of host cells is important for viral invasion of HSV-1, but that a minimal length of 10-12 monosaccharides is also critical. The analysis also shows that 6-O-sulfation may play a more prominent role in viral invasion and that N-sulfation is less important.

Cancer progression is also strongly linked to differences in the fine structure of heparan sulfate proteoglycans. These differences have been associated with tumor progression, angiogenesis,[27-30] and metastasis.[31-35] Perlecan, an extracellular matrix heparan sulfate proteoglycan, represents a major storage site for fibroblast growth factor-2 (FGF-2), a protein which stimulates the growth of a wide variety of cells,[36] in the blood vessel wall. It has been demonstrated that perlecan can stimulate FGF-2-mediated angiogenesis which is an important factor in tumor growth.[34] Kuniyasu, et al. also found that heparan sulfate, in the extracellular matrix, stimulates invasion of human colon carcinoma cell lines that express a variant of CD44 glycoprotein (CD44v3).[33]

1.4 Heparin

1.4.1 Structure of Heparin

Heparin, also a member of the glycosaminoglycan family, is similar to heparan sulfate (HS) in that it is composed of the same sulfated uronic acid/D-glucosamine dissacharide unit. The disaccharides in a typical heparin oligosaccharide have an average

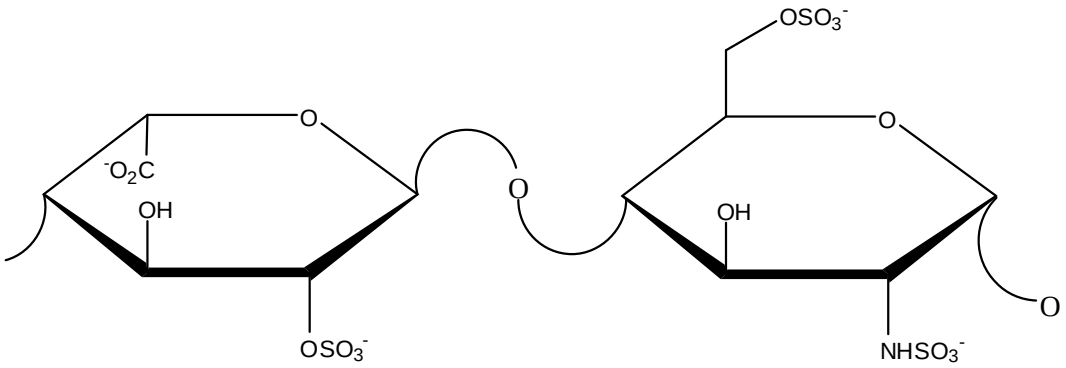

Fig. 1.6. Major repeat disaccharide sequence of heparin.

mass of 600 daltons[37] and each saccharide is about 4 Å across.[38] Heparin is synthesized by the same biosynthetic pathway as heparan sulfate, but is less information dense, meaning that sulfation patterns on heparin vary to a lesser degree than in heparan sulfate as it is primarily composed of the trisulfated disaccharide unit IdoA(2S)-(1,4)-GlcNS(6S), Fig. 1.6. The trisulfated disaccharide sequence makes up 70 to 90% of the polysaccharide chain from porcine intestinal mucosa and bovine lung, respectively.[9] Heparin is synthesized within mast cells as a proteoglycan (Mr 750000-1000000). Subsequently the polysaccharide chains of the proteoglycan are cleaved to give a heterogeneous dispersion of smaller polysaccharide chains (Mr 5000-25000).[9,14,30] These smaller chains are noncovalently bound to basic proteases within the cytoplasmic secretory granules of mast cells.

1.4.2 Ring Conformation

Heparin's monosaccharide building blocks of uronic acid and glucosamine can have the possible ring conformations in Fig. 1.7. Theoretical studies and X-ray diffraction analysis have confirmed that the GlcA and GlcNAc residues prefer the $^4C_1$ chair conformation.[39-41] Data from ^{1}H-NMR spectroscopy indicate that IdoA(2S), the sulfated C-5 epimer of GlcA, prefers the $^1C_4$ chair conformation.[42] Work done by Ferro et al. demonstrated that IdoA(2S) exhibits greater flexibility depending on the sulfation pattern of adjacent residues. ^{1}H-NMR data and force field calculations of a synthetic oligosaccharide representing the binding sequence to Antithrombin III (ATIII), show that IdoA(2S) is in equilibrium between the $^1C_4$ chair and the $^2S_0$ skew boat conformation. The monosaccharide, methyl 2-O-sulfo-α-L-iduronate, is primarily in the $^1C_4$ conformation with a ratio of $^1C_4$ to $^2S_0$ of 90:10. When IdoA(2S) is between two GlcNS(6S) residues, the ratio decreases to about 60:40 of $^1C_4$ to $^2S_0$. An IdoA(2S) internal residue located adjacent to a GlcNS(6S(3S)) residue, as in the ATIII binding sequence, again decreases the ratio of $^1C_4$ to $^2S_0$ to about 30:60. Although the $^4C_1$ conformation of IdoA is of similar potential energy to the $^1C_4$ and $^2S_0$ conformations, the $^4C_1$ conformation only occurs for IdoA residues located at the nonreducing terminus of heparin oligosaccharides.[43] These results indicate that IdoA(2S), an abundant residue in heparin, has a conformational flexibility that may play a part in specific binding to certain proteins, a prime example of that being the binding of ATIII by heparin. The 3-O-

A.

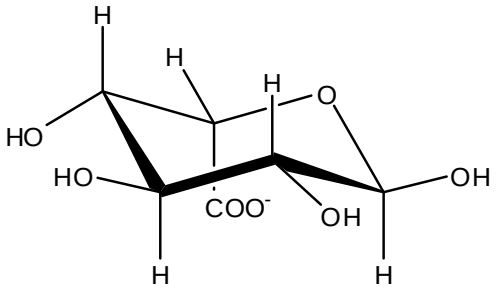

$^{4}C_{1}$

B.

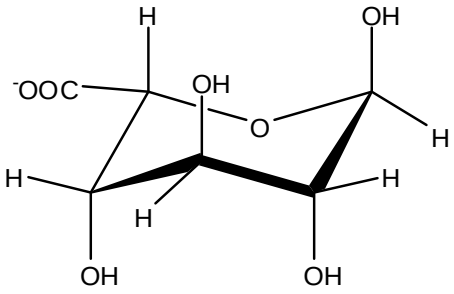

$^{1}C_{4}$

C.

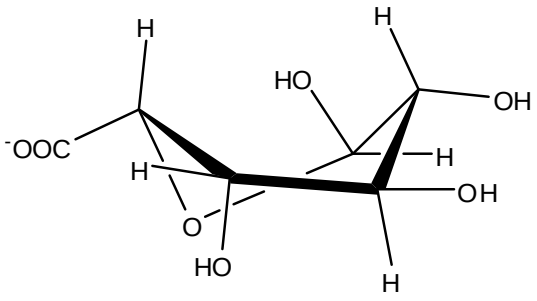

$^{2}S_{0}$

Fig. 1.7.A. and **B.** show the chair conformations and **C.** shows the skew boat conformation of the iduronate residue of heparin.

sulfation of GlcNS(6S(3S)) is critical for high-affinity binding to ATIII, which upon binding induces a change in the conformer equilibrium.[44]

1.4.3 Discovery of Heparin

The first step in the process of the discovery of heparin was initiated by Jay McLean, a second-year medical student working for William Henry Howell, at Johns Hopkins Medical School, in 1916. His research focused on purifying the key procoagulant component, thought to be cephalin, a phosphatide, from a crude extract from the brain tissue of dogs that exhibited thromboplastic properties. The purification process proved difficult and so McLean started exctracting other phosphatides from other organs that contain less cephalin in an effort to find a compound with procoagulant properties that may be extracted with cephalin from the brain as an impurity. In this endeavor, he found in the literature extraction processes that may result in cephalin from the heart (cuorin) and liver (heparphosphatide). After the extraction of heparphosphatide, the cephalin portion deteriorated over time weakening its thromboplastic properties. An impurity from that extraction proved to be a potent anticoagulant, which was not obvious due to the procoagulant effect of the cephalin. [45-47] Howell continued working on anticoagulants although McLean further researched cephalins. By 1922, Howell and another medical student, L. Emmett Holt Jr., isolated, what was identified as glucuronic acid with anticoagulant properties from canine liver, then termed “heparin”, by Howell. After refinement of methods for purification and characterization of heparin, by 1935,

heparin was finally administered into human volunteers with no detrimental side effects, hence promoting heparin, in its present form, into clinical use for the treatment of thrombolic disorders by the 1940's.[47, 48]

1.4.4 Clinical Uses of Heparin

During cardiopulmonary bypass, blood passing through the foreign surfaces of the bypass system induces a strong activation of the inflammatory and coagulation pathways.[49, 50] Attenuation of the coagulation pathway is necessary to prevent thrombosis during cardiac surgery implementing cardiopulmonary bypass. In 1953, heparin was first used for this purpose and since then has continued to be used as the primary anticoagulant.[51] Heparin works by accelerating the rate at which antithrombin, a serine protease inhibitor, inhibits coagulation proteases.[52] Patients with chronic kidney failure can also be treated with heparin to prevent thromboembolism during hemodialysis.[53, 54] Heparin is also the drug of choice for the treatment of deep vein thrombosis.[55, 56] Venous thrombosis is caused by a myriad of factors including: surgery, cardiac failure,[57] prolonged immobility, or genetic disorders[58] with the majority of thromboemboli occurring in the legs.[59] In some clinical situations where it is necessary to neutralize the anticoagulant activity of heparin, protamine is the drug used for this purpose.[60]

1.4.4.1 Protamine

Protamine is a family of highly cationic proteins consisting of about 67% arginine residues and has an average molecular weight of about 4500 Da. Protamine was discovered in 1868 by Friedrick Miescher in salmon sperm and was the basis for the advancement of protein chemistry as protamine had the simplest amino-acid sequence at the time.[61] Protamine is now used to reverse the anticoagulant activity of heparin. Due to its polycationic nature, protamine displaces antithrombin III by ionic interactions with the anionic groups of heparin. Depending on the size and source of heparin, the binding affinity has been determined to be anywhere from $5.4X10^{6}\ M^{-1}$ for low-molecular-weight heparin to $1.22X10^{8}\ M^{-1}$ and $2.12X10^{8}\ M^{-1}$ for unfractionated heparin from porcine mucosa and beef lung sources, respectively.[37] In this case, binding affinity of heparin preparations and protamine were determined by titrating heparin into a protamine solution and detecting the change in potentiometric response by a heparin-sensitive electrode.

The administration of protamine can also induce adverse side-effects.[61, 62] A study conducted by Lowenstein, et al.[63] describes severe systemic hypotension and other cardiovascular changes after the administration of protamine in patients for the reversal of heparin's anticoagulant activity. The life-threatening events, they surmise, were associated with activation of the complement system by protamine-heparin complexes, and by protamine acting as a substrate for C-reactive protein, another activator of the complement system. The activation of the complement system resulted

in severe pulmonary vascular constriction. According to the data from another study,[64] protamine infusion precipitated hypotension by vasodilation. It was hypothesized that protamine acts on endothelial cell receptors, of the systemic arteries thereby increasing the release of endothelial-derived relaxing factor (EDRF). The release of EDRF decreases vascular resistance by regulating vascular tone, similar to that of a nitrovasodilator. Anaphylactoid response to protamine has also been reported in patients with fish allergy[62] in which protamine is cross-reactive with the fish antigen and in diabetics who have been exposed to protamine-zinc-insulin.[65] Symptoms of anaphylactoid response can include: severe bronchospasm, edema, and cardiovascular collapse.[62]

Considering the adverse side-effects of protamine administration for the neutralization of heparin, it is of interest to develop suitable replacements for protamine. Previously, polycations (poly-DL-Lysine, poly-L-ornithine, and lysine-rich and arginine-rich histone fractions) were tested using the kaolin-activated partial thromboplastin time test for the neutralization of heparin.[66] In these studies, the histone fractions were less effective at neutralizing heparin's anticoagulant activity compared to protamine. The polycation peptides were comparable in their activity to protamine; unfortunately, the two polycationic peptides are toxic to humans. Since it has been shown that polycations can neutralize heparin, it may be possible to design polycationic peptides, peptoids, or peptide/peptoid hybrids that are as effective as protamine in neutralizing heparin and that are nontoxic to humans.

1.4.4.2 Overview of the Coagulation Cascade

The sequence of reactions in the coagulation cascade is shown in Fig. 1.7. There are two pathways in the coagulation cascade, the intrinsic and the extrinsic. Both pathways are initiated by vascular damage and lead to the polymerization of fibrin, forming a clot.[67] A number of blood-circulating proteins, such as prothrombin and factors V, VII, VIII, IX, X, XI, XII, and XIII, are involved in the coagulation process, and are subsequently converted to active serine proteases in a stepwise manner. The initiation of the extrinsic pathway occurs during vascular injury when tissue factor, residing in the subendothelium, is exposed to blood. Tissue factor and factor VII form a complex which, in the presence of Ca^{2+}, activates factor VII to an active serine protease, VIIa. The tissue factor (TF)/ factor VIIa complex leads to the activation of other factors which results in the formation of fibrin. Thrombin, the activated serine protease of prothrombin, initiates the intrinsic pathway. Both pathways converge in the activation of factor X to factor Xa. Factor Xa is a cofactor in the conversion of prothrombin to thrombin which in turn catalyzes fibrinogen to fibrin which is crosslinked to form a clot.[68]

Antithrombin, a serine protease inhibitor, controls the process of coagulation. Inhibition of coagulation begins at the reactive center loop (RCL) of antithrombin which has a sequence of amino acids complementary to the active sites of target proteases. After binding to the RCL, proteases initiate cleavage of the RCL which starts a mechanism whereby the proteases are subsequently deformed thereby inactivating their coagulant activity.[69] Two of antithrombin's primary targets are

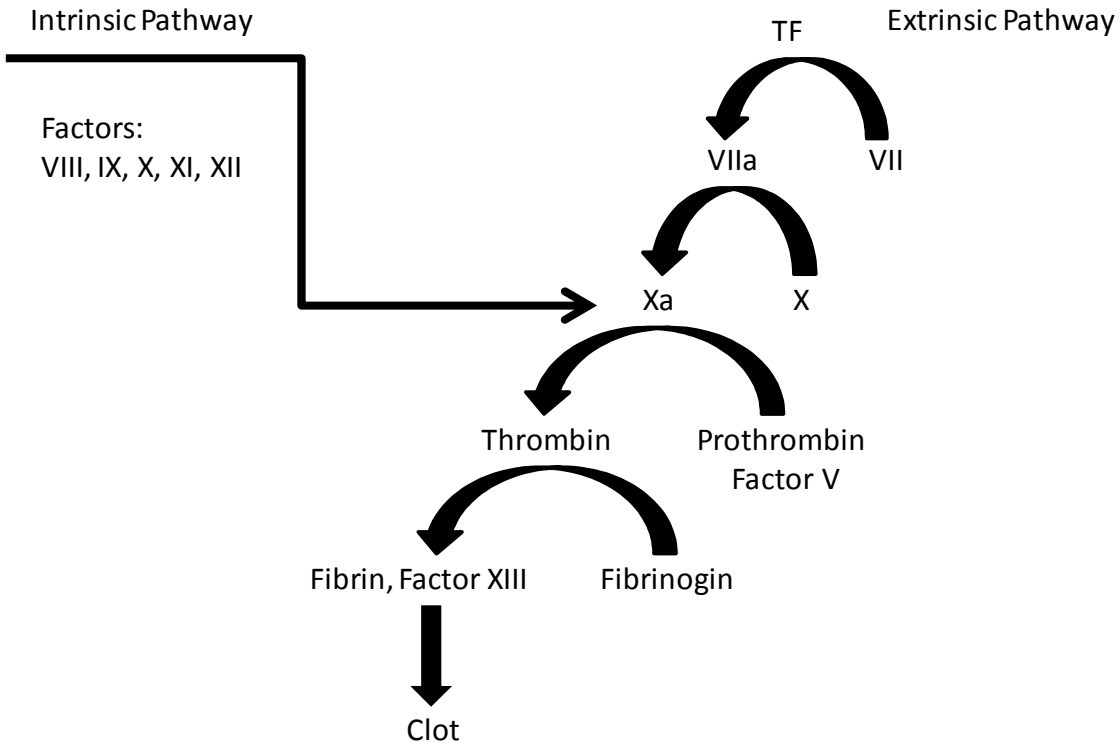

Fig. 1.8. Overview of the coagulation cascade. The formation of a clot begins with a series of conversions of serine proteases to their active form at both intrinsic and extrinsic pathways which converge at the conversion of Factor X to Xa. For simplicity, the details of the roles of factors: VIII, IX, X, XI, and XII, which take part in the intrinsic pathway in the coagulation cascade, are not shown.

thrombin and factor Xa.[69] Although antithrombin inactivates thrombin and factor Xa, at plasma levels, the rate of inactivation is below that which is necessary to inhibit protease activity.[52] It is thought that heparan sulfate lining the endothelium is responsible for mediating antithrombin's anticoagulant activity in the same manner as heparin.[52, 70, 71]

1.4.4.3 Antithrombin

Antithrombin is a 58 kDa protein that is a serine protease inhibitor produced in the liver. Its structure consists of three β-sheets and nine α-helices. Although its structure is highly conserved, it exists in two forms, 10% as the β-form and 90% as the α-form.[69] The difference between the two is the amount of glycosylation; the β-form lacks a carbohydrate at Asn^{135}. The lack of carbohydrate on Asn^{135} renders the β-form the major inhibitor of serine proteases.

Fluorescence[72] and X-ray[73] diffraction studies show that heparin binds to antithrombin, which causes antithrombin to undergo a conformational change. The conformational change results in its reactive center loop (RCL), which is partially inserted in a five-stranded β-sheet called the A-sheet, becoming more exposed. The RCL can therefore interact with serine proteases, such as thrombin and factor Xa, much more readily, thereby promoting anticoagulation. However in α-antithrombin, the carbohydrate on Asn^{135} sterically hinders this conformational change resulting in a lower affinity for serine proteases.[73]

The binding of heparin to antithrombin accelerates its binding to serine proteases, such as thrombin, by several thousandfold,[38] resulting in the formation of a ternary complex. Although a minimum five-saccharide sequence is necessary for high-affinity binding of heparin to antithrombin, eighteen monosaccharides are necessary to form the complex. [74] Chain length of heparin also determines its affinity for antithrombin. Lower-molecular weight heparin of about 7,900 Da binds to antithrombin with a binding constant of about $6.6X10^5$ M^{-1} and a binding ratio of 2:1. Heparin with a molecular weight of 14,300 Da to 21,600 Da has been determined to bind to antithrombin with a binding constant of $2.89X10^6$ M^{-1} and a binding ratio of 1:1.[75]

Using chromatographic and NMR methods to evaluate selective chemical and enzymatically cleaved oligosaccharides of heparin, a pentasaccharide, Fig. 1.8, was found to be the minimal length to bind antithrombin with high affinity and to elicit anti-factor Xa activity.[76, 77] The binding constant of this heparin pentasaccharide to antithrombin was found to be $7.10X10^6$ M^{-1}. [76] It was assumed that a recurring 3-O-sulfate on the central residue of the pentasaccharide was critical due to its appearance in the high-affinity pentasaccharide. The importance of the 3-O-sulfo group was determined by synthesizing a similar antithrombin-binding pentasaccharide in which the 3-O-sulfo group was absent.[78] The synthetic pentasaccharide was evaluated by the use of clotting or amidolytic assays and was shown to have no measurable binding affinity to antithrombin or to have anti-factor Xa activity, thus settling the critical nature of the 3-O-sulfo group.

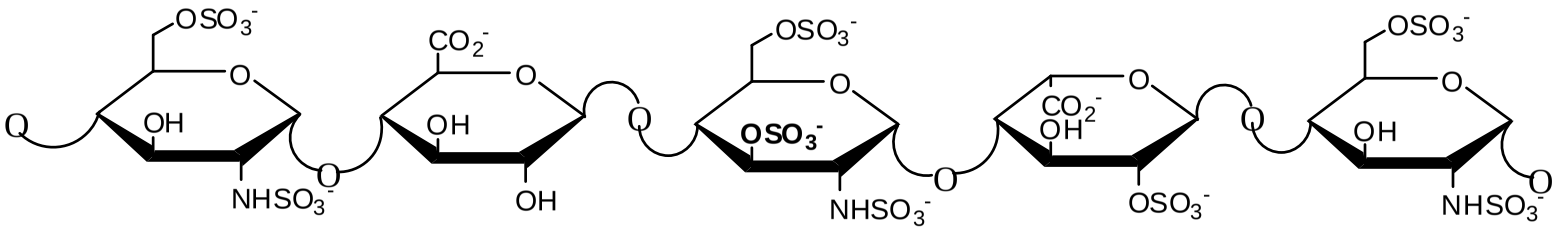

Fig. 1.9. The unique antithrombin-binding pentasaccharide sequence of heparin with the critical 3-O-sulfate group in bold.

1.4.5 Heparin and Its Affect on Other Biological Processes

Heparin has also been found to affect biological processes similarly to that of heparan sulfate. Two areas of interest where heparin has shown biological modulation are in viral invasion, including invasion by HIV[79-81] and herpes,[82-85] and angiogenesis and tumor growth.[86-89]

1.4.5.1 Infection by Human Immunodeficiency Virus

Nagumo et al. showed in 1988 the biological basis of how heparin inhibits infectivity of the Human Immunodificiency Virus (HIV) *in vitro*.[79] In this research, heparin, low-molecular weight heparin, de-N-sulfated heparin, and protamine sulfate were used to test their ability to prevent infection of MT-4 cells by two isolates of HIV: HTLV-III_b and GUN-1. HTLV-III_B cells were incubated in different culture media, each one containing one of the four drugs above. Subsequently, suspensions of MT-4 cells were added to each medium and tested for the expression of HIV antigens by immunofluorescence assay. Results indicated that at concentrations of 10 and 50 ug/ml, heparin almost completely inhibited infection. MT-4 cells were infected with the GUN-1 isolate with and without heparin. Under similar assay conditions, 30-40% of MT-4 cells tested positive for HIV antigens, in the absence of heparin, whereas, less than 1% tested positive in the presence of heparin. Further research by Rider, et al., found that heparin inhibited infectivity by binding specifically to the V3 loop located on gp120, a glycoprotein found on the viral coat of HIV type-1. This binding, although it did not

interfere with the initial binding step of gp120 to CD4 receptors on target cells, probably interfered with a critical step in the plasma membrane-viral coat fusion process.[80]

1.4.5.2 Angiogenesis and Cancer

Angiogenesis is the development of new blood vessels from those that are preexisting. Several biological processes depend on angiogenesis such as wound healing, embryonic development, and tumor growth.[88] Tumor cell proliferation depends on angiogenesis so that new capillaries may supply the growing tumor with nutrients and oxygen, and as an outflow for metabolic waste products.[90] Fibroblast growth factor (FGF) and vascular endothelial growth factor (VEGF) are two important mitogenic proteins that stimulate proliferation of vascular endothelial cells.[90-92] Heparin has been shown to bind to these two growth factors, thereby modulating their angiogenic activity both *in vitro* [86, 93, 94] and *in vivo*.[95]

1.4.6 Heparin-Ligand Binding

Although no 3-D structures of protein-heparin complexes have been solved, studies involving heparin-binding peptides have uncovered several characteristics that may indicate the active site of a heparin-binding protein. These heparin-binding peptides have been shown to have a high cationic charge density, conform to a helical structure upon binding to heparin, and have a sequence which confers upon them amphipathicity when induced into a helical structure.[38, 96, 97]

Furthermore, Cardin and Weintraub have elucidated amino acid sequences common in a number of heparin-binding proteins which may compose the heparin-binding region.[98] The sequences are: XBBXBX and XBBBXXBX where B is a basic residue such as lysine or arginine, and X is any other residue. Peptides comprised of this sequence have been found to bind heparin with high affinity,[99] and form amphipathic, α-helices upon binding to heparin.[98] The induction of α-helices by the ridged, polyanionic structure of heparin will align cationic residues on one face of the helix to maximize electrostatic interactions.[100]

Although the primary binding force between heparin and positively charged peptides is electrostatic,[100, 101] residues other than those containing basic side chains are also important in heparin binding. For example, amino acids such as alanine, leucine, and glycine[38, 96, 97, 102] appear to have a propensity to stabilize helical structure which would facilitate amphipathicity.

1.4.7 Studying Heparin/Ligand Binding Affinity

There are a variety of techniques that can be used to determine the binding affinity of heparin/ligand interactions. These techniques include capillary electrophoresis,[103, 104] surface plasmon resonance,[105, 106] isothermal titration calorimetry,[107-109] and nuclear magnetic resonance.[110, 111]

Gunnarsson et al. demonstrated the utilization of capillary zone electrophoresis for the binding of low-affinity heparin to antithrombin. The goal of the study was to

develop a method to determine binding constants of low-affinity interactions with relatively small sample amounts and short analysis time. By measuring the difference in electrophoretic mobility between the free antithrombin and the heparin-antithrombin complex at various heparin concentrations, a binding curve of relative mobility as a function of heparin concentration was used to determine the binding constant. The resulting binding constant of low-affinity heparin to antithrombin was reported as $K_b \approx 5.3X10^4\ M^{-1}$.[103]

In another study,[106] biotinylated heparin was immobilized to a surface plasmon resonance sensor chip coated with covalently bound streptavidin. The aim of this study was to determine the site of the binding domain of fibrinogen using two fibrinogen fragments, E and D which were both previously proposed to participate in heparin binding. The fibrinogen fragments were eluted over the sensor chip and the association and dissociation rate constants were measured by constructing a binding curve of plasmon-resonance response as a function of time. The binding affinity can then be determined as a ratio of the two rate constants. The technique of surface plasmon resonance was able to exclude fragment E as part of the heparin binding domain as it exhibited no binding to the bound heparin. Fragment D, however was found to bind tightly to the immobilized heparin with a measured binding affinity of $K_b = 1.8X10^6\ M^{-1}$.

Rabenstein et al., used ITC to determine the binding constant of heparin interacting protein analogue peptide, constructed of D-amino acids (D-HIPAP), of heparin interacting protein.[107] The study was done to compare binding activity of

synthetic peptides and antithrombin to heparin. The results show that the K_b for D-HIPAP ranged from $3.8X10^4$ to $4.5X10^4$ M^{-1} depending on the Na^+ concentration. D-HIPAP also showed anticoagulant activity using the Coatest method. As peptides of D-isomers are resistant to proteolytic activity, the data indicate that synthetic analogue peptides with similar binding affinity to heparin may have potential as a protamine replacement.

Nuclear magnetic resonance (NMR) has also been applied to determine the binding affinity (K_b) of heparin to urokinase-type plasminogen activator (u-PA).[111] According to the authors of this study, u-PA plays an important role in several physiological processes including invasive behavior of malignant cells. Some of these processes are stimulated by heparin. Differences of ^{1}H-NMR chemical shift data of histidine residues, adjacent to the proposed heparin-binding site of u-PA (called u-PA kringle domain) were measured by titrating solutions of u-PA kringle fragments with low-molecular weight heparin. After plotting the changes in histidine singlets as a function of the ratio of the concentrations of heparin to kringle fragment, a non-linear least squares model was used to fit the data. The results give a K_b of $5.78X10^4$ M^{-1}. The ^{1}H-NMR data along with data from other techniques used in the study seem to indicate that the u-PA kringle domain is indeed the heparin-binding site.

1.5 Research in This Dissertation

Although Protamine is the drug of choice for reversing heparin's anticoagulant activity, as mentioned above, the administration of this drug results in several severe side-effects. Although some attempts have been made to produce a suitable substitute for protamine, no suitable replacements have been found. In this work, several families of peptides, peptoids, and peptide-peptoid hybrids have been synthesized and their binding interactions, along with their secondary structure have been characterized by several techniques, namely, isothermal titration calorimetry, heparin affinity chromatography, and circular dichroism. Synthetic methods and other details are presented in chapter 2.

In chapter 3, peptides are synthesized by way of rational design utilizing an amino acid sequence pattern found in many heparin-binding proteins. Subsequently, their binding interaction with heparin is characterized. In chapter 4, peptoids, a class of peptidomimetics, are synthesized with sequences designed to produce amphipathic structures with faces of cationic charge and their interaction with heparin is characterized. By synthesizing peptoids with residues which force a stable secondary structure, and incorporating a cationic residue in every third position of the sequence, it is possible to control the orientation of cationic residues to increase binding affinity to heparin via heparin's anionic sulfate and carboxylate groups. In chapter 5, peptide/peptoid hybrids are synthesized using the same chemical synthesis methods used for peptoids in combination with traditional solid-phase peptide chemistry, and

their interaction with heparin is studied. In this case, the amino acids lysine or arginine are used in place of the peptoid monomer with a lysine-like side chain.

1.6 References

1. Zaia, J., *Mass Spectrom. Rev.* **2008,** *28*, 254-272.

2. Gandhi, N. S.; Mancera, R. L., *Chem. Biol. Drug Des.* **2008,** *72*, 455-482.

3. Sugahara, K.; Kitagawa, H., *Curr. Opin. Struct. Biol.* **2000,** *10*, 518-527.

4. Volpi, N., *Curr. Med. Chem.* **2006,** *13*, 1799-1810.

5. Volpi, N.; Maccari, F.; Linhardt, R. J., *Electrophoresis* **2008,** *29*, 3095-3106.

6. Toole, B. P., *J. Clin. Invest.* **2000,** *106*, 349-360.

7. Iozzo, R. V., *Proteoglycans: Structure, Biology, and Molecular Interactions*. Marcel Dekker, Inc.: New York, 2000.

8. Trowbridge, J. M.; Gallo, R. L., *Glycobiology* **2002,** *12*, 117R-125R.

9. Rabenstein, D. L., *Nat. Prod. Rep.* **2002,** *19*, 312-331.

10. Raman, R.; Sasisekharan, V.; Sasisekharan, R., *Chem. Biol.* **2004,** *12*, 267-277.

11. Alexopoulou, A. N.; Multhaupt, A. B.; Couchman, J. R., *Int. J. Biochem. Cell Biol.* **2007,** *39*, 505-528.

12. Iozzo, R. V., *J. Clin. Invest.* **2001,** *108*, 165-167.

13. Sasisekharan, R.; Venkataraman, G., *Curr. Opin. Chem. Biol.* **2000,** *4*, 626-631.

14. Garg, H. G.; Linhardt, R. J.; Hales, C. A., *Chemistry and Biology of Heparin and Heparan Sulfate*. Elsevier: Boston, 2005.

15. Vai, M. X.; Shueren, V. D.; Cassiman, J.; Berghe, H. V. D.; David, G., *J. Histochem.* **1994,** *42*, 1043-1053.

16. Rapraeger, A. C.; Krufka, A.; Olwin, B. B., *Science* **1991,** *252*, 1705-1708.

17. Inatani, M.; Haruta, M.; Honjo, M.; Oohira, A.; Kindo, N.; Takashi, M.; Honda, Y.; Tanihara, H., *Brain Res.* **2001,** *920*, 217-221.

18. Johnson, C. E.; Crawford, B. E.; Stavridis, M.; Dam, G.; Wat, S. L.; Rushton, G.; Ward, C. M.; Wilson, V.; Van Kuppevelt, T. H.; Esko, J. D.; Smith, S.; Gallagher, J. T.; Merry, C. L. R., *Stem Cells* **2007,** *25*, 1913-1923.

19. Qiao, D.; Yang, X.; Meyer, K.; Friedl, S., *Mol. Biol. Cell* **2008,** *19*, 2789-2801.

20. Roderiquez, G.; Orvecz, T.; Yanagishita, M.; Chequer, D.; Bou-Habib, D. C.; Mostowski, H.; Norcross, M. A., *J. Virol.* **1995,** *69*, 2233-2239.

21. Crublet, E.; Pierre-Jean, A.; Vives, R. R.; Jacob-Lortat, H., *J. Biol. Chem.* **2008,** *283*, 15193-15200.

22. Vidricaire, G.; Bgauthier, S.; Tremblay, M. J., *J. Infect. Dis.* **2007,** *195*, 1461-1471.

23. Schulze, A.; Gripon, P.; Urban, S., *Hepatology* **2007,** *46*, 1759-1768.

24. Wang, F.; Akula, S. M.; Pramod, N. P.; Zeng, L.; Chandran, B., *J. Virol.* **2001,** *75*, 7517-7527.

25. Feyzi, E.; Trybala, E.; Bergstrom, T.; Lindahl, U.; Spillmann, D., *J. Biol. Chem.* **1997,** *272*, 24850-24857.

26. Herold, B. C.; WuDunn, D.; Noltys, N.; Spear, P. G., *J. Virol.* **1991,** *65*, 1090-1098.

27. Iozzo, R. V.; San Antonio, J. D., *J. Clin. Invest.* **2001,** *108*, 349-355.

28. Qiao, D.; Meyer, K.; Mundhenke, C.; Drew, S. A.; Friedl, A., *J. Biol. Chem.* **2003,** *278*, 16045-16053.

29. Roy, M.; Marchetti, D., *J. Cell. Biochem.* **2009,** *106*, 200-209.

30. Sharma, B.; handler, M.; Eichstetter, I.; Whitelock, J. M.; Nugent, M. A.; Iozzo, R. V., *J. Clin. Invest.* **1998,** *102*, 1599-1608.

31. Yang, Y.; MacLeod, V.; Bendre, M.; Huang, Y.; Theus, A. M.; Miao, H.; Kussie, P.; Yaccoby, S.; Epstein, J.; Suva, L. J.; Kelly, T.; Sanderson, T. K., *Blood* **2005,** *105*, 1303-1309.

32. Iozzo, R. V.; Sharma, B., *J. Biol. Chem.* **1998,** *273*, 4642-4646.

33. Kuniyasu, H.; Oue, N.; Tsutsumi, M.; Tahara, E.; Yasui, W., *Clin. Cancer Res.* **2001,** *7*, 4067-4072.

34. Kolset, S. O.; Fjeldstad, K., *Current Drug Targets* **2005,** *6*, 665-682.

35. Sanderson, D. R., *Cell Devel. Biol.* **2001,** *12*, 89-98.

36. Prestrelski, S. J.; Fox, G. M.; Arakawa, T., *Biochem. Biophys. Res. Commun.* **1992,** *293*, 314-319.

37. Ramamurthy, N.; Baliga, N.; Wakefield, T. W.; Andrews, P. C.; Yang, V. C.; Meyerhoff, M. E., *Anal. Biochem.* **1999,** *266*, 116-124.

38. Ferran, D. S.; Sobel, M.; Harris, R. B., *Biochemistry* **1992,** *31*, 5010-5016.

39. Nagarajan, M.; Rao, V. S. R., *Biopolymers* **1979,** *18*, 1407-1420.

40. Virudachalam, R.; Rao, V. S. R., *Carbohyr. Res.* **1976,** *51*, 135-139.

41. Johnson, L., *Acta Cryst.* **1966,** *21*, 885-892.

42. Gatti, G.; Casu, B. P., A. S., *Biochem. Biophys. Res. Commun.* **1978,** *85*, 14-20.

43. Conrad, H. E., *Heparin-Binding Proteins*. Academic Press: San Diego, 1998.

44. Ferro, D. R.; Provasoli, A.; Ragazzi, M.; Torri, G.; Casu, B.; Gatti, G.; Jacquinet, J. C.; Sinay, P.; Petitou, M.; Choay, J., *J. Am. Chem. Soc.* **1986,** *108*, 6773-6778.

45. McLean, J., *Circulation* **1959,** *19*, 75-78.

46. Kelling, D.; Wardrop, D., *Br. J. Haematol.* **2008,** *141*, 757-763.

47. Mueller, R.; Scheidt, S., *Circulation* **1994,** *89*, 432-449.

48. Marcum, A. J., *J. Hist. Med. Allied Sci.* **2000,** *55*, 37-66.

49. Casati, V.; Gerli, C.; Franco, A.; Valle, P. D.; Benussi, S.; Alfieri, O.; Torri, G.; D'Angelo, A., *Anesthesiol.* **2001,** *95*, 1103-1109.

50. Boisclair, M. D.; Lane, D. A.; Philippou, H.; Esnouf, M. P.; Sheikh, S.; Hunt, B.; Smith, K. J., *Blood* **1993,** *82*, 3350-3357.

51. Yavari, M.; Becker, R. C., *J. Thromb. Thrombolysis* **2008,** *26*, 218-228.

52. Scully, M. F.; Ellis, V.; Shah, N.; Kakkar, V., *Biochem. J.* **1989,** *262*, 651-658.

53. Dieval, J.; Moriniere, P.; Gross, S.; d'Azemar, P.; Fournier, A.; Delobel, J., *Thromb. Res.* **1990,** *58*, 555-560.

54. Spagnuolo, P. J.; Bass, S. H.; Smithg, M. C.; Danviriyasup, K.; Dunn, M. J., *Blood* **1982,** *60*, 924-929.

55. Hirsh, J., *Circulation* **1998,** *98*, 1575-1582.

56. Hansen, J.; Sandset, P. M., *Thromb. Res.* **1998,** *91*, 177-181.

57. Kakkar, V., *Circulation* **1975,** *51*, 8-19.

58. Watson, H. G., *Blood Rev.* **2005,** *19*, 235-241.

59. Brozovic, M., *J. R. Soc. Med.* **1979,** *72*, 602-605.

60. Byun, Y.; Singh, V. K.; Yang, V. C., *Thromb. Res.* **1999,** *94*, 53-61.

61. Horrow, J. C., *Anesth. Analg.* **1985,** *64*, 384-361.

62. Horrow, J. C., *J. Cardiothorac. Vasc. Anesth.* **1988,** *2*, 225-242.

63. Lowenstein, E.; Johnston, W. E.; Lappas, D. G.; D'Ambra, M. N.; Schneider, R. C.; Daggett, W. M.; Akins, C. W.; Philbin, D. M., *Anesthesiol.* **1983,** *59*, 470-473.

64. Pearson, P. J.; Evora, P. R. B.; Ayrancioglu, K.; Schaff, H. V., *Circulation* **1992,** *86*, 289-294.

65. Walker, W. S.; Reid, K. G.; Hider, C. F.; Davidson, I. A.; Boulton, F. E.; Yap, P. L., *Br. Heart J.* **1984,** *52*, 112-114.

66. Fabian, I.; Aronson, M., *Thromb. Res.* **1980,** *17*, 239-247.

67. Davie, E. W., *J. Protein Chem.* **1986,** *5*, 247-253.

68. Davie, E. W.; Fujikawa, K.; Kisiel, W., *Biochemistry* **1991,** *30*, 10363-10370.

69. Quinsey, N. S.; Greedy, A. L.; Bottomley, S. P.; Whisstock, J. C.; Pike, R. N., *Int. J. Biochem. Cell Biol.* **2004,** *36*, 386-389.

70. Weitz, J. I., *J. Clin. Invest.* **2003,** *111*, 952-954.

71. Pejler, G.; Backstrom, G.; Lindahl, U., *J. Biol. Chem.* **1987,** *262*, 5036-5043.

72. Huntington, J. A.; Olson, S. T.; Fan, B.; Gettins, P. G. W., *Biochemistry* **1996,** *35*, 8495-8503.

73. McCoy, A. J.; Pei, X. Y.; Skinner, R.; Abrahams, J.; Carrell, R. W., *J. Mol. Biol.* **2003,** *326*, 823-833.

74. Danielsson, A.; Raub, E.; Lindahl, U.; Bjork, I., *J. Biol. Chem.* **1986,** *261*, 15467-15473.

75. Piepkorn, M. W.; Lagunoff, D.; Schemer, G., *Biochem. Biophys. Res. Commun.* **1978,** *85*, 851-856.

76. Choay, J.; Petitou, M.; Lormeau, J. C.; Sinay, P.; Casu, B.; Gatti, G., *Biochem. Biophys. Res. Commun.* **1983,** *116*, 492-499.

77. Thunberg, L.; Backstrom, G.; Lindahl, U., *Carbohyr. Res.* **1982,** *100*, 393-410.

78. Petitou, M.; Duchaussoy, P.; Lederman, I.; Choay, J., *Carbohyr. Res.* **1988,** *179*, 163-172.

79. Nagumo, T.; Hoshino, H., *Jpn. J. Cancer Res.* **1988,** *79*, 9-11.

80. Rider, C. C.; Coombe, D. R.; Harrop, H. A.; Hounsell, E. F.; Bauer, C.; Feeney, J.; Mulloy, B.; Mahmood, N.; Hay, A.; Parish, C. R., *Biochemistry* **1994,** *33*, 6974-6980.

81. Batinic, D.; Robey, F. A., *J. Biol. Chem.* **1992,** *267*, 6664-6671.

82. Nahmias, J. A.; Kibrick, s., *J. Bacteriol.* **1964,** *87*, 1060-1066.

83. Herold, B. C.; Gerber, S. I.; Polonsky, T.; Belval, B. J.; Shaklee, P. N.; Holme, K., *Virol.* **1995,** *206*, 1108-1116.

84. Shieh, M.; Spear, P. G., *J. Virol.* **1994,** *68*, 1224-1228.

85. Copeland, R.; Balasubamaniam, A.; Vaibhav, T.; Fuming, Z.; Arlene, B.; Linhardt, R. J.; Shukla, D.; Liu, J., *Biochemistry* **2008,** *47*, 5774-5783.

86. Pisano, C.; Aulicino, C.; Vesci, L.; Casu, B.; Naggi, A.; Torri, G.; Ribatti, D.; Belleri, M.; Rusnati, M.; Presta, M., *Glycobiology* **2004,** *15*, 1C-6C.

87. Michaeli-Ishai, R.; Svahn, C. M.; Weber, M.; Shaul-Chajek, T.; Korner, G.; Ekre, H. P.; Vlodavsky, I., *Biochemistry* **1992,** *31*, 2080-2088.

88. Folkman, J.; Shing, Y., *J. Biol. Chem.* **1992,** *267*, 10931-10934.

89. Presta, M.; Leali, D.; Stabile, H.; Ronca, R.; Camozzi, M.; Coco, L.; Moroni, E.; Liekens, S.; Rusnati, M., *Curr. Pharm. Des.* **2003,** *9*, 553-566.

90. Nicosia, R. F., *Am. J. Pathol.* **1998,** *153*, 11-16.

91. Seghezzi, G.; Patel, S.; Ren, C. J.; Gualandris, A.; Pintucci, G.; Robbins, E. S.; Shapiro, R. L.; Galloway, A. C.; Rifkin, D. B.; Mignatti, P., *J. Cell. Biol.* **1998,** *141*, 1659-1673.

92. Rak, J.; Kerbel, R. S., *Nature Med.* **1997,** *3*, 1083-1084.

93. Ito, N.; Claesson-Welsh, L., *Angiogenesis* **1999,** *3*, 159-166.

94. Lundin, L.; Larsson, H.; Kreuger, J.; Kanda, S.; Lindahl, U.; Salmivirta, M.; Claesson-Welsh, L., *J. Biol. Chem.* **2000,** *275*, 24653-24660.

95. Hasan, J.; Shnyder, S. D.; Clamp, A. R.; McGown, A. T.; Bickness, R.; Presta, M.; Bibby, M.; Double, J.; Craig, S.; Leeming, D.; Stevenson, K.; Gallagher, J. T.; Jayson, G. C., *Cancer Therapy: Preclinical* **2005,** *11*, 8172-8179.

96. Wu, C. W.; Jayaraman, G.; Chien, K. Y.; Liu, Y. J.; Lyu, P. C., *Peptides* **2003,** *24*, 1853-1861.

97. Jayaraman, G.; Wu, C. W.; Liu, Y. J.; Chien, K. Y.; Fang, P. C.; Lyu, P. C., *FEBS Lett.* **2000,** *482*, 154-158.

98. Cardin, A. D.; Weintraub, H. J. R., *Arteriosclerosis* **1989,** *9*, 21-32.

99. Verrecchio, A.; Germann, M. W.; Schick, B. P.; Kung, B.; Twardowski, T.; San Antonio, J. D., *J. Biol. Chem.* **2000,** *275*, 7701-7707.

100. Cardin, A.; Demeter, D. A.; Weintraub, H. J. R.; Jackson, R. L., *Methods Enzymol.* **1991,** *203*, 556-583.

101. Mascotti, D. P.; Lohman, T. M., *Biochemistry* **1995,** *34*, 2908-2915.

102. Kelly, M. A.; Chellgren, B. W.; Rucker, A. L.; Troutman, J. M.; Fried, M. G.; Miller, A.; Creamer, T. P., *Biochemistry* **2001,** *40*, 14376-14383.

103. Gunnarsson, K.; Valtcheva, L.; Hjerten, S., *Glycoconj. J.* **1997,** *14*, 859-862.

104. McKeon, J.; Holland, L. A., *Electrophoresis* **2004,** *25*, 1243-1248.

105. Bjorquist, P.; Bostrom, S., *Thromb. Res.* **1997,** *85*, 225-236.

106. Raut, S.; Gaffney, P. J., *Thromb. Res.* **1996,** *81*, 503-509.

107. Wang, J.; Rabenstein, D. L., *Biochemistry* **2006,** *45*, 15740-15747.

108. Hileman, R. E.; Jennings, R. N.; Linhardt, R. J., *Biochemistry* **1998,** *37*, 15231-15237.

109. Hernaiz, M. J.; LeBrun, L. A.; Wu, Y.; Sen, J. W.; Linhardt, R. J.; Heegaard, J. H. H., *Eur. J. Biochem.* **2002,** *269*, 2860-2867.

110. Sibille, N.; Sillen, A.; Leroy, A.; Wieruszeski, J.-M.; Mulloy, B.; Landrieu, I.; Lippens, G., *Biochemistry* **2006,** *45*, 12560-12572.

111. Stephens, R. W.; Bokman, A. M.; Myohanen, H. T.; Reisberg, T.; Tapiovaara, H.; Pedersen, T.; Grondahl-Hansen, J.; Llinas, M.; Vaheri, A., *Biochemistry* **1992,** *31*, 7572-7579.

Chapter 2

Materials and Methods

2.1 Peptide Synthesis

2.1.1 Peptide Synthesis Materials

Piperidine (PIP), 99.5%+ biotech grade, and triisopropylsilane (TIPS), 99%, were purchased from Sigma-Aldrich. 2-(1H-benzotriazole-1-yl)-1,1,3,3-tetramethyluronium hexafluorophosphate (HBTU), N-hydroxybenzotriazole (HOBT) 1 M in N-methyl-2-pyrrolidone (NMP), and N-diisopropylethylamine (2 M in NMP), were obtained from Applied Biosystems. N,N-dimethylformamide (DMF) ACS grade, was purchased from Mallinckrodt Chemicals. Glacial acetic acid (HPLC grade) was purchased from Fisher Scientific, and trifluoracetic acid (TFA) was acquired from Impex International Inc. Rink amide-methylbenzhydrylamine (MBHA) resin and 9-fluorenylmethoxycarbonyl (Fmoc)-protected amino acids were obtained from Novabiochem and Advanced Automated Peptide Protein Technologies, respectively.

2.1.2 Peptide Synthesis Overview

Solid-phase peptide synthesis (SPPS) was introduced by Bruce Merrifield in 1963.[1] As the peptide is attached to a solid support during synthesis, SPPS is a practical replacement for solution phase chemistry in which one could encounter solubility issues and tedious purifications between synthesis steps.

In SPPS, the first amino acid residue is covalently attached, via its carboxyl terminus, to an insoluble support; this covalent attachment allows the resin, along with the growing peptide chain, to be washed of excess reagents and filtered.[2] Amino acids are then added in a stepwise manner, and the peptide is synthesized from the C - to the N- terminus. The N-terminal amine on each incoming amino acid has to be protected to prevent self-coupling. Amino acid side chains also have to be protected to prevent unwanted side reactions. After the coupling step, the N-terminal amino group of the last amino acid residue to be added needs to be deprotected and the incoming amino acid is activated for the next coupling step.[3] The three steps of deprotection, rinsing (of excess reagents), and coupling are repeated until synthesis of the desired peptide is complete. The peptide is then cleaved from the resin, which simultaneously removes side-chain protecting groups, and filtered.

The two most common methods utilized in SPPS are: tert-butyloxycarbonyl (tBoc) and 9-fluorenylmethoxycarbonyl (Fmoc).[4] In the tBoc method, the N-terminus of the amino acid is protected by the tBoc group and reactive side-chains are protected by acid labile protecting groups. In this case, the side-chain protecting groups and the amino protecting group are more acid labile then the bond supporting the peptide to the solid-support. Therefore, the removal of these groups is facilitated by a mild acid and the cleavage of the peptide from the solid-support by a strong acid. This allows for the possibility of structural changes to the peptide under these relatively harsher conditions. In the Fmoc procedure, an orthogonal approach is used in which

deprotection of the N-terminus (protected by the Fmoc group) and side-chain protecting groups is facilitated by a mild base, and cleavage of the peptide from the support by a mild acid. The Fmoc method allows for milder conditions to be used during the cleavage of the peptide from the support and is thus now the most common method used in peptide synthesis. The Fmoc method of SPPS is used in this research and so will be discussed further.

2.1.3 Automated Fmoc Peptide Synthesis Overview

The peptides used in this work were synthesized on an Applied Biosystems ABI 433A automated peptide synthesizer.The synthesizer is computer controlled by a Power Mac G4 workstation using SynthAssist Version 2.0 software. The workstation includes chemistry programs for a variety of synthesis methods. In this research, the *FastMoc* option was utilized using the 0.10 mmol scale. In automated SPPS, all necessary reagents are contained in bottles that are attached to the front of the synthesizer, and four-liter solvent bottles are located just outside the synthesizer. Cartridges, filled with amino acids, are lined up in sequential order within a groove on the outside of the instrument. A pusher block then pushes each cartridge under a syringe needle which then draws up the dissolved amino acid into a reaction vessel, in which the solid-support is placed, for coupling. Deprotection and amino acid coupling, occurs within the reaction vessel which enhances the reactions by vortexing. Solvent and reagent delivery to the

amino acid cartridges and reaction vessel, and mechanical operation of the synthesizer are all mediated by pressurized nitrogen gas set at around 65 psi.

Several steps take place during the synthesis and are repeated throughout until the peptide is complete. The steps are: deprotection of the resin (and thereafter the Fmoc-protected N-terminus of the amino acid residue), activation of the incoming amino acid, and coupling of the activated amino acid to the deprotected N-terminus of the previously added amino acid. Between each of these steps, washing steps occur to remove any excess reagents.

2.1.4 Fmoc SPPS Method for Automated Synthesis

Using the 0.1 mmol scale, approximately 0.1786 g of Rink Amide MBHA resin, Fig. 2.1, was placed in an 8 ml reaction vessel. The resin had a substitution of 0.56 mmol/g and was of 100-200 mesh. Rink Amide MBHA resin is a polystyrene material crosslinked with 1% divinylbenzene with a covalently attached MBHA linker. Initally, the resin in the reaction vessel is allowed to swell, with 6 mL NMP, to about 10X its original dried volume. The swelling is due to solvation of the interior of the polymer bead which enhances coupling efficiency by exposing more coupling sites to reagents. Cleavage of the peptide from this resin results in an amidated C-terminus. Before the first deprotection step, NMP from the solvent bottle is delivered to the reaction vessel to allow the resin to swell. The MBHA linker is protected by an Fmoc group which must be removed to allow the C-terminus of the first amino acid of the peptide to be coupled to

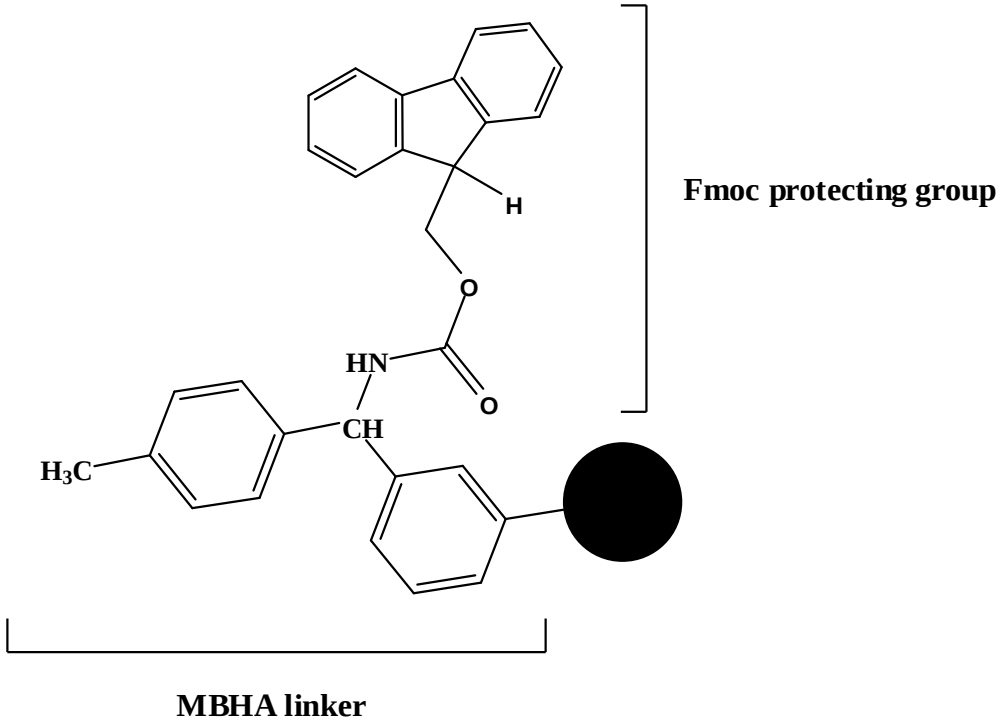

Fig. 2.1. Rink Amide MBHA resin with the polystyrene bead (black dot), the MBHA linker, and the Fmoc protecting group. The linker is cleaved between the carbonyl carbon and the amide nitrogen leaving a free amine which is coupled to an incoming, activated amino acid.

the linker. This is accomplished by delivering 20% piperidine in NMP to the reaction vessel and vortexing for about 10 min. Piperidine deprotonates the Fmoc group at the β-carbon, Fig. 2.2. The high acidity of this hydrogen is due to the electron withdrawing fluorene ring system of the Fmoc group allowing it to be extracted by a weak base to form a dibenzylfulvene carbanion intermediate.[5] This intermediate is then susceptible to attack by piperidine, forming a fulvene-piperidine adduct; this adduct can be monitored by UV absorbance at 301 nm to establish deprotection efficiency. After deprotection,

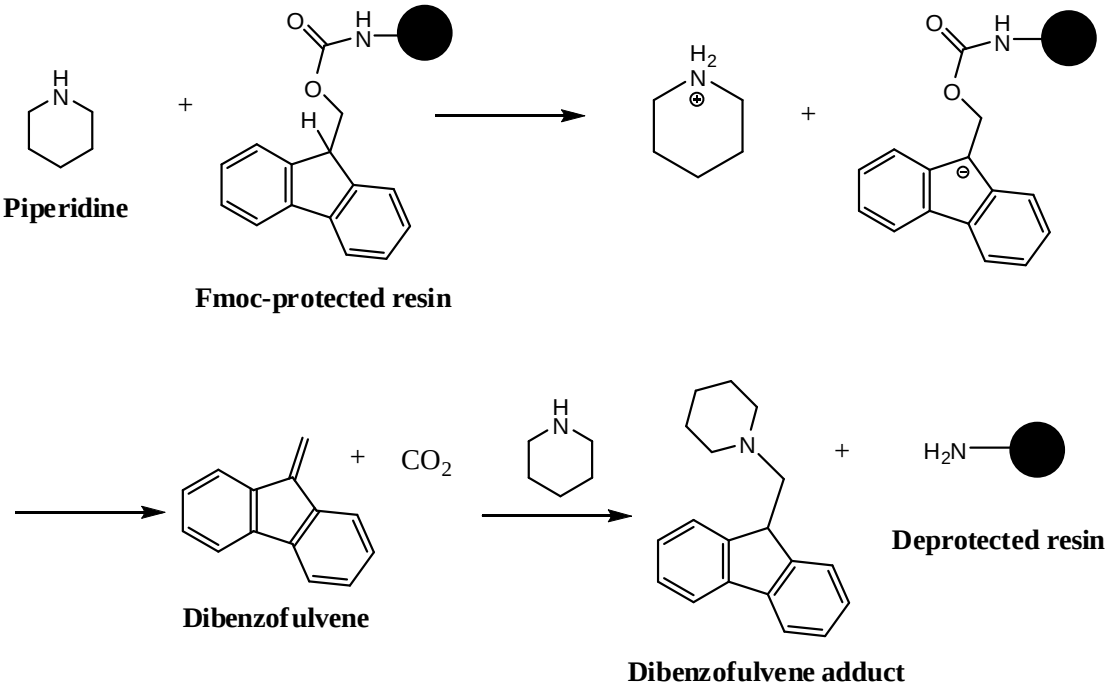

Fig. 2.2. The first deprotection of the Fmoc-protected MBHA linker. Subsequent deprotections occur similarly for each added Fmoc-protected amino acid.

the resin is thoroughly washed with NMP and the incoming Fmoc-protected amino acid is activated by HBTU for coupling to the now free amine of the MBHA linker.

Activation of the carboxylate group of the incoming amino acid is necessary since it will not react in a practical time period with the free amine, Fig. 2.3. To prepare the activation reagent, 200 ml of 0.5 M HOBt in NMP are poured into a 450 ml bottle containing 100 mmol of HBTU which is subsequently attached to the manifold of the synthesizer. The addition of HOBt to the 100 mmol of HBTU dilutes the 0.5 M HOBT to 0.45 M. 2.0 g of 0.45 M HBTU/HOBt in DMF, and 0.8 mL NMP is injected into the amino

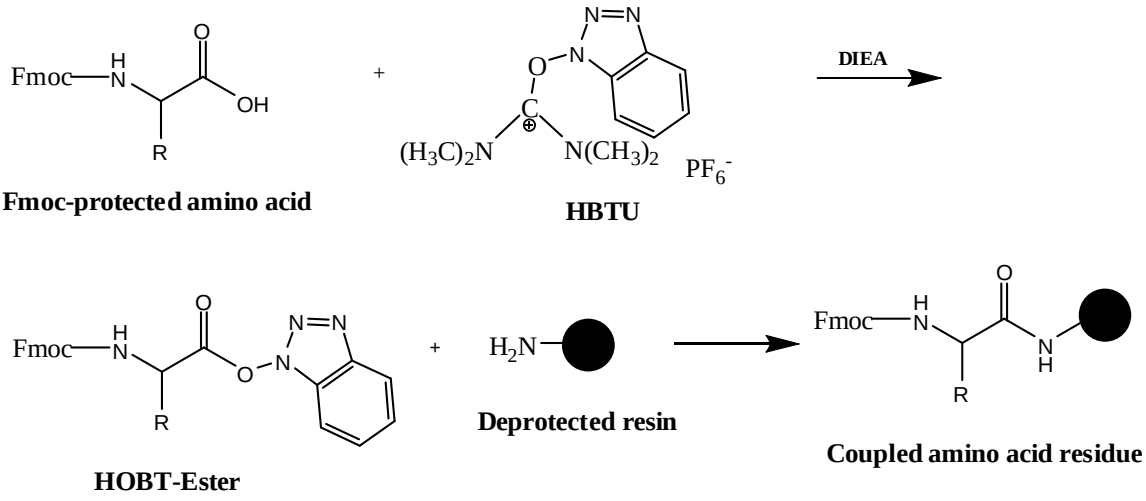

Fig. 2.3. Activation and coupling of Fmoc-protected amino acids to a free, resin-bound, amine.

acid cartridge to dissolve the Fmoc-protected amino acid. 1 ml of 2 M DIEA is delivered to the cartridge to activate the carboxylic group of the amino acid and mixed by bubbling with N_2 for about 6 min. A ratio of 5X the amount of amino acid to coupling sites on the resin bead is used to ensure high coupling efficiency. DIEA is necessary to form a carboxylate of the amino acid which will then react with HBTU forming an HOBt ester.[4] The activated amino acid solution is then transferred to the reaction vessel for coupling for 9 min.

Between each reaction in the reaction vessel, the resin is washed 5X with about 6 ml of NMP. All peptides synthesized for this research were acylated on the N-terminus to avoid end-charge affects. This was done by adding 60 µL of glacial acetic acid to the last amino acid cartridge and utilizing the same steps in the amino acid coupling process.

The above steps were repeated (except for the final acylation step) until the peptide synthesis was complete.

When the peptide synthesis was complete the resin with attached peptide was rinsed thoroughly with methanol by vacuum filtration to remove any residual solvents and then dried overnight before cleavage. The side-chain protecting groups were removed and the peptide-linker bond cleaved by reaction with cleavage solution for about 2 hrs. The cleavage solution was 95% TFA, 2.5% water, and 2.5% TIPS. The TIPS is necessary to scavenge carbocations, formed from side-chain protecting groups released during the cleavage process that could otherwise irreversibly bond to the side chains of certain amino acid residues. In this research the sensitive side chains are those of histidine, lysine, and arginine residues. The side-chain protected Fmoc amino acids are shown in Fig. 2.4.

After cleavage, the peptide/resin solution was filtered by vacuum filtration to remove the resin. The crude material was then analyzed by MALDI-TOF-MS to ensure the target peptide was synthesized. The filtrate was then placed in a rotovaporator to reduce its volume to a more practical working level, and subsequently frozen with liquid N_2 for about 30 min. The frozen filtrate was lyophilized overnight, typically to a brown, oily, residue. The residue was then dissolved in about 5-10 mL of water and the peptide was then isolated by preparative scale HPLC. Each major peak in the HPLC chromatogram was analyzed by MALDI-TOF-MS to determine which peak contained the

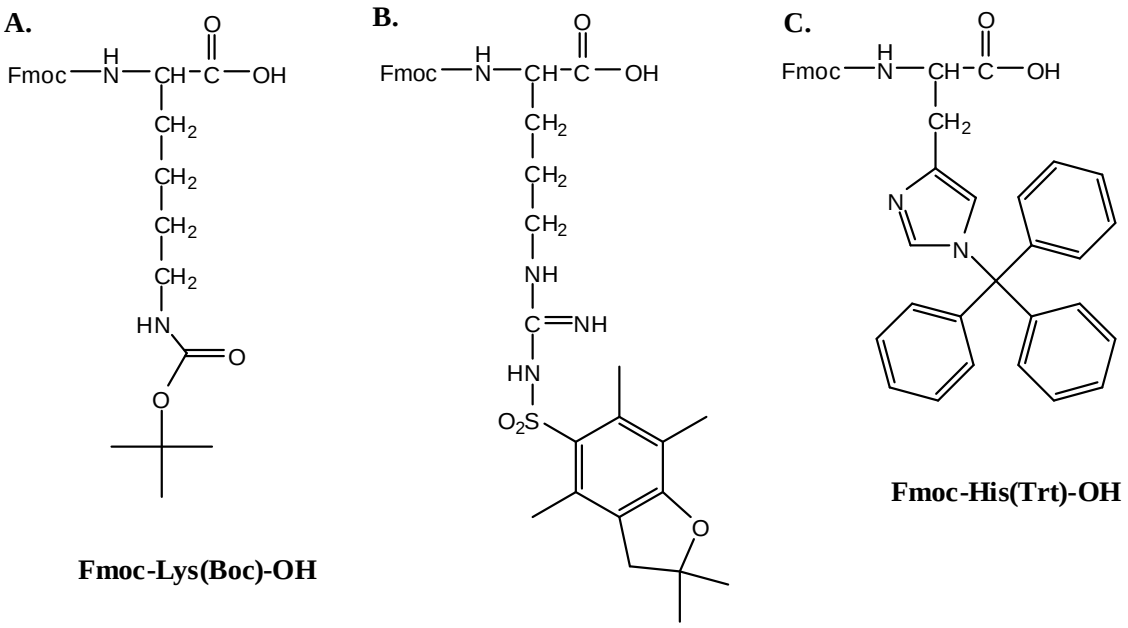

Fmoc-Lys(Boc)-OH

Fmoc-Arg(Pbf)-OH

Fmoc-His(Trt)-OH

Fig. 2.4.A. Fmoc-protected lysine amino acid with the tert-butyloxycarbonyl (Boc) side-chain protecting group. **B.** Fmoc-protected arginine amino acid with the 2,2,4,6,7-pentamethyldihydrobenzofuran-5-sulfonyl (Pbf) side-chain protecting group. **C.** Fmoc-protected histidine amino acid with the trityl (Trt) side-chain protecting group.

target peptide. The peak corresponding to the target peptide was then collected. The purified peptide in HPLC solvent was again placed in a rotovaporizor to bring the solution down to a practical working level. The solution was then frozen with liquid N_2 and lyophilized down to a crystalline powder form that was used in heparin-binding experiments.

2.2 Peptoid Synthesis

2.2.1 Peptoid Synthesis Materials

Piperidine 99.5% biotech grade, triisopropylsilane 99% (TIPS), bromoacetic acid 97% GR ACS (BrAc), (R)-(+)-α-methylbenzylamine 98% (rpe) and (S)-(-)-α-methylbenzylamine (spe) were all purchased from Sigma-Aldrich. N-N'-diisopropylcarbodiimide (DIC), (S)-(+)-sec-butylamine (ssb), and N-(tert-butoxycarbonyl)-1,4-diaminobutane were all obtained from TCI America. N-methyl-2-pyrrolidone (NMP) was purchased from Applied Biosystems, and n-butylamine (nb) was purchased from Acros Organics. A Benchmixer vortex mixer was purchased from Southwest Science, and 20 ml Teflon syringes with fritted disks for solid phase synthesis were acquired from Torviq. Rink amide-methylbenzhydrylamine (MBHA) resin was obtained from Novabiochem. Trifluoroacetic acid (TFA) was purchased from Impex International Inc.

2.2.2 Peptoid Synthesis Overview

Synthesis of peptoids can be realized by the efficient submonomer solid-phase synthesis method, Fig. 2.5, developed by Zuckermann et al.[6] In this method, the peptoid is linked to a rink amide solid-support and synthesized by incorporating peptoid monomers from the C-terminus to the N-terminus of the peptoid sequence, as in regular solid-phase peptide synthesis. Submonomer units are added sequentially until the peptoid synthesis is complete. First, bromoacetic acid is activated by diisopropylcarbodiimide; this is used to acylate the deprotected rink amide resin. The side-chain group is then added to form a peptoid monomer residue by an SN2 displacement reaction with a primary amine in which bromine acts as an efficient leaving-group. The two-step process is continued until the synthesis of the peptoid is complete. Cleavage of the peptoid from the rink amide resin results in an amidated C-terminus. One of the advantages of using this method of synthesis is the availability of primary amines which can endow peptoids with a variety of side-chain chemistries.

2.2.3 Manual Peptoid Synthesis Method

In this research peptoids were syntheisized manually using 20 mL Teflon syringes, with fritted disks, as reaction vessels. The syringes were held tip-down by the syringe plunger by a three fingered clamp attached to a ring stand, Fig. 2.6. The tip of the syringe was placed on top of the working-end of a vortex mixer which was used for agitation of the reaction mixtures inside the syringe during the deprotection, acylation, amidation, and

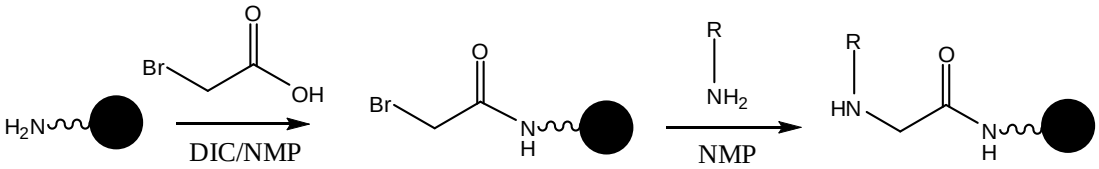

Fig. 2.5. The first acylation and SN2 displacement step of the submonomer method, forming a peptoid monomer.

washing steps to enhance reaction efficiency. The vortexer was set to a moderate mixing speed.

All syntheses were run on a 0.1 mmol scale which required about 0.1786g of Fmoc-protected Rink Amide MBHA resin with a 0.56 mmol/g substitution. After the resin was placed in the syringe, it was allowed to swell for 30 min in NMP. After swelling, the Fmoc-protected resin was deprotected with a solution of 20% piperidine in NMP for 30 min. The resin was subsequently washed 5X with 5 ml of NMP for about 1 min for each wash. Between each subsequent acylation and amidation step a washing step was incorporated using the same above procedure. The next step was the acylation in which 6 ml of a 1.2 M BrAc solution in NMP and 1.25 mL of DIC were added to the resin and vortexed for 30 min. The amine solutions were 2.5 M or 1 M in NMP; Fig. 2.7 shows the amines used. 6 mL of amine solution was used for the addition of the primary amine, and coupled for 2 hrs using the 2.5 M solutions of the primary amines or 4 hrs using the 1 M solutions; the difference in concentration used was due to expense, with the N-Boc-1,4-diaminobutane and (S)-sec-butyl reagents being more expensive; for these amines, 1 M was used but the reaction time was increased from 2 hrs to 4 hrs.

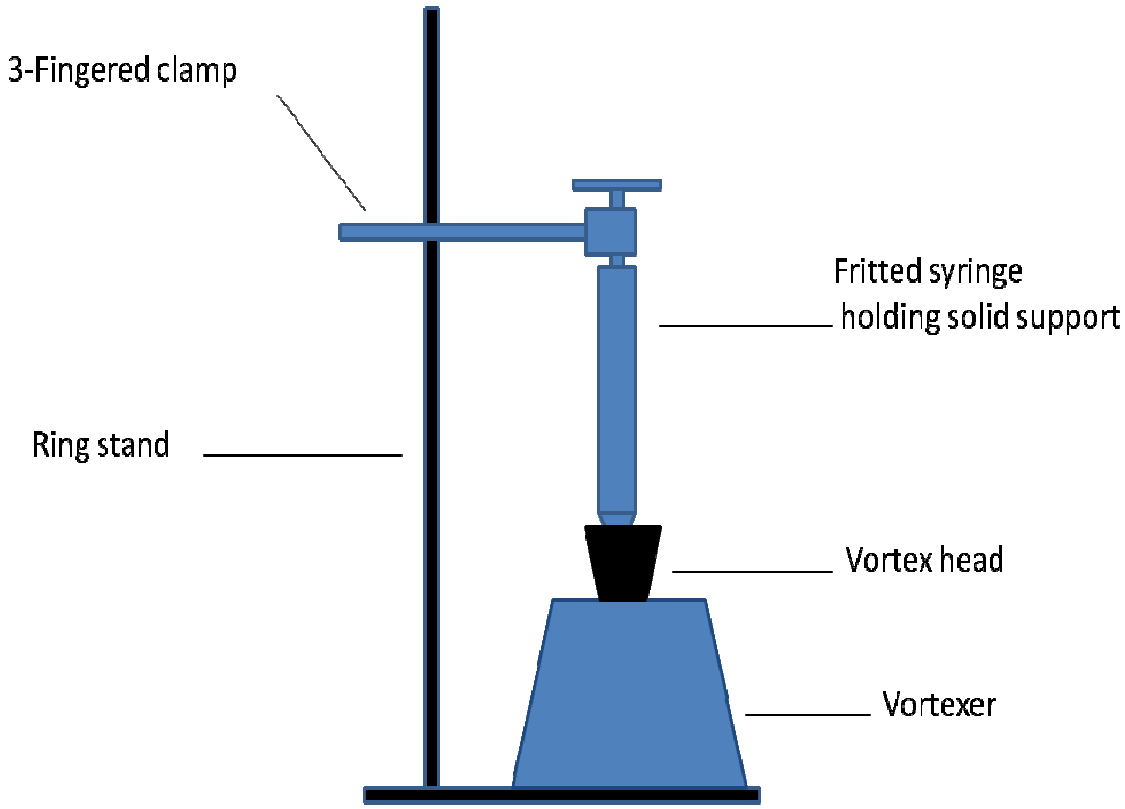

Fig. 2.6. Manual peptoid/hybrid synthesizer with the tip of a fritted syringe (reaction vessel) placed in the vortex head which is held in place by a 3-fingered clamp.

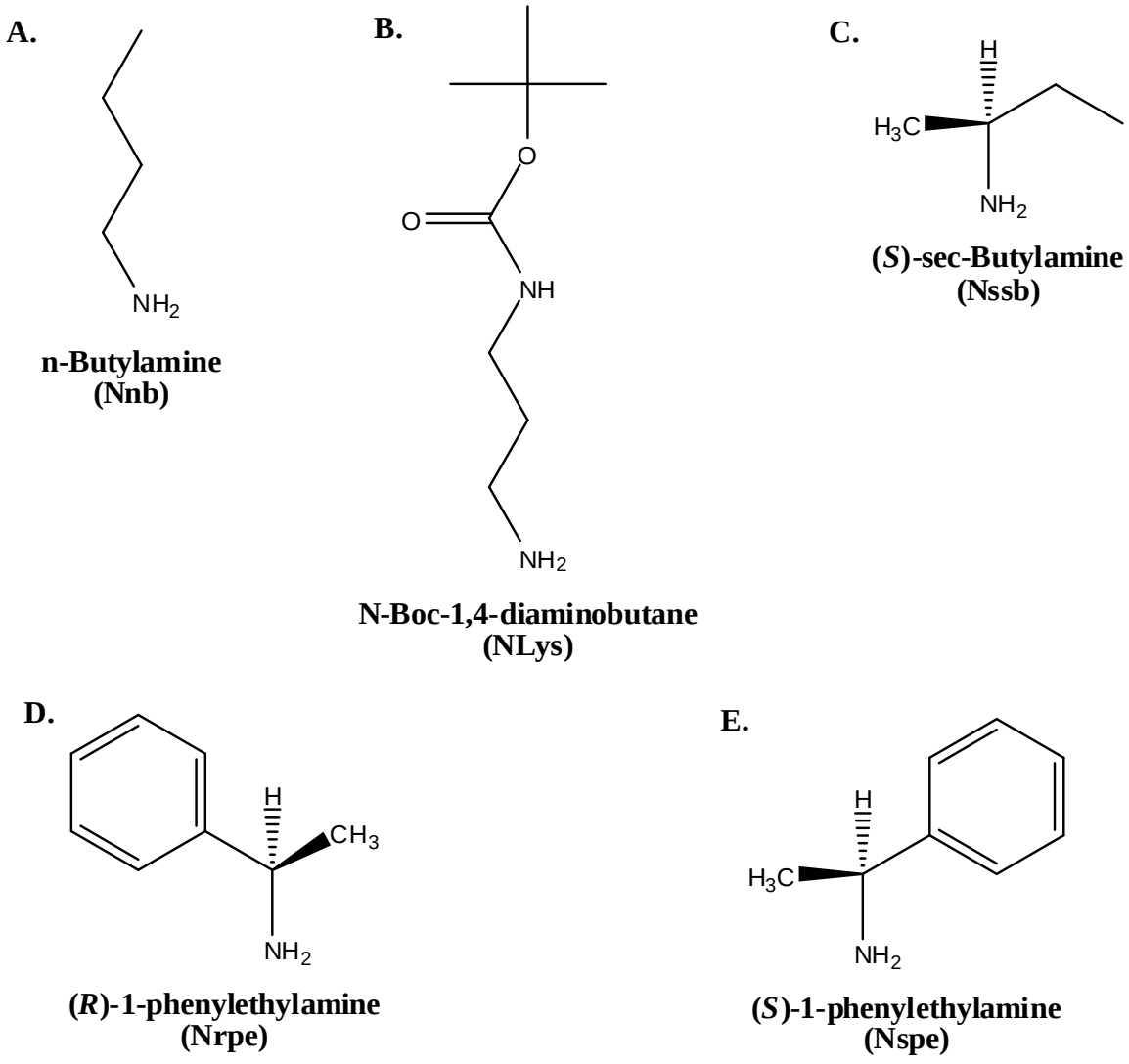

Fig. 2.7. Primary amines used in this research, with the corresponding abbreviations used to indicate the fully formed monomer within a peptoid in parentheses. For example, a peptoid containing peptoid monomer units formed from n-butylamine, (S)-sec-butylamine, and (R)-1-phenylethylamine, in order from the N-terminus, would be written as: Nnb-Nssb-Nrpe.

After the first and only deprotection step in the synthesis, acylation and amidation steps were repeated until the desired peptoid was synthesized. After the synthesis was complete, the resin with bound peptoid was washed 5X with 5 mL of methanol to rid the resin of residual NMP. The resin was then placed on weigh paper and air dried overnight before cleavage. For the cleavage step, the resin plus bound peptoid was weighed to determine the necessary amount of cleavage reagent to use. In all cases the volume of cleavage cocktail used was 3 mL per 0.1g of resin plus bound peptoid. The cleavage cocktail consisted of 95% TFA, 2.5% water, and 2.5% TIPS, with the TIPS again serving to scavenge reactive carbocations produced from the side-chain protecting groups during cleavage.

After the cleavage, the peptoid/resin solution was filtered by vacuum filtration and the crude material was analyzed by MALDI-TOF-MS to ensure the target peptoid was synthesized. The filtrate was then placed in a rotovaporator to reduce its volume to a more practical working level, and subsequently frozen with liquid N_2 for about 30 min. The frozen filtrate was lyophilized overnight to a brown, oily, residue. About 5-10 mL of water were then added to dissolve the oily residue, and then the peptoid was isolated by HPLC. The major peaks of the HPLC separation were collected and analyzed by MALDI-TOF-MS to identify which peak contained the target peptoid. The peak containing the corresponding peptoid was then collected. The purified peptoid, in HPLC solvent, was again placed in a rotovaporator. After the peptoid solution was reduced to

a practical working volume, it was frozen with liquid N_2 and lyophilized to a crystalline powder form for use in heparin-binding experiments.

2.2.1.1 Synthesis of N-tert-butoxycarbonyl-1,4-diaminobutane

2.2.1.1.1 N-tert-butoxycarbonyl-1,4-diaminobutane Synthesis Materials.

1,4-diaminobutane and di-tert-boc-dicarbonate were purchased from TCI America. 1,4-dioxane was purchased from Acros Organics. Dichloromethane and Na_2SO_4 (anhydrous) were acquired from Fisher.

2.2.1.1.2 Method of Synthesis for N-tert-butoxycarbonyl-1,4-diaminobutane

An initial 8:1 ratio of 1,4-diaminobutane to di-tert-boc-dicarbonate is required for the optimal yield of N-tert-butoxycarbonyl-1,4-diaminobutane, Fig. 2.7. To this end, 95 mL and 30 mL of dioxane were added to 27 mL of 1,4-diaminobutane and to 6 g of di-tert-boc-dicarbonate, respectively. The di-tert-boc-dicarbonate solution was then added drop-wise, under N_2 and over 3 hrs, to the 1,4-diaminobutane solution. After this addition, the reaction was continued for 24 hrs with vigorous stirring. The mixture was rotovaporized at 40 ^{o}C. Then 100 mL of water was added resulting in the formation of a white precipitate containing di-boc-protected 1,4-diaminobutane. The filtrate was isolated and the unprotected and mono-boc-protected 1,4-diaminobutane, were extracted, 3 times, with dichloromethane. A water extraction was performed on the dichloromethane layer to remove any unprotected 1,4-diaminobutane, isolating the

desired product, mono-boc-protected 1,4-diaminobutane. This solution was then dried using anhydrous Na_2SO_4, vacuum-filtered, and then rotovaporized. To the resulting oil, enough NMP was added to make a 1 M solution of N-tert-butoxycarbonyl-1,4-diaminobutane for peptoid synthesis.

2.3 Peptide/Peptoid Hybrid Synthesis

2.3.1 Peptide/Peptoid Hybrid Synthesis Materials

All materials used in peptide/peptoid hybrid (hybrid) synthesis were the same as those used for peptide and peptoid synthesis, as described above.

2.3.2 Manual Hybrid Synthesis Method

All hybrids were synthesized using a manual method similar to that used in the synthesis of peptoids. About 0.1786g of Fmoc-protected Rink Amide MBHA resin (0.1 mmol scale) was placed into a fritted syringe and allowed to swell in NMP for about 30 min. The syringe was hung on a ring stand by the syringe plunger (with the tip down) by a three-fingered clamp, and the tip of the syringe was placed on the vortexing cup. This position allowed the syringe to be vortexed when the mixer was turned on. Deprotection of the Rink Amide Fmoc-protecting group was initiated by adding in 6 mL of a 20% piperidine solution in NMP, and vortexing for 30 min. Acylation was the next step in which 6 mL of a 1.2 M solution of BrAc in NMP and 1.125 mL of DIC was mixed

and poured into the syringe barrel and vortexed for 30 min. Coupling of a primary amine, such as (R)-1-phenylethylamine, was done by adding 6 mL of a 2.5 M solution of the primary amine in NMP to the resin. The mixture was then allowed to react for 2 hrs. The first two steps of acylation and amidation were the same for each addition of a primary amine. For the coupling of Fmoc-protected amino acid, 6 mL of a solution containing a five-fold excess of the amino acid, compared to the 0.1 mmol scale used in this synthesis, was prepared. To this mixture, 1.125 mL of DIC was added and then this solution was poured into the syringe barrel. Since it was found to be difficult to efficiently couple the amino acid to the secondary amine of the peptoid residue, as compared to a primary amino group in peptide synthesis, the coupling mixture was allowed to vortex for 24 hrs. After coupling of the amino acid, a deprotection step was needed since the amino acid has an Fmoc-protecting group bound to its primary amine. This was done in the same way as the deprotection step of the Rink Amide resin. Between each acylation and coupling step, the resin was washed of excess reagents 5X with 5 mL of NMP each. After the last washing of NMP, the resin was washed 5X with 5 ml of methanol each for desolvation of the resin.

After the synthesis was complete, the resin was placed on weighing paper to dry overnight. The hybrid was cleaved from the resin using a cleaving solution consisting of 95% TFA, 2.5% TIPS, and 2.5% water. The volume of cleaving solution used was determined by the final mass of the resin plus hybrid: for every 0.1 g of resin plus

hybrid, 3 mL of cleaving solution was used. The cleaving solution was allowed to react with the resin-bound hybrid for 2 hrs.

After cleaving the hybrid from the resin, the cleaving solution was filtered from the resin by vacuum filtration and the resin rinsed with about 10 mL of water. The solution was then rotovaporized to bring the volume down to a practical working level (about 5 mL). The solution was then purified by reverse-phase HPLC.

During HPLC, the major peaks resulting from the separation were collected and analyzed by MALDI-TOF-MS to identify which peak contained the target hybrid. After identification, the target hybrid's corresponding peak was then collected and again rotovaporized before freezing with liquid N_2 and lyophilized for experimentation.

2.4 Isothermal Titration Calorimetry

2.4.1 Isothermal Titration Calorimetry Materials

Sodium monobasic phosphate, monohydrate, GR ACS was purchased from EMD Chemicals. Heparin sodium salt from porcine intestinal mucosa (average molecular weight of 12,000 Da, 180 USP units/mg, Lot 105K1114) was purchased from Sigma. All buffers were prepared using Millipore water. All ITC experiments were performed on a Microcal VP-ITC MicroCalorimeter. Data were analyzed using Origin 5.0 sofware.

2.4.2 Isothermal Titration Calorimetry Overview

Isothermal titration calorimetry has been used to determine the thermodynamic parameters of a variety of biomolecular reactions such as: DNA-drug interactions,[7] protein folding and unfolding,[8] and enzyme kinetics.[9] Although ITC can be utilized to measure various biological interactions, the binding affinity of the interaction must satisfy certain criteria to obtain accurate results; specifically, K_b values should be in the 10^3 to 10^9 M^{-1} range.[10] Indirect techniques have been developed to determine association constants above[11] and below this range.[12]

The strong point of ITC is that it measures, directly, enthalpy changes associated with binding interactions.[13] In a single experiment, ITC can be used to determine the binding constant K_b, the number of binding sites n, and the change in enthalpy ΔH of a binding interaction.[14] The free energy of the reaction ΔG and entropy ΔS can be calculated from these parameters by the relationship:[15]

$$\Delta G = -RTlnK_b = \Delta H - T\Delta S \qquad 2.1$$

Since the heat of the binding interaction is the measured signal, there is no need to immobilize or modify any of the reactants.[8] The calorimeter accomplishes this by utilizing an injection syringe, under computer control, which injects aliquots of titrant (typically the ligand) into a sample cell containing the binding partner (typically the macromolecule). However, depending on the type of binding interaction, the ligand may be placed in the sample cell, and the macromolecule in the injection syringe, as in most cases of this research. Each injection of the ligand or macromolecule into the sample cell

results in heat, either absorbed or evolved, from the binding interaction . The sample cell, together with a reference cell (containing buffer only) are located in an adiabatic jacket, and kept at a constant, small differential temperature by feedback control circuits, Fig. 2.8. The resulting change in temperature of the sample cell, associated with the binding interaction, triggers the feedback system to either increase (in the case of an endothermic reaction) or decrease (in the case of an exothermic reaction) power to the sample cell to maintain the same temperature offset prior to injection; this is the signal that is recorded by the calorimeter. As the titrations continue, the recorded signal for each binding event diminishes as the equilibrium is pushed farther to the right; as a consequence, fewer and fewer binding sites are available for the ligand. Each injection is plotted as a change in power as a function of time. This data is subsequently integrated to give the molar enthalpy as a function of the molar ratio of ligand to macromolecule. The integrated isotherm is then fit with an appropriate binding model to generate the above thermodynamic parameters.[7]

Figs. 2.9 and 2.10 show an example of raw titration data and the results of the data after integration and fitting with an appropriate model. This example involves the binding of 2'-CMP and Ribonuclease A, which is a reference titration for the calorimeter. The results confirm the calorimeter is producing results which are within the expected error. Several binding models are available with the instrument software for fitting the integrated titration data. The simplest and most commonly applied is one in which there

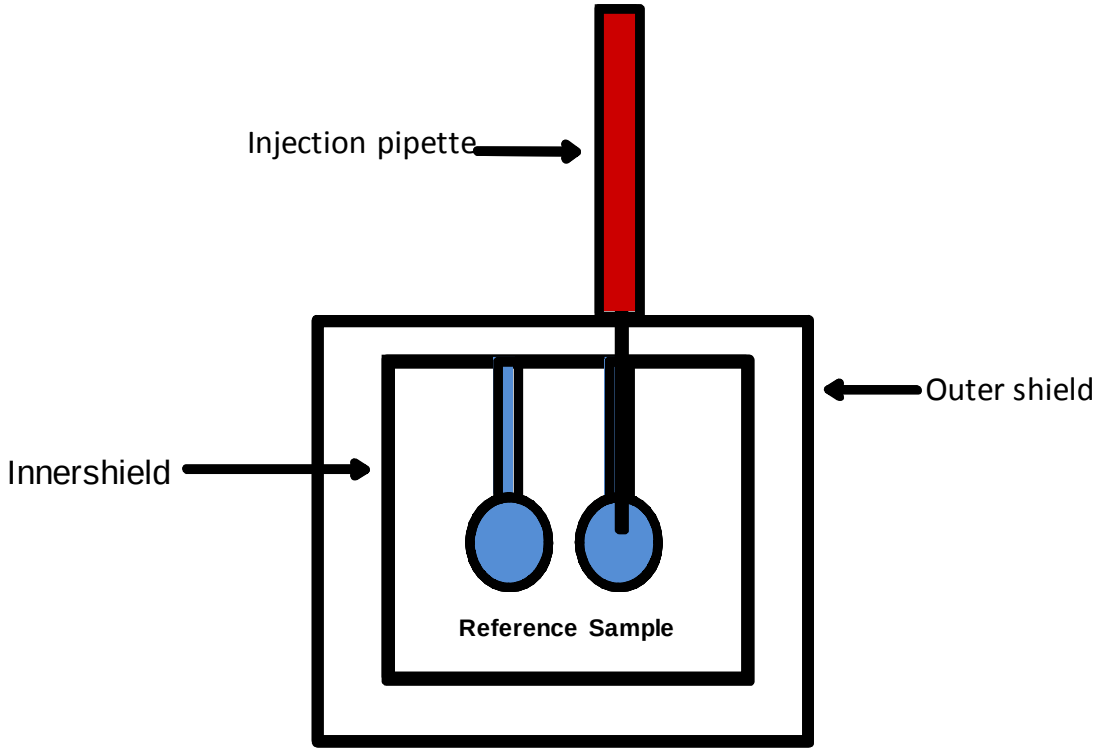

Fig. 2.8. Schematic of the reference and sample cells housed in the adiabatic jacket of the isothermal titration calorimeter, with the pipette injector inserted into the sample cell.

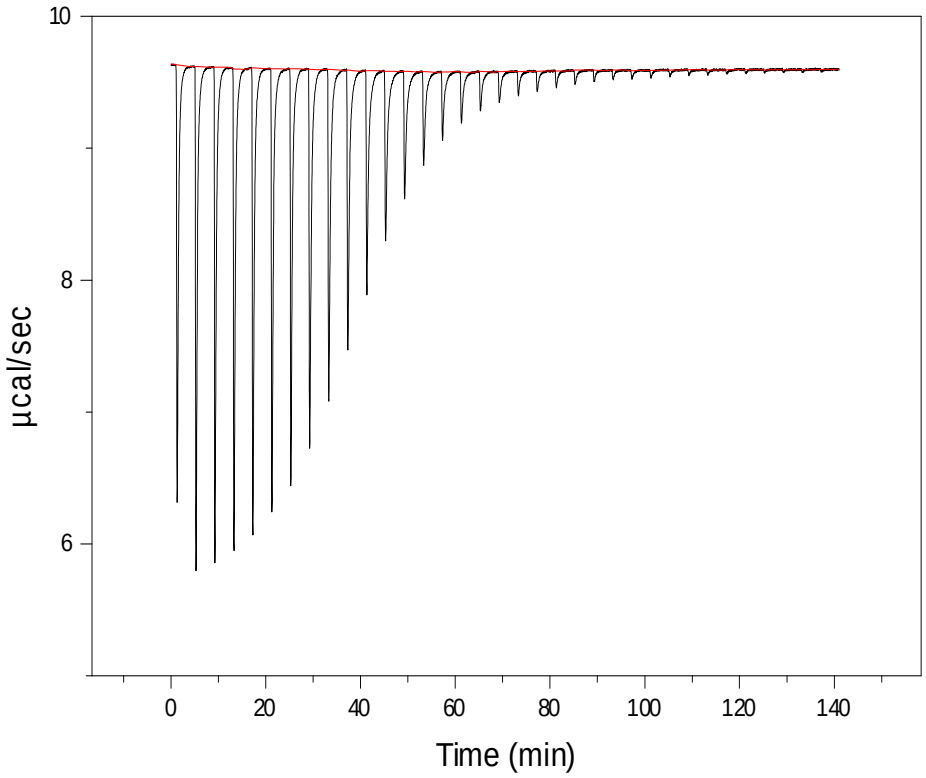

Fig. 2. 9. Raw titration data for the titration of Ribonuclease A with 2' CMP. This particular titration is used to determine instrument accuracy. Each peak represents the differential power decrease as the sample cell temperature increases with each titration, characteristic of an exothermic binding interaction.

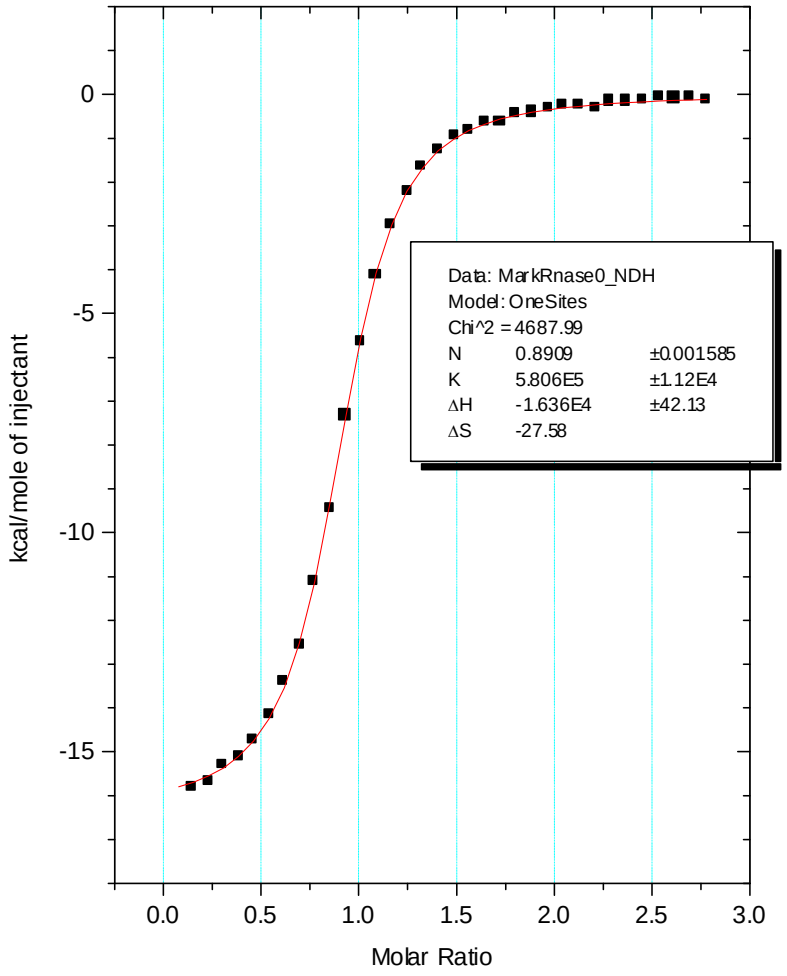

Fig. 2.10. The integrated raw data of that shown in Fig. 2.9. Data is fit with a one-set-of-single-binding-sites model to give the thermodynamic parameters shown in the inset.

is multiple sets of independent binding sites on the macromolecule;[16] this model was used in this research.

For the equilibrium

$$M + X \leftrightarrow MX \tag{2.2}$$

where M is a binding site on a macromolecule and X is a ligand, the equilibrium expression, K_b, is

$$K_b = \frac{[MX]}{[M][X]} \tag{2.3}$$

If $[M]$ is the concentration of free binding sites and $[M_t]$ is the total macromolecule concentration, then the total concentration of binding sites is $n[M_t]$ where n is the total number of binding sites on the macromolecule. In fractional terms

$$\frac{[M]}{n[M_t]} = 1 - \frac{[MX]}{[M] + [MX]} \tag{2.4}$$

Let θ be the fraction of $n[M_t]$ bound by X so

$$\theta = \frac{[MX]}{[M] + [MX]} \tag{2.5}$$

The concentration of free M is then

$$[M] = [1 - \theta]n[M_t] \tag{2.6}$$

Then equ. 2.3 can become

$$K_b = \frac{\theta n[M_t]}{[1 - \theta]n[M_t][X]} \tag{2.7}$$

Then by cancellation

$$K_b = \frac{\theta}{[1 - \theta][X]} \tag{2.8}$$

Let $[X_t]$ be the total amount of ligand, $[X]$ the amount of free ligand and n the number of binding sites on the macromolecule, so

$$[X_t] = [X] + [M_t]\theta n \quad 2.9$$

Equ. 2.8 can be rearranged so that

$$[X] = \frac{[\theta]}{[1-\theta]K_b} \quad 2.10$$

Equ. 2.9 can be rearranged so that

$$[X] = [X_t] - \theta n[M_t] \quad 2.11$$

By substituting equ. 2.11 into 2.10

$$[X_t] - [M_t]\theta n = \frac{[\theta]}{[1-\theta]K_b} \quad 2.12$$

Rearranging equ. 2.12 into a quadratic equation gives

$$\theta^2 - \theta\left(1 + \frac{X_t}{nM_t} + \frac{1}{nK_bM_t}\right) + \frac{X_t}{nM_t} = 0 \quad 2.13$$

The heat Q associated with the total of bound binding sites after each injection is:[17]

$$Q = \Delta HV\theta n[M_t] \quad 2.14$$

Where ΔH is the molar enthalpy of the binding interaction, and V is the reaction volume.

By solving the above quadratic equation and substituting for θ into equation 2.14 becomes:

$$Q = \frac{\Delta Hn[M_t]V}{2}\left[1 + \frac{[X_t]}{n[M_t]} + \frac{1}{K_bn[M_t]} - \sqrt{\left(1 + \frac{X_t}{n[M_t]} + \frac{1}{K_bn[M_t]}\right)^2 - \frac{4[X_t]}{n[M_t]}}\right] \quad 2.15$$

A value is calculated for Q by an initial estimation of the independent parameters ΔH, K_b, and n, and compared to the experimental data. The estimates of the parameters are then adjusted and the procedure repeated to fit the experimental data to the theoretical model.[10] The parameters that give the best fit to the data are obtained by doing a non-linear least squares fit of the data to this model using the Origin software, which uses the Marquardt non-linear least squares algorithim.

However, due to the complexity of the one-set-of-sites binding model there can be significant error associated with the thermodynamic values determined by the model. This is most likely due to the individual errors associated with the guesses made by Origin on the values of n, K_b, and ΔH. Therefore, an average of the percent error associated with the thermodynamic values resulting from the fitting of the ITC data in this research has been calculated. The percent error for n, K_b, and ΔH are 1.3%, 10%, and 1.5%, respectively. Origin does not calculate error for the value of ΔS.

2.4.3 Isothermal Titration Calorimetry Method

Peptide, peptoid, or hybrid solutions were prepared with concentrations in the 0.1 mM to 0.5 mM range. The concentration of heparin titrant solutions ranged anywhere from 0.125 mM to 1.5 mM. The ratio of heparin to analyte at the end of each ITC titration was such that the number of binding sites on heparin was at least 2X in excess of the peptide, peptoid, or hybrid. All samples were prepared in a 50 mM sodium phosphate buffer at pH 7.4. Since the amount of peptide, peptoid, or hybrid was in short

supply relative to the amount of heparin, they were placed in the sample cell of the ITC instrument and heparin was loaded into the syringe as the titrant.

Before experiments were performed, the reference solution, sample solution, and heparin solutions were placed in 4 ml plastic vials, and degassed for 30 min in the Microcal Thermovac which comes with the instrument. The temperature of the solutions was brought to several degress below that of the experimental parameters to decrease the time necessary for the solutions to reach the experimental temperature of 25 ^{o}C once in the ITC. The parameters of the ITC experiments varied, such as injection volume, spacing between injections, and total number of injections, according to the strength of binding and concentrations used. All experiments were conducted with a cell temperature of 25 ^{o}C, the number of injections ranged from between 15 and 30 with an injection volume of anywhere from 4-10 µl. The spacing between injections was 360 sec. and stirring speed was 310 revolutions/min. All parameters were input into the VPViewer2000 which is the software that controls the VP-ITC instrument.

The sample and reference solutions were loaded into their respective cells with the 2.5 ml glass loading syringe that came with the instrument. At least 2.5 ml of sample and reference were degassed to make sure that when the cells are filled the syringe still has enough solution so as to prevent air bubbles from being introduced into the cells (each cell has a volume of about 1.8 ml). Bubbles that may have resided on the upper part of the cells during loading were removed by abruptly spurting about 0.25 ml of solution, quickly in and out of the cells with the glass syringe. After removing any air

bubbles, each cell was overflowed with solution and the syringe was place on the inner edge of the opening of the cell and any excess solution was removed to make sure each cell had the same amount in it before running the experiment, as the data is sensitive to the actual volume of sample and concentration input.

Heparin solution was loaded into the auto-pipette by placing the heparin solution, in a plastic vial, over the pipette tip, while still held in the pipette stand, and using the plastic loading syringe, attached to the fill port of the pipette, to suck up heparin solution from the plastic vial. After the injection syringe was filled, it was subsequently purged 3X to make sure no air bubbles remained.

Between experiments with the various peptides, peptoids, and hybrids, the sample cell was cleaned using at least 50 ml of Millipore water injected into the cell using the 2.5 ml glass filling syringe and then extracted, while utilizing the same reference solution. Between sets of experiments the sample and reference cells were thoroughly cleaned using the filling and extraction needles with at least 2 ml of 5% Contrad 70 solution with agitation and let to sit for at least one hour. Then the cells were rinsed with at least 100 ml of Millipore water, and rinsed with about 2 ml of buffer if another experiment were to take place. The syringe of the auto-pipette was cleaned by a vacuum setup with first about 50 ml of 5% Contrad 70, then 50 ml of Millipore water, and then 50 ml of methanol. The pipette was then dried by vacuum for at least 15 min. after the cleaning to ensure no water was left in the syringe.

2.5 Circular Dichroism

2.5.1 Circular Dichroism Materials

Sodium monobasic phosphate, monohydrate, GR ACS was purchased from EMD Chemicals. Heparin sodium salt from porcine intestinal mucosa (average molecular weight of 12,000 Da, 180 USP units/mg) was purchased from Sigma. 1 mm quartz crystal QX cuvettes were purchased from Fisher Scientific. All CD experiments were performed on a Jasco J-815 spectrometer.

2.5.2 Circular Dichroism Overview

Circular dichroism is a spectroscopic method that can aid in the determination of protein or peptide secondary structure.[18, 19] Chiral molecules will absorb circularly polarized light differently depending on their enantiomeric orientations. Solutions containing different enantiomers will also have different refractive indices for circularly polarized light and thus will exhibit circular dichroism.

Plane polarized light is made up of two electric field components rotating in opposing directions when observed from its direction of travel.[19] A chiral molecule will absorb one of these components to a different extent than the other. If plane polarized light is directed at a 45^{o} angle, it will be made up of two electric field vectors oscillating in a horizontal and vertical direction relative to the plane polarized light. These two electric field vectors will result in circularly polarized light rotating either left or right depending on a 90^{o} shift in their phase. In practice, plane polarized light is directed through a photo-elastic modulator which is birefringent to the horizontal and vertical

components of the incident plane polarized light. By alternately shifting the phase of the vertical and horizontal components by 90^{o}, at about 50 kHz, the sample will be exposed alternately to left-handed and right-handed plane polarized light. [20]

The peptide bond is the primary chromaphore in peptides, peptoids, and hybrids which absorbs circularly polarized light and gives secondary-structure information.[21] The peptide bond absorbs over the range of 180 – 240 nm. Secondary structure of the peptide or peptoid, such as α-helices, polyproline-type helices, or β-sheets, can be discerned by characteristic CD absorption spectra.[22] The electronic transitions responsible for the characteristic absorption spectra are the n→π* and π→π* transitions of the lone pair electrons and π electrons of the carbonyl group and nitrogen atom of the peptide bond. Although the instrument measures differences in absorption, the absorption spectrum is plotted as molecular ellipticity θ_{me}(which is a measure of the ellipticity formed by an electric field vector resulting from the differences in absorbance of left and right-handed circularly polarized light) versus wavelength. The units of molecular ellipticity are degrees cm^2/dmol, and can be derived from differences in absorption as follows:[18]

The tangent of the minor and major axes of the ellipse that is theoretically traced due to the difference in absorption of left and right circularly polarized light is

$$\tan\theta = \frac{minor\ axis}{major\ axis} \qquad 2.16$$

and if θ is in radians

$$tan\theta \approx \theta_r \quad 2.17$$

In terms of the difference in the absorption of left and right circularly polarized light, A_l and A_r, respectively

$$\theta_r = \frac{2.303}{4}(A_l - A_r)[rad] \quad 2.18$$

Converting to degrees gives

$$\theta_d = \frac{2.303}{4}(A_l - A_r)\frac{180}{\pi}[deg] \quad 2.19$$

Equ. 2.19 is then normalized by concentration (g/cm^3), molar mass (g/dmol), and path length of the sample cell (cm) to get molecular ellipticity (θ_{me})

$$\theta_{me} = \frac{\theta_d M}{Cl} = \frac{\deg g}{dmol} \cdot \frac{cm^3}{g} \cdot \frac{1}{cm} = \frac{deg \cdot cm^2}{dmol} \quad 2.20$$

2.5.3 Circular Dichroism Method

2-3 ml of 200 µM solutions of peptides, peptoids, or hybrids (analyte) were prepared in a 10 mM sodium phosphate, pH 7.4 buffer. A stock solution of 200 µM heparin was prepared in the same buffer (all buffers were prepared with Millipore water). From the stock solution of analyte and heparin, six solutions were prepared. Each of the six vials contained 200 µL of analyte and varying volumes of the heparin stock solution. The final volume of each solution was brought to 400 µL by adding buffer to give six different solutions of 0, 2, 5, 10, 20, and 50 µM of heparin and a final concentration of 100 µM of analyte. The idea was to observe any changes in secondary structure of the peptide, peptoid, or hybrid in the absence and presence of heparin. A

300 µl volume of the heparin-analyte solution was placed in the 1 mm cuvette and its CD spectrum was acquired. The CD parameters were: sensitivity, 100 mdeg; start λ, 240 nm; end λ, 190 nm; data pitch, 1 nm; scan mode, continuous; scan speed, 100 nm/min; response, 1 sec; accumulations, 3. The spectrometer was purged with N_2 at 20 psi for 5 minutes before, and throughout the analysis.

2.6 Heparin Affinity Chromatography

2.6.1 Heparin Affinity Chromatography Materials

Sodium monobasic phosphate, monohydrate, GR ACS was purchased from EMD Chemicals. Sodium chloride, certified ACS, was purchased from Fisher Scientific. HiTrap heparin HP affinity colums (1 ml volume) were purchased from GE Healthcare Bio-Sciences. Porcine heparin linked to a matrix of 6% cross-linked agarose was the stationary phase in the Hi-Trap heparin affinity columns. The average particle size of the stationary phase was 34 µm. All heparin affinity chromatography experiments were performed on a Dionex 500 HPLC system utilizing polyether ether ketone (PEEK) tubing and ceramic pump heads (to resist corrosion due to salt in the mobile phase), and PeakNet software.

2.6.2 Heparin Affinity Chromatography Overview

Heparin affinity chromatography is a separation technique based on the differing binding affinities of biological compounds for heparin such as plasma proteins,[23] and

growth factors.[24, 25] It can also be used as a cation exchange separation technique to separate compounds that exhibit nonspecific binding, due to heparin's anionic sulfate groups.[26, 27] An aqueous mobile phase, usually consisting of NaCl, is used to elute the analyte through the column.

2.6.3 Heparin Affinity Chromatography Method

Two mobile phases were prepared, mobile phase 'A' and mobile phase 'B'. Both mobile phases were made with Millipore water and buffered to pH 7.4 with 50 mM sodium phosphate. Mobile phase 'B' also contained 1 M NaCl. The two mobile phases were then filtered using vacuum filtration with a 0.45 µm filter. About 20 µl of sample was injected onto the column. After injection a linear gradient elution was initiated by a GP40 gradient pump system starting with 100% mobile phase 'A' and increasing mobile phase 'B' one percent/min until the sample was eluted, with a flow rate of 0.65 ml/min. As heparin is a polyelectrolyte, the Na^+ ions essentially compete with the ligands for the heparin stationary phase. Therefore, the gradient increases the NaCl concentration to elute compounds sequentially which bind heparin with increasing affinity. The analyte was detected by an AD20 absorbance detector set at 215 nm. For each sample, three injections were made, and the average retention times were used as results.

2.7 High Performance Liquid Chromatography

2.7.1 High Performance Liquid Chromatography Materials

Acetonitrile HPLC grade was purchased from Fisher Scientific. Trifluoroacetic acid (TFA) was purchased from Impex International Inc. Purification of peptides, peptoid, and hybrids was performed on a Varian ProStar 210 HPLC system manufactured by Varian Analytical Instruments. The Varian HPLC system was equipped with a SunFire preparative C18 19 X 250 mm column, with Optimum Bed Density design, manufactured by Waters Corp. The column was packed with a silica based C18 stationary phase with a particle size of 5 µm.

2.7.2 High Performance Liquid Chromatography Overview

All peptides, peptoids, and hybrids were separated using the reversed-phase separation mode (RP-HPLC). In RP-HPLC, the stationary phase is very non-polar and the mobile phase is a relatively polar aqueous solution infused with an organic solvent such as acetonitrile.[28] The most common stationary phase in use is octadecylsilane (C18) covalently bound to the silanol groups of a silica base. This mode of separation is practical for the separation of biological compounds as this technique is capable of separating analytes with a wide range of polarity.[29] The ability to resolve biological compounds with varying degrees of hydrophobicity makes RP-HPLC the dominant mode for the purification of target peptides after peptide synthesis, not only from synthetic

peptide impurities but also from crude synthesis solutions containing small organic molecules.[30]

RP-HPLC usually employs a gradient elution in which two mobile phases are used, one consisting of water and another consisting of an organic solvent. Normally the separation starts with a gradient of a low proportion of organic solvent and then, incrementally ramps up the organic solvent proportion to elute the more hydrophobic compounds as they would more strongly interact with the relatively more hydrophobic stationary phase. The eluting peptides are then detected using UV absorbance detection set at 215 nm as the peptide bond strongly absorbs light of this wavelength.[30]

2.7.3 High Performance Liquid Chromatography Method

All peptides, peptoids, and hybrids were purified by RP-HPLC from their crude synthesis mixtures. First, two mobile phases were prepared, mobile phase 'A' and mobile phase 'B', for gradient elution. Mobile phase 'A' consisted of Millipore water with the addition of 0.1% TFA and mobile phase 'B' consisted of HPLC grade acetonitrile also with 0.1% TFA (2.7 ml of TFA per 4 L bottle). Prior to use the mobile phases were degassed with N_2 for at least 5 min. Most analytes eluted within 30 min. using a gradient that started with 0% mobile phase 'B' and increased in proportion by 2%/min. with a flow rate of 10 ml/min. Equilibration time was 15 min. Each of the major peaks from the crude synthesis mixture were collected and submitted to MALDI-TOF mass spectrometry to identify the peak corresponding to the target; detection of analyte was by UV

absorbance set at 215 nm wavelength. Thereafter, the peak corresponding to the target analyte was collected, and after purification was frozen with liquid N_2 for lyophilization.

2.7.4 Lyophilization

Before lyophilization, samples were rotavaporized using a Buchi 461 Rotavapor manufactured by Brinkmann Instruments Inc. to reduce sample volumes to about 20 ml. Samples were placed either in glass vials or plastic centrifuge tubes, and frozen with liquid N_2 for about 30 min. After freezing, the sample containers were placed in a glass drying flask and freeze dried in a Virtis Sentry Benchtop 3L lyophilizer manufactured by The Virtis Co. Inc. The lyophilizer was set to a temperature of -52 ^{o}C and a pressure of about 1200 mTorr. Samples were usually completely freeze dried overnight to a white crystalline or powder form that was used in heparin binding studies.

2.8 Matrix Assisted Laser Desorption Ionization Time-of-Flight Mass Spectrometry (MALDI-TOF-MS)

2.8.1 MALDI-TOF-MS Materials

HPLC grade methanol and HPLC grade acetonitrile were purchased from Fisher Scientific. Trifluoracetic acid (TFA) was obtained from Impex International Inc. α-Cyano-4-hydroxycinnamic acid (CHCA) was acquired from Aldrich. All MALDI-TOF-MS spectra were measured on a Voyager-DE STR Biospectrometry MALDI-TOF-MS Workstation, using the WinNT Data system, manufactured by PerSeptive Biosystems.

2.8.2 MALDI-TOF-MS Overview

The technique of MALDI-TOF-MS is useful for the identification of biomolecules as it is a soft ionization method, therefore, biomolecules are not significantly degraded during the ionization process.[31] Due to the soft ionization process, most ions are the singly-charged parent ions, which can be easily and directly identified in the mass spectrum.

The sample is embedded in a matrix of a small organic compound which crystallizes after being placed on a sample stage. A laser is then pulsed onto the sample/matrix. Energy is absorbed from the laser by the matrix which helps prevent the fragmentation of the analyte,[32] and facilitates desorption and ionization of the analyte, which is decomposed into a cloud of particles and ions.[33] Ions are then extracted and accelerated from the cloud by an electric field, and sent down a field-free flight path to the detector. The mass-to-charge ratios of the molecular ions are calculated from how long it takes them to reach the detector (time-of-flight) after the extraction with a fixed kinetic energy, with larger ions taking longer to reach the detector than smaller ones.

2.8.3 MALDI-TOF-MS Method

To determine the molecular weight of the peptides, peptoids, and hybrids, MALDI matrix was prepared by adding CHCA to a microvial and enough solution of 50% methanol, 50% acetonitrile, with approximately 0.1% TFA to create a saturated solution of CHCA. The solution was vortexed and then centrifuged. 1.5 µL of crude or purified compound (in cleavage solution or HPLC solvent, respectively) of interest was added to a separate microvial, and to the same microvial was added 9 µl of the saturated CHCA solution. The microvial was subsequently vortexed and centrifuged. 1.5 µl of the CHCA/compound solution was then placed on a stainless

steel sample stage and the solution was allowed to evaporate leaving behind the cocrystalline mixture of CHCA and sample. The sample stage was then placed in the MALDI-TOF-MS workstation for analysis.

2.9 References

1. Merrifield, R. B., *J. Am. Chem. Soc.* **1963,** *85*, 2149-2154.

2. Barany, G.; Kneib-Cordonier, N.; Mullen, D. G., *Int. J. Pept. Protein Res.* **1987,** *30*, 705-739.

3. Merrifield, R. B., *Methods Enzymol.* **1997,** *289*, 3-13.

4. Howl, J., *Peptide Synthesis and Applications*. Humana Press: Totowa, 2005.

5. Fields, G. B.; Noble, R. L., *Int. J. Pept. Protein Res.* **1990,** *35*, 161-214.

6. Zuckermann, R. N.; Kerr, J. M.; Kent, S. B. H.; Moos, W. H., *J. Am. Chem. Soc.* **1992,** *114*, 10646-10647.

7. Ladbury, J. E.; Chowdhry, B. Z., *Biocalorimetry: Applications of Calorimetry in the Biological Sciences*. John Wiley & Sons: New York, 1998.

8. Liang, Y., *J. Iran. Chem. Soc.* **2006,** *3*, 209-219.

9. Okhrimenko, O.; Jelesarov, I., *J. Mol. Recognit.* **2008,** *21*, 1-19.

10. Ladbury, J. E.; Chowdhry, B. Z., *Chem. Biol.* **1996,** *3*, 791-801.

11. Campoy, A. V.; Freire, E., *Nat. Protoc.* **2006,** *1*, 186-191.

12. Tellinghuisen, J., *Anal. Biochem.* **2008,** *373*, 395-397.

13. Buurma, N. J.; Haq, I., *Methods Enzymol.* **2007,** *42*, 162-172.

14. Wiseman, T.; Williston, S.; Brandts, J. F.; Lin, L., *Anal. Biochem.* **1989,** *179*, 131-137.

15. Campoy, A. V.; Freire, E., *Biophys. Chem.* **2005,** *115*, 115-124.

16. Wang, J. Characterization of the Interaction of HIP Analog Peptides by Heparin. Ph.D. Dissertation, University of California, Riverside, 2005.

17. Freire, E.; Mayorga, O. L.; Straume, M., *Anal. Chem.* **1990,** *62*, 950A-959A.

18. Greenfield, N. J., *Nat. Protoc.* **2006,** *1*, 2876-2890.

19. Woody, R. W., *Methods Enzymol.* **1995,** *246*, 34-37.

20. Kelly, S. M.; Jess, T. J.; Price, N. C., *Biochim. Biophys. Acta* **2005,** *1751*, 119-139.

21. Berova, N.; Koji, N.; Woody, R. W., *Circular Dichroism: Principles and Applications*. Wiley-VCH: New York, 2000.

22. Rodger, A.; Norden, B., *Circular Dichroism and Linear Dichroism*. Oxford University Press: Oxford, 1997.

23. Josic, D.; Bal, F.; Schwinn, H., *J. Chrom.* **1993,** *632*, 1-10.

24. Lobb, R. R.; Fett, J. W., *Biochemistry* **1984,** *23*, 6295-6299.

25. Klagsbrun, M.; Sullivan, R.; Smith, S.; Rybka, R.; Shing, Y., *Methods Enzymol.* **1987,** *147*, 95-105.

26. Wang, J.; Rabenstein, D. L., *Biochemistry* **2006,** *45*, 15740-15747.

27. Hari, S. P.; McAllister, H.; Chuang, W.-L.; Christ, M. D.; Rabenstein, D. L., *Biochemistry* **2000,** *39*, 3763-3773.

28. Meyer, R. V., *Practical High-Performance Liquid Chromatography*. 4th ed.; Wiley: Chichester, 2004.

29. Lough, W. J.; Wainer, I. W., *High Performance Liquid Chromatography: Fundamental Principles and Practice*. Blackie Academic & Professional: London, 1996.

30. Mant, C. T.; Hodges, R. S., *High-Performance Liquid Chromatography of Peptides and Proteins: Separation, Analysis, and Conformation*. CRC Press: Boca Raton, 1991.

31. Jurinke, C.; Oeth, P.; van den Boom, D., *Mol. Biotech.* **2004,** *26*, 147-163.

32. Pan, C.; Xu, S.; Zhou, H.; Fu, Y.; Ye, M.; Zou, H., *Anal. Bioanal. Chem.* **2007,** *387*, 193-204.

33. Bonk, T.; Humeny, A., *The Neuroscientist* **2001,** *7*, 6-12.

Chapter 3

Heparin-Binding Peptides

3.1 Introduction

3.1.1 Peptide/Heparin Binding

Peptide/heparin binding is mediated, in large part, by electrostatic interactions between cationic groups of the peptide and anionic groups of heparin.[1] As heparin is a polyelectrolyte, due to its high negative charge density, a fraction of its negative charge is neutralized by bound counterions, such as Na^+.[2] The counter ions are bound to the polyelectrolyte in two ways: site-specifically bound, in which the counterion is directly associated with a specific anionic site on the polyelectrolyte; and territorially bound, in which the counterions are associated with the polyelectrolyte by its strong polyanion field and are considered to be delocalized. Rabenstein et al. determined that for beef lung heparin the fraction of charge neutralized by Na^+ is 0.59 or 2.12 sodium ions per heparin disaccharide unit. Therefore, it can be expected that the ionic contacts made between the cationic sites of a peptide and heparin would displace a number of counter ions associated with heparin.[3] It has been shown experimentally that 1.78 Na^+ ions are displaced when the H_2A^{2+} form of histamine binds to beef lung heparin. Therefore, release of counterions from peptide/heparin interactions results in a favorable entropic contribution to the free energy of binding, as shown in Equ. 3.1.[1]

$$\text{Peptide} + \text{Heparin}(Na^+)_x \leftrightarrow \text{Peptide-Heparin}(Na^+)_{x-n} + nNa^+ \qquad 3.1$$

The dependence of the strength of peptide/heparin binding on the concentration of Na^+ ions also exemplifies the electrostatic nature of the binding interactions.[1, 3] Equation 3.2 shows the dependence of the binding affinity on the concentration of Na^+ ions:

$$\log K_b = \log K_{nonionic} - Z\psi[Na^+] \qquad 3.2$$

where Zrepresents the number of ionic interactions made between peptide and heparin, ψ represents both the fraction of anionic charge on heparin neutralized by a Na^+ ion, θ, and the screening effect of condensed Na^+ ions on residual anionic charges on heparin. K_b is the measured binding constant and $K_{nonionic}$ is the contribution of nonionic interactions to the binding constant. Equation 3.2 shows that as the concentration of Na^+ increases, the measured binding constant decreases.

Although hundreds of proteins have been found that bind to heparin via non-specific electrostatic interactions,[4] researchers have elucidated patterns in amino acid sequences which may indicate specific heparin-binding regions on proteins. For example, Cardin and Weintraub found that various heparin-binding proteins such as apolipoprotein B-100, apolipoprotein E, vitronectin, and platelet factor 4, contain heparin binding regions of similar amino acid motifs.[5] Each of these binding regions contains stretches of basic residues that electrostatically interact with the anionic groups of heparin. By comparing forty-nine similar regions of 21 other heparin-binding proteins, they found, using matrix analyses, the frequency of occurrence of certain types of residues in particular positions of that region. For example, they found that the

heparin-binding proteins fibronectin, thrombospondin, and endothelial growth factor, contain a distribution pattern of X-B-B-X-B-X, where B represents a high occurrence of a basic residue, such as lysine or arginine, and in position X, a high probability of a hydropathic residue. Other heparin-binding proteins such as γ-interferon, protein C inhibitor, and β-thromboglobulin contain a region with a distribution pattern of X-B-B-B-X-X-B-X where B and X represents a basic and hydropathic residue, respectively.

Although, during the study, these regions have not been experimentally shown to bind heparin, they could indicate a potential heparin-binding region. Further confirmation of this potentiality was demonstrated in subsequent studies. It was shown by circular dichroism, that the heparin-binding region of apolipoprotein E, upon binding with heparin, increased α-helical content by greater than 50%.[6] The heparin-binding region contains the consensus sequence X-B-B-B-X-X-B-X, which by a helical wheel diagram, shows that the basic charges are distributed primarily on one side of the helix, conferring amphipathicity to the helix.[5] By using predictive algorithms, similar regions of other proteins were determined to have strong amphipathic character. This amphipathic nature of the helix permits it to bind more effectively to the anionic portions of heparin. So for heparin-binding regions that are α-helical, the binding motif of X-B-B-B-X-X-B-X may be a nucleation point in protein/heparin binding.

By using affinity coelectrophoresis, Verrecchio et al. demonstrated the binding capacity of sets of peptides based on the X-B-B-X-B-X and X-B-B-B-X-X-B-X motifs. The peptides were designed as such: $(AKKARA)_n$ and $(ARKKAAKA)_n$ where n was 1-6 and 1-5

respectively.[7] No affinity could be detected for either set where n = 1, however as n increased, so did binding affinity. When the 6-mer and the 8-mer repeats reached about 30 amino acids, the affinity leveled off with a maximum binding of $K_b = 1.1X10^7\ M^{-1}$ and $K_b = 2.5X10^7\ M^{-1}$ respectively. Each peptide displayed random coil character in circular dichroism studies. Upon titration with heparin, the stronger binding peptides converted into α-helices giving them amphipathic character, whereas the weaker binding peptides, did not change conformation upon titration with heparin. These results show that peptides consisting of the consensus sequences of Cardin and Wientraub have the capacity for high binding affinity to heparin, and that upon binding change conformation to an α-helix which provides a face of high charge density for binding to the anionic portions of heparin.

In another study, Margalit, et al.[8] used binding sites that have already been shown to bind heparin to determine any structural similarity between them. They first observed already established structures in a 3-D graphics technique to distinguish the distribution of basic residues. The final data set included 18 sequences from which secondary structure was already established, or modeled after an α-helix or β-strand. Some of the sequences were taken from protein C inhibitor, apolipoprotein E, and platelet factor 4. The 3-D structures for each sequence, whether α-helix or β-strand, were superimposed and compared for distribution of basic residues. In each sequence, about a 20 Å distance was found between two basic residues located on opposite sides of the structure. They hypothesized that because the two basic residues were on

opposite sides of the sequence, that heparin may wrap around the peptide backbone making a coiled coil type structure, causing a conformational change in the protein. The results above, and those of Cardin and Weintraub may be of use in designing sequences for heparin-binding peptides.

In this research, we have designed a number of peptides all based on the X-B-B-B-X-X-B-X motif where B is either a lysine, arginine, or histidine residue. Representing residue X are alanine, luecine, valine, and glycine, Table 3.1. The residues chosed for X are known helix formers, as discussed in Section 1.4.6, except valine.[9] This pattern is expected to promote peptide-heparin binding by facilitating the formation of an amphipathic helix. Heparin-binding interactions of these peptides are also characterized. Fig. 3.1 shows structural formulas of CPK4, CPR4, and CPH4.

Peptide Name	Peptide Sequence
CPK3	**Ac-G-A-K-K-K-L-A-NH_2**
CPR3	**Ac-G-A-R-R-R-L-A-NH_2**
CPK4	**Ac-G-A-K-K-K-L-A-K-V-NH_2**
CPR4	**Ac-G-A-R-R-R-L-A-R-V-NH_2**
CPH4	**Ac-G-A-H-H-H-L-A-H-V-NH_2**
CPK7	**Ac-G-A-K-K-K-L-A-K-V-A-K-K-K-L-NH_2**
CPR7	**Ac-G-A-R-R-R-L-A-R-V-A-R-R-R-L-NH_2**

Table 3.1. Left hand column shows the peptide name: consensus peptide (CP) and number of basic amino acid residues. For example CPK3 is consensus peptide containing three lysine residues. The right hand column shows the sequence of the peptide.

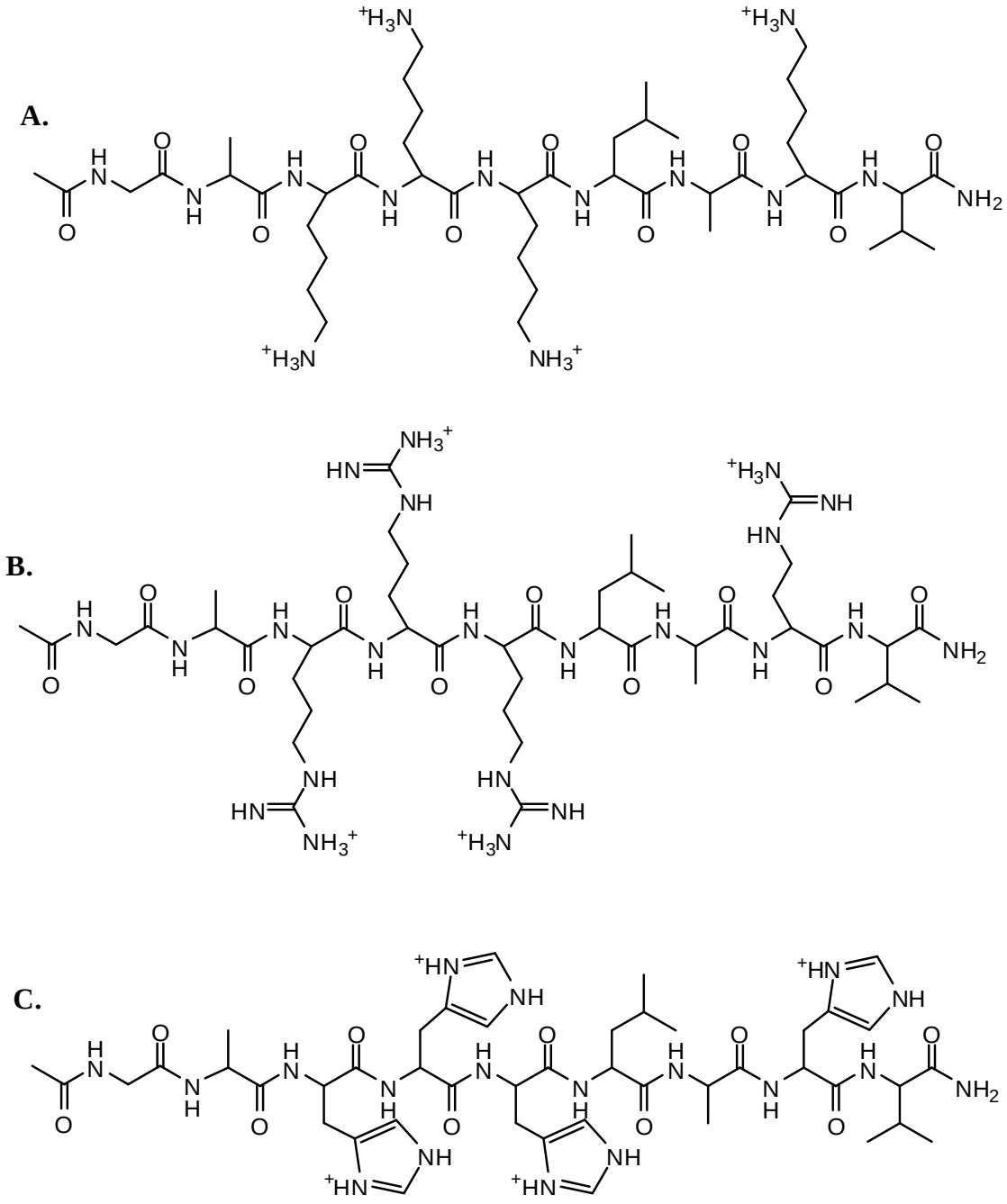

Fig. 3.1. Structural formulas representative of consensus peptides showing **A.** CPK4, the lysine-containing peptide, **B.** CPR4, the argining-containing peptide, and **C.** CPH4, the histidine-containing peptide. The lysine side chains of **A**, the arginine side chains of **B**, and the histidine side chains of **C**, are shown in the heparin-binding protonated form.

3.1.2 Secondary Structure of Peptides.

Peptides, especially those containing less than or equal to 13 residues, have difficulty forming stable secondary structures such as an α-helix, except under specific conditions and when meeting certain design criteria.[10-12] However, studies done on peptides which were thought to lack secondary structure have shown that these peptides are not entirely devoid of stable local conformation.[13, 14]

The structure of homopolymers of lysine, glutamic acid, and alanine, as determined by molecular modeling calculations and experimental evidence, is characterized as a left-handed helix similar to that of a polyproline II helix with about 3 residues per turn.[13, 15-18] The circular dichroism (CD) spectra of these structures show a positive peak at about 220 nm and a negative peak at about 200 nm. The disappearance of the 220 nm band correlates to a transition to an unordered state. [17] Stabilization of the left-handed helix may occur through the repulsion of side chain charges which force the peptide to orient itself in a way to minimize potential energy. This factor applies to long homo-lysine and glutamic acid polymers which form α-helices upon charge neutralization at high pH or by high salt concentrations.[17]

Short poly-lysine peptides consisting of seven lysine residues, and unable to form α-helices upon charge neutralization, have also been studied.[19] The study showed that even when lysine charges are neutralized, significant poly-proline II character still exists. The conclusion was that the backbone will orientate itself to maximize favorable interactions with solvent molecules via hydrogen bonding. Thus, longer flexible side

chains such as lysine and leucine residues will maximize exposure of the backbone to solvent molecules. Kelly et al. developed a host-guest system of a poly-proline peptide in which proline residues were substituted with a variety of other amino acids to determine the propensity of certain residues to conform to a polyproline-type II helix. They found that alanine and glycine, amino acids with little or no side chains had a high propensity to adopt such a conformation.[9] They attributed this propensity, again, to maximizing accessibility of the backbone to solvation. Monte Carlo simulations were also performed on the conformation of polyalanine in water which also showed that solvation free energy of a polyproline II helix conformation is favored over other conformers.[15] The peptides studied in this research contain a large number of polyproline II-favoring residues which increases their propensity to form this type of structure.

3.2 Results

3.2.1 Binding Constants

3.2.1.1 Lysine-Containing Peptides

Binding constants for the interaction of the peptides in Table 3.1 were determined by isothermal titration calorimetry (ITC). Fig. 3.2 shows data obtained for a typical titration of a peptide in the CPK series of peptides (Table 3.1). The titration data consist of a series of positive peaks indicating an endothermic binding interaction following the addition of each aliquot of titrant. The area under each peak is plotted in

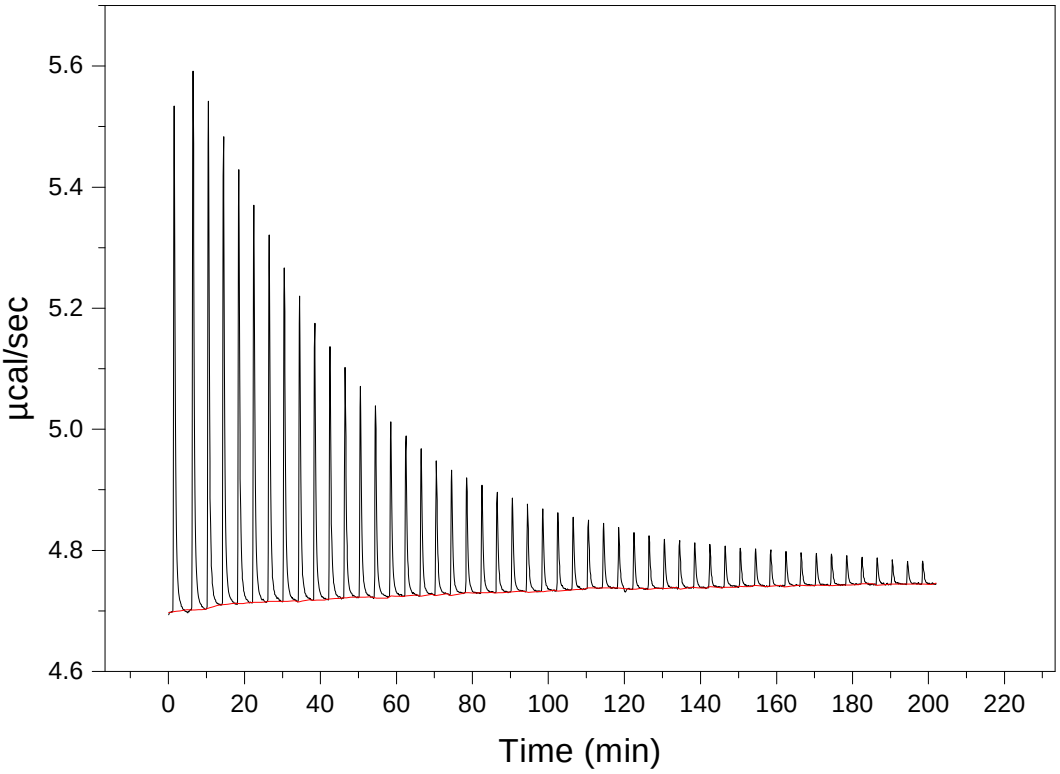

Fig. 3.2. Typical raw ITC data for the CPK series of peptides, in this case, data for heparin titrated into a solution of CPK4. Upward deflecting peaks signify an endothermic binding event. Parameters are: total injections, 50; cell temperature, 25 ^{o}C; heparin titrant concentration, 1.4 mM; CPK4 concentration, 0.5 mM; injection volume, 5 µL; injection spacing, 240 s.

Fig. 3.3. The binding constant was obtained by fitting these data to a single-set-of-binding sites model. The binding constants obtained by ITC for the CPK peptides are reported in Table 3.2. The results in Table 3.2 show that forthe lysine-containing peptides the binding affinity increases with the number of cationic lysine residues. Peptide CPK3, which contains only three lysine residues, has such a weak binding interaction that a binding constant could not be determined (ND) by ITC. As discussed in Section 2.4.2, the binding constants must be greater than 10^3 M^{-1} to be measured by the ITC method. The largest lysine-containing peptide studied in this research CPK7, which contains seven lysine residues, has the largest binding affinity with a K_b of $1.2X10^5$ M^{-1}. The calorimetric data show that, on average, 11.8 peptides of CPK4 and 9.1 peptides of CPK7 bind per heparin chain.

3.2.1.2 Arginine-Containing Peptides

Figs. 3.4 and 3.5 show typical titration data from the CPR series of peptides. Results from the ITC measurements, as reported in Table 3.3, show that the arginine-containing peptides have a higher binding affinity than the corresponding lysine-containing peptides (Table 3.2). For example, CPR3 actually had a measurable binding signal, in contrast to CPK3, in the ITC experiments which gave an average binding constant of 1800 M^{-1}. CPR7 had a much higher binding affinity for heparin with a binding constant of $6.5X10^6$ M^{-1} compared to $1.8X10^5$ M^{-1} for CPK7. The number of binding sites

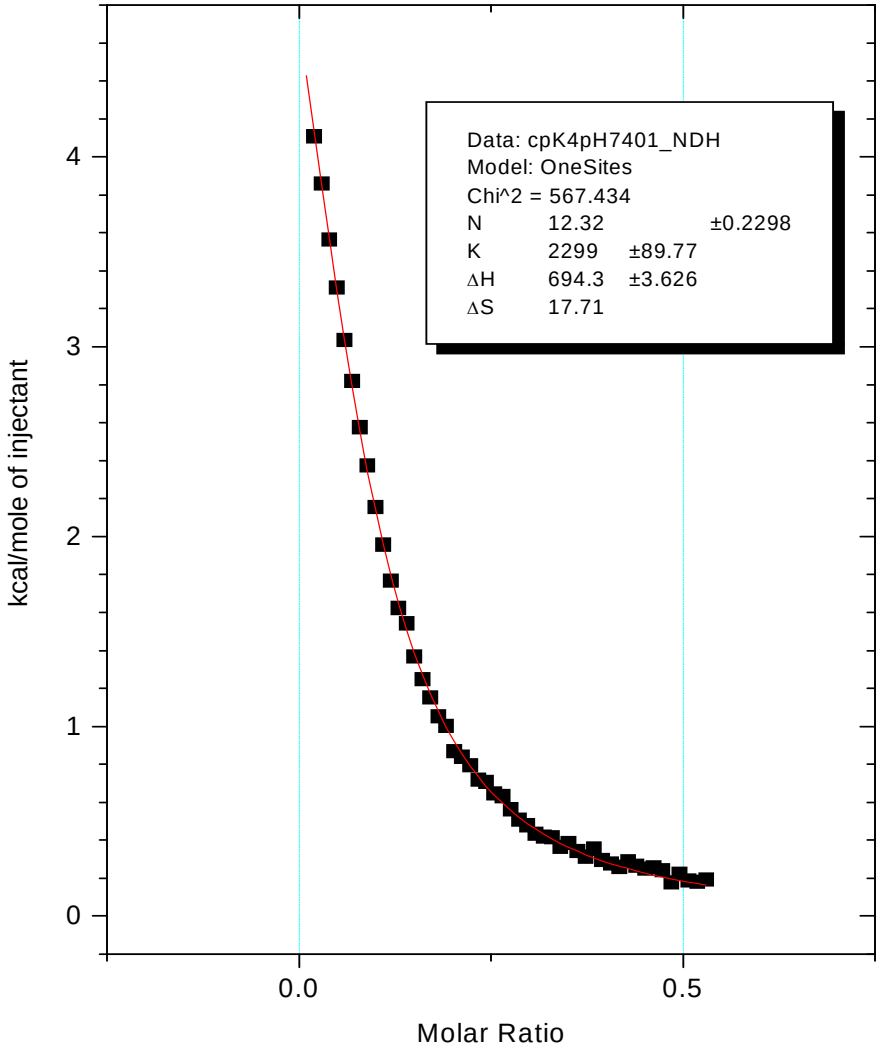

Fig. 3.3. The integrated raw data of the CPK4 titration (indicated by the solid squares), and the fit of the data to a single-set-of-identical-binding sites model. Thermodynamic values of the resulting fit are given in the figure.

Peptide	K_b (M^{-1})	N	ΔH (cal/mol)	ΔS (cal/mol·°C)
CPK3	ND	ND	ND	ND
CPK4	2490 ± 317	11.8 ± .5	689 ± 20	17.8 ± .2
CPK7	(1.2 ± .2)X10^5	9.1 ± .2	1286 ± 86	27.6 ± .06

Table 3.2. Average thermodynamic values for the CPK series of peptides as determined by ITC: K_b, binding constant; N, number of binding sites per heparin molecule; ΔH, change in enthalpy; and ΔS, change in entropy for the binding interaction. CPK7 values are the average from three replicate titrations, CPK4 is the average of two, showing associated standard deviations, and ranges, respectively.

(n) on heparin for CPR3, CPR4, and CPR7 were determined to be: 19.9, 21.2, and 7.51, respectively.

3.2.1.3 Histidine-Containing Peptides

The ITC data at pH 7.4 indicated that binding constants could not be determined for the histidine-containing peptides; the pKa of the histidine side chain imidazolium group is 6.0, indicating that only about 10% of the free histidine side chains are protonated at pH 7.4. Therefore, ITC experiments were conducted by varying the pH of the buffered solutions to 6.5, 6.0, 5.5, and 5.0 to determine the extent of heparin-binding upon protonation of the histidine side chains. Figs. 3.6 and 3.7, show a typical isothermal titration of CPH4 at pH 5.5; the thermodynamic binding parameters are presented in Table 3.4.

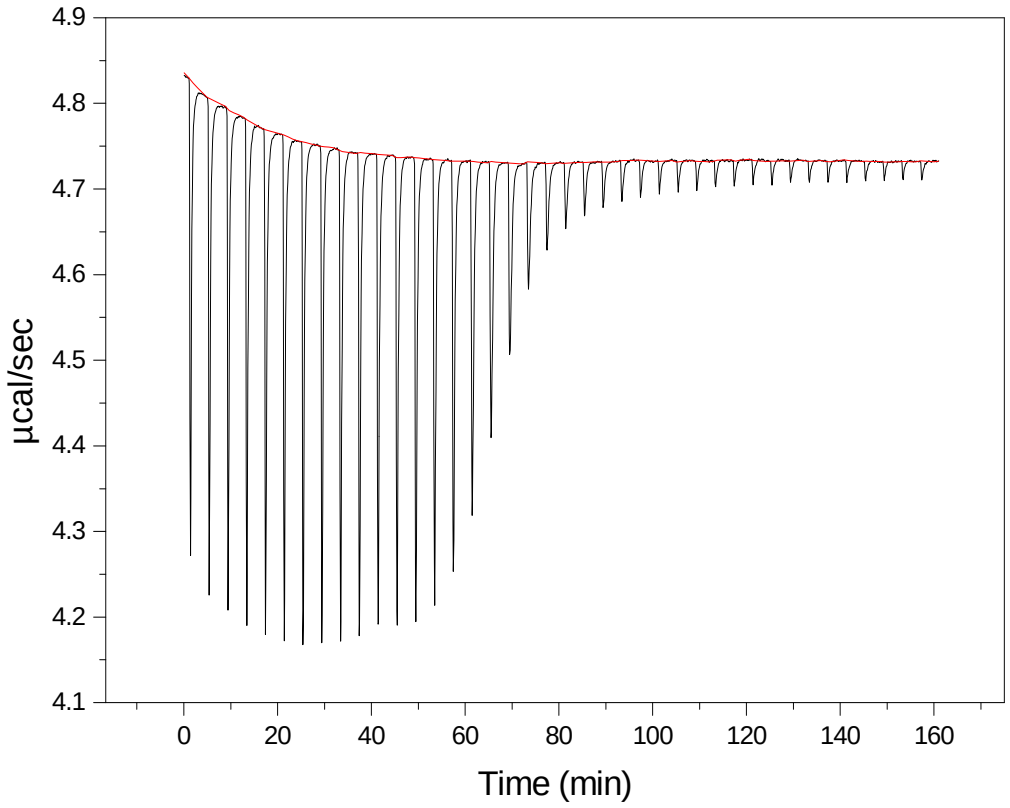

Fig. 3.4. Typical raw ITC data for the CPR series of peptides, showing CPR7 titrated into heparin. Downward deflecting peaks signify an exothermic binding event. Parameters are: total injections, 40; cell temperature, 25 ^{o}C; CPR7 titrant concentration, 0.7 mM; heparin concentration, 0.006 mM; injection volume, 2 µL; injection spacing, 240 s.

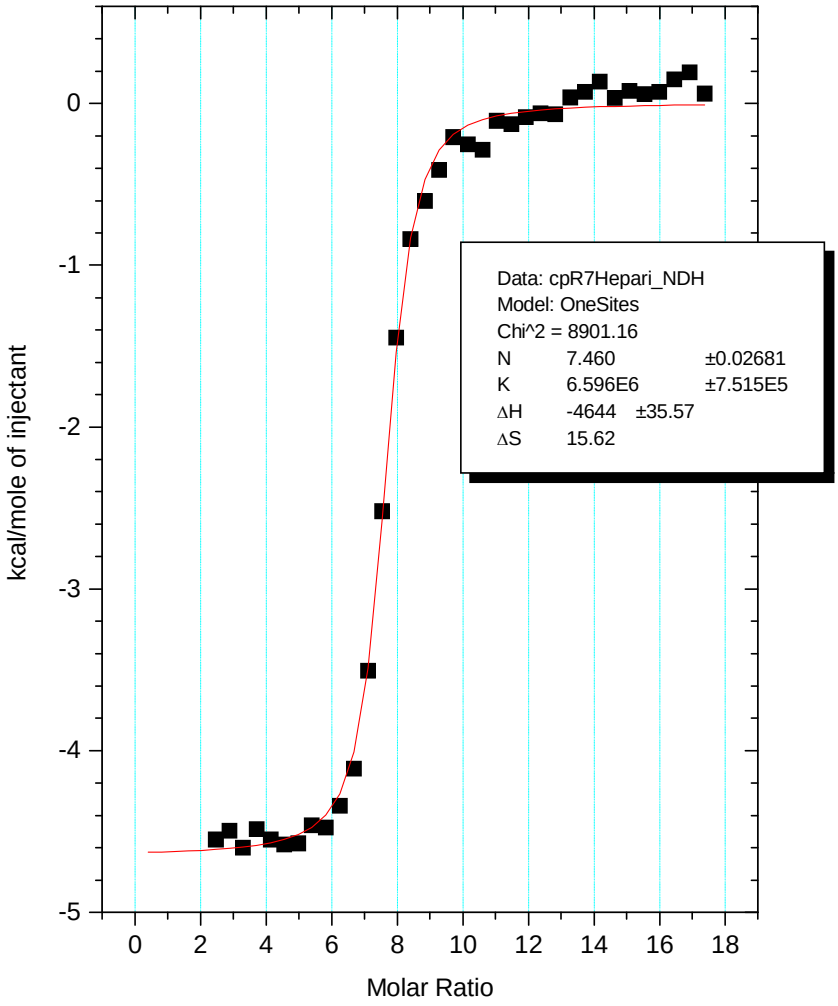

Fig. 3.5. The integrated raw data of the CPR7 titration (indicated by the solid sqares), and the fit of the data to a single-set-of-identical-binding sites model. Thermodynamic values of the resulting fit are given in the figure.

Peptide	K_b (M^{-1})	N	ΔH (cal/mol)	ΔS (cal/mol·°C)
CPR3	1800 ± 156	19.9 ± .9	-696 ± 21	12.6 ± .2
CPR4	$(2.0 \pm .2)X10^4$	21.2 ± .9	-1200 ± 52	15.6 ± .2
CPR7	$(6.5 \pm .4)X10^6$	7.51 ± .18	-4670 ± 28	15.5 ± .1

Table 3.3. Average thermodynamic values for the CPR series of peptides as determined by ITC: K_b, binding constant; N, number of binding sites per heparin molecule; ΔH, change in enthalpy; and ΔS, change in entropy for the binding interaction.

An average of the measured K_b values of 1900 M^{-1}, at pH 6.5, indicate that binding is still relatively weak. At pH 5.0, at which point the imidazole group is fully protonated, the binding constant increases to $3.7X10^4$ M^{-1}. The results also show that as the pH increases the binding interaction becomes more exothermic, from -2850 to -9900 cal/mol. Conversely, the change in entropy decreases from 11 to -18 cal/mol·°C.

3.2.2 Circular Dichroism.

CD measurements of the peptides synthesized in this research show a similar CD spectrum as that reported by Creamer et al. for a poly-lysine peptide at pH 12.0, purported to exist in a predominantly polyproline II conformation.[19] The CD spectra of CPK4 and CPR4 in Figs. 3.8 and 3.9, show a strong minimum at about 195 nm and a maximum at about 215 nm, respectively, typical of this conformation; all CPK and CPR

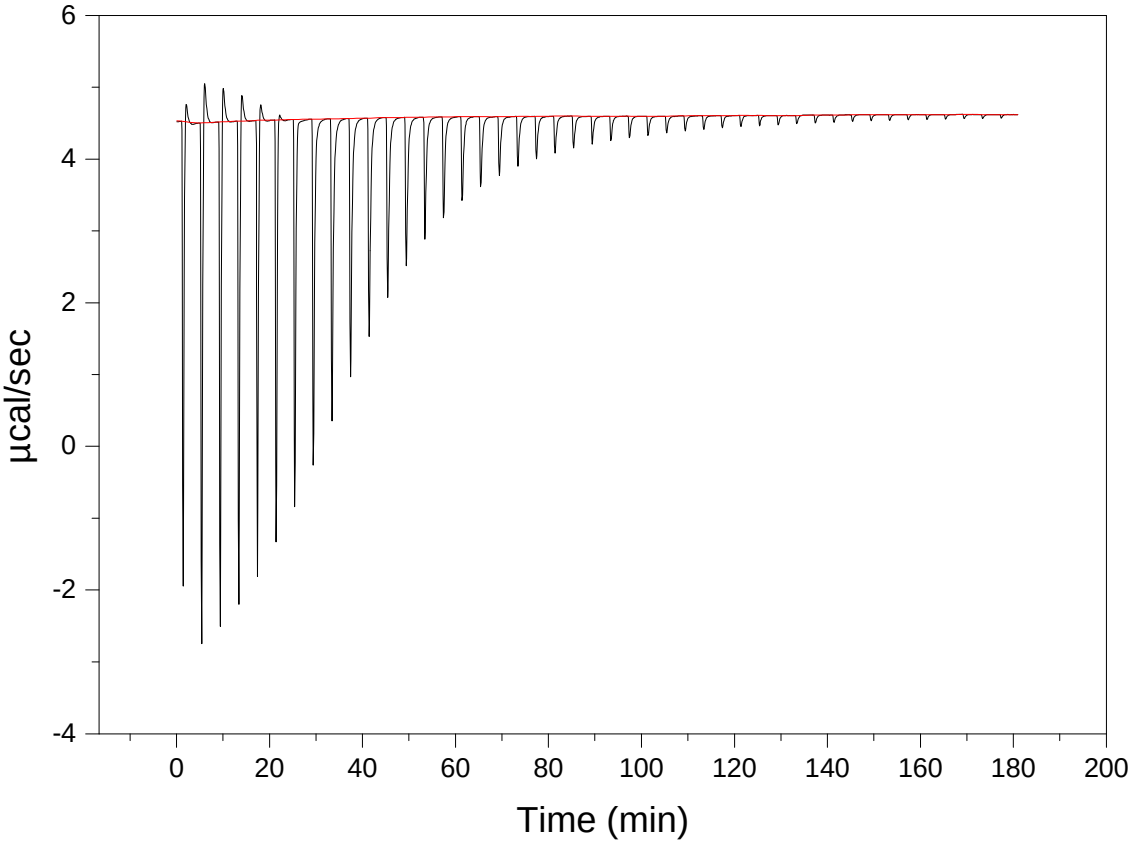

Fig. 3.6. Typical raw ITC data for CPH4, showing heparin titrated into a solution of CPH4 at pH 5.5. Downward deflecting peaks signify an exothermic binding event. Parameters are: total injections, 45; cell temperature, 25 ^{o}C; heparin titrant concentration, 1.04 mM; CPH4 concentration, 0.45 mM; injection volume, 5 µL; injection spacing, 240 s.

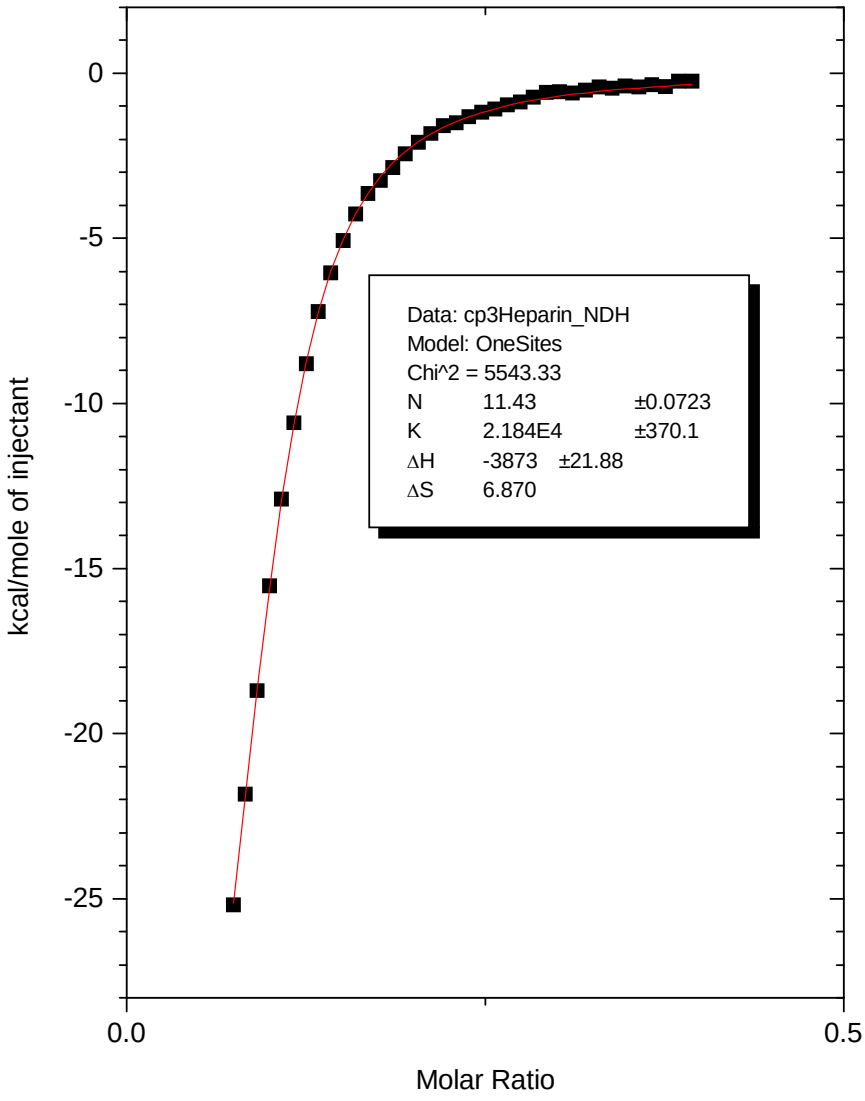

Fig. 3.7. The integrated raw data of the CPH4 titration (indicated by the solid squares), and the fit of the data to a single-set-of-identical-binding sites model. Thermodyamic values of the resulting fit are given in the figure.

pH	K_b (M^{-1})	N	ΔH (cal/mol)	ΔS (cal/mol·°C)
7.4	ND	ND	ND	ND
6.5	1900 ± 13	10.8 ± .13	-9900 ± 149	-18.2 ± 1
6.0	8800 ± 41	9.90 ± .01	-4790 ± 3	1.98 ± .02
5.5	$2.1X10^4$ ± 720	10.74 ± .69	-4040 ± 164	6.2 ± .6
5.0	$(3.6 \pm .08)X10^4$	11.3 ± .2	-2900 ± 190	11.2 ± .7

Table 3.4. Average thermodynamic values for the CPH4 peptide at varying pH, as determined by ITC: K_b, binding constant; N, number of binding sites per heparin molecule; ΔH, change in enthalpy; and ΔS, change in entropy for the binding interaction. Eact titration is the average of two trials, uncertainties are ranges.

series of peptides show this characteristic CD signature. The peptides in this research contain a large portion of residues that have a propensity to form a peptide with a polyproline II-like conformation, [9, 19-22] so it is possible that the peptides, in this work, are adopting a local repeating conformation and are not completely devoid of secondary structure.

Upon titration with heparin (0 μM to saturation) there was no enhancement or change in the CD spectra, indicating no change in secondary structure (data not shown). This was also the case with similarly designed peptides (in sequence and length) in work reported by Verrecchio et al.[7] The only change observed upon titration with heparin was a decrease in peak intensity, most likely a result of aggregation which was seen as a white, cloudy precipitate in the sample cells.

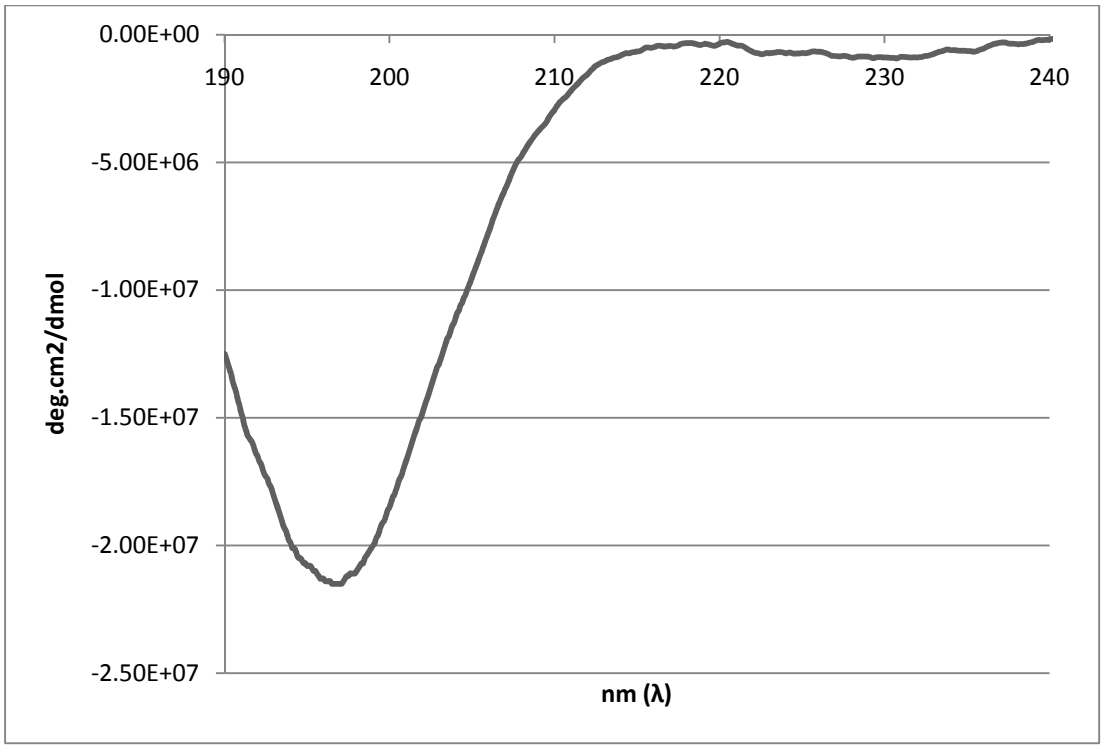

Fig. 3.8. CD spectrum of CPK4 in the absence of heparin. The minimum at about 195 nm and the maximum at 215 nm are indicative of a local polyproline-type II conformation.

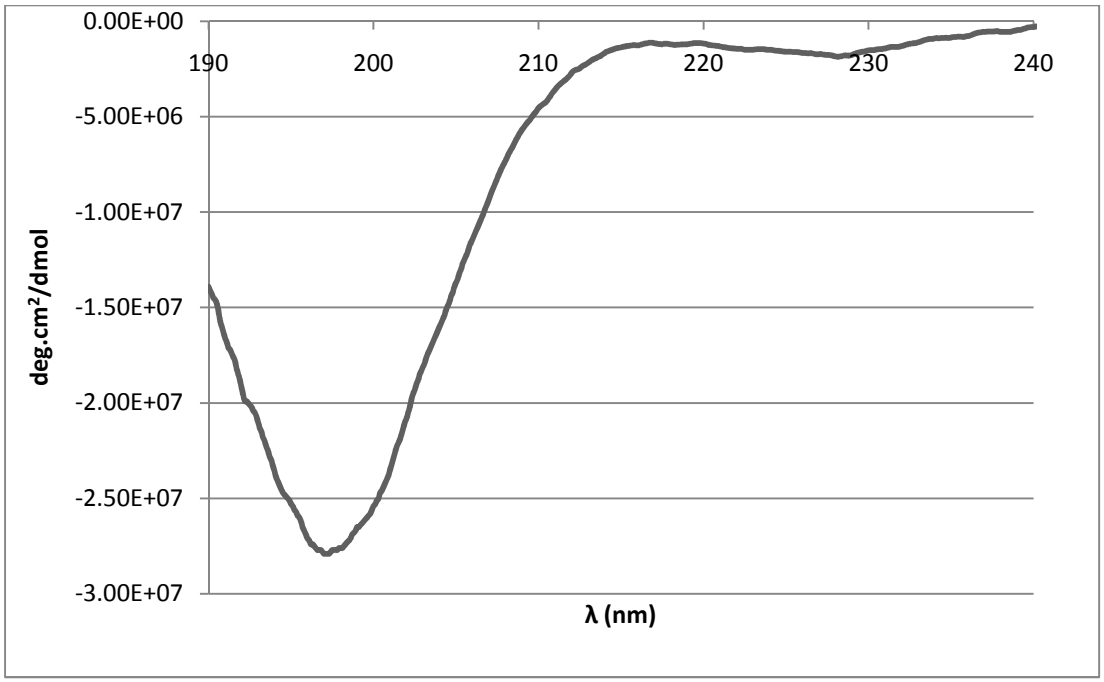

Fig. 3.9. CD spectrum of CPR4 in the absence of heparin. The minimum at about 195 nm and a maximum at 215 nm are indicative of a local polyproline-type II conformation.

The imidazolium ring of histidine makes a significant contribution to absorption in the CD range used in this work to determine secondary structure, therefore, CD studies were not performed.[23] However, it can be predicted that the CPH4 peptide will have less local ordered structure than CPK4 and CPR4 peptides since histidine has been shown to have less of a propensity to adopt a polyproline II-like conformation.[24]

3.2.3 Heparin Affinity Chromatography

To further characterize binding of the peptides in Table 3.1 by heparin, their relative binding affinities were determined by heparin affinity chromatography. Fig. 3.10 shows a sample chromatogram for CPK4. As discussed previously, binding interactions with heparin and the peptides CPK3 and CPH4 (at pH 7.4) were too weak to evaluate by ITC. If heparin-peptide binding occurs primarily via electrostatic interactions between the cationic residues of lysine and arginine, and the anionic groups of heparin, then the affinity of CPK and CPR peptides for the heparin-stationary phase, should increase with the number of cationic residues. As a mobile phase containing a higher concentration of NaCl is necessary to elute longer peptides, this would seem to indicate that elution of the peptides is based on a cation exchange mechanism; peptides containing larger numbers of cationic residues need higher concentrations of Na^+ ions to displace them from the anionic heparin-stationary phase.

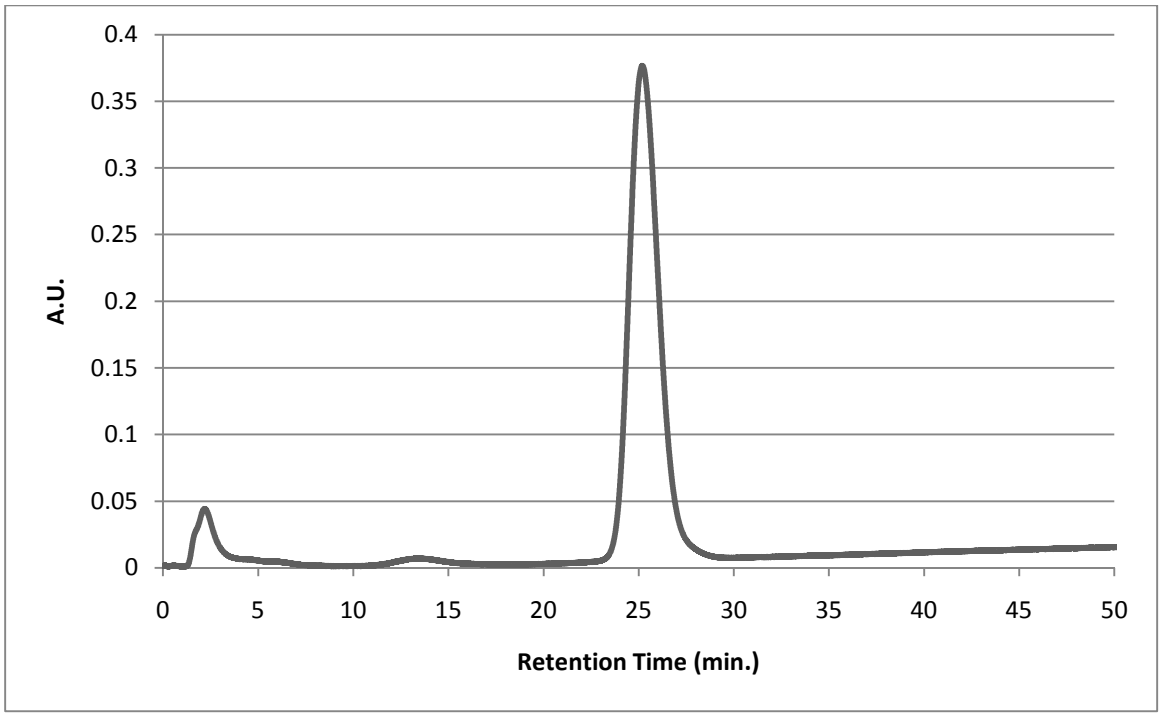

Fig. 3.10. Heparin affinity chromatogram of CPK4 showing a retention time of 25.18 min As calculated from the NaCl gradient and the elution time, the CPK4 peptide elutes at a NaCl concentration of about 0.25 M.

Results in Table 3.5 indicate that longer peptides from both the CPK and CPR series of peptides are retained for a longer time period in the column. Retention times for the CPK series averaged 13.69 min for CPK3 to 42.17 min for CPK7. For the CPR series retention times ranged from an average of 20.72 min to 55.55 min Table 3.5 shows a comparison of retention times for CPK and CPR series of peptides with their binding constants determined by ITC.

Given that a linear NaCl gradient is used for eluting the peptides from the heparin stationary phase, the retention time between each peptide should be proportional to its heparin-binding affinity. Equ. 2.1 shows that ΔG is proportional to $\ln(K_b)$, the heparin-binding constant of the peptides as determined by ITC. Given this proportionality, ΔG of binding of peptides to heparin in the calorimeter and the heparin affinity column should also be proportional. Therefore, a linear correlation of $\log(K_b)$ to the retention time has been established and plotted in Fig. 3.11. By substituting a retention time of 13.69 min. for "X", a K_b of 232 M^{-1} is calculated for CPK3.

As can be seen, the CPR series of peptides are retained for a longer time period than their corresponding CPK peptide. This reiterates that the arginine-containing peptides have a higher binding affinity for heparin than the lysine-containing peptides, for reasons discussed in section 3.1.2.

At pH 7.4, binding between heparin and CPH4 was not strong enough to generate a binding curve due to lack of protonation of the imidazole group of the histidine residues. By lowering the pH of the mobile phase by 0.5 increments, the effect

Peptide	Avg RT (min)	Avg K_b (M^{-1})
CPK3	13.69	231
CPR3	20.72	1800
CPK4	25.10	2490
CPR4	31.86	$2.0X10^4$
CPK7	42.17	$1.2X10^5$
CPR7	55.55	$6.5X10^6$

Table 3.5. Average retention times (RT) of the CPK and CPR series of peptides compared to their corresponding binding constants (K_b) as determined by ITC. K_b of CPK3 was calculated from the equation of the line in Fig. 3.11.

of protonation of the imidazole ring on heparin binding could be quantitatively determined, and compared to the CPK and CPR series of peptides. Results in Table 3.6 show that as the pH of the mobile phase decreases, binding affinity of CPH4 for the heparin stationary phase increases. The retention time of CPH4 in the column increases from 3.45 min at pH 7.4 to 38.76 min at pH 5.0. This also correlates with binding constants measured by ITC experiments as a function of pH. As the pH decreases the imidazolium ring of histidine becomes more protonated suggesting that electrostatic interactions play a dominant role in heparin-binding affinity. Data show that CPH4, at pH 5.0, has a longer retention time than the corresponding CPR4, at pH 7.4, although both

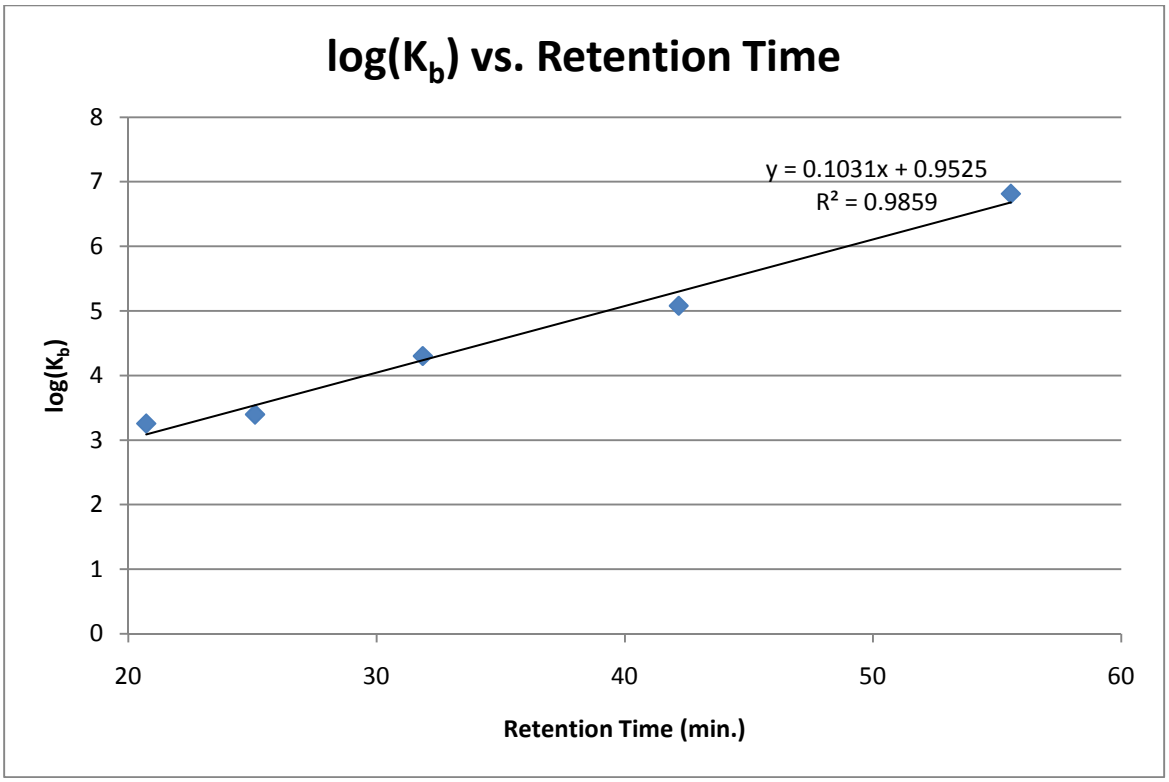

Fig. 3.11. Plot of log(K_b), determined by ITC vs the retention time as measured by heparin affinity chromatography for the CPR and CPK series of peptides. A linear least squares fit of the data gives the equation: logK_b = 0.0147(retention time) + 0.932. Using this equation and retention time, a binding constant of 232 M^{-1} was estimated for CPK3.

pH	RT (min)	K_b (M^{-1})
7.4	3.45	ND
6.5	10.70	1880
6.0	24.68	8830
5.5	30.25	$2.1X10^4$
5.0	38.76	$3.7X10^4$

Table 3.6. The average retention time (RT) for CPH4 at varying pH compared to its corresponding heparin-binding constant (K_b).

are fully protonated at their respective pH. This may suggest that site-specific bonding of the imidazolium ring to heparin is reinforcing the binding interaction.

3.3 Discussion

The ITC data for the binding interactions between heparin and the lysine-containing peptides show that this binding results in an unfavorable positive enthalpy which is compensated by a positive entropy. As heparin is a polyelectrolyte, it is associated with a number of charged counterions in solution. The association of bound counterions adds order to the solution and so is entropically unfavorable. The binding of a peptide to heparin displaces these counterions and adds favorably to the free energy of peptide/heparin binding.[25] This is exemplified by the positive entropy. As the change

in enthalpy is positive, the binding interaction is driven by the positive entropy change resulting from the counterion release. It may be that the ionic binding interaction between the lysine residues on the peptides and the anionic groups on heparin is too weak to compensate for the positive enthalpy associated with the counterion release, hence the net positive enthalpy. This suggests that the binding interaction is primarily electrostatic.[26]

Both lysine- and arginine-containing peptides exhibit a positive change in entropy as a result of the binding interaction, however, binding interactions with the arginine-containing peptides are exothermic while those with the lysine-containing peptides are endothermic. A possible reason for the difference in binding affinity of lysine- and arginine-containing peptides is that hydrogen bonding may play a larger role in the binding interaction of the guanidinium group of arginine than in the ammonium group of lysine.[26] The hydrogen bond angle of the N-H groups on the ammonium and guanidinium groups to the oxygen atoms of the sulfate groups of heparin is different.[27] Molecular modeling suggests that the guanidinium group can form two hydrogen bonds with a sulfate group in which the bond angle is almost exactly 180^{o}, while the ammonium group can form one hydrogen bond in which the bond angle is 180^{o}. This suggests that, although counterions of heparin are released upon binding of both lysine-containing and arginine-containing peptides (shown by the positive change in entropy values), hydrogen bonding between the guanidinium groups and sulfate groups is strong

enough to compensate for the positive change in enthalpy due to the counterion release, as shown by a negative enthalpy value.

Since peptide/heparin binding is driven, to a large degree, by electrostatic interactions, CPH4 would not be expected to strongly interact with heparin at pH 7.4, because the histidine side chains are in the neutral imidazole form. Hence the undetermined binding constant. The pKa's of lysine and arginine are 10.54 and 12.48,[28] respectively; thus at physiologic pH, the lysine- and arginine-containing side chains are fully protonated. However, the imidazolium ring of histidine has a pKa of 6.0 and so is only about 10% protonated at pH 7.4.[29] The ITC data generated at pH 6.5 show a negative enthalpy and relatively large negative entropy contribution, as shown in Table 3.4. This suggests that binding is mainly driven by forces other than electrostatic interactions as the negative entropy is not characteristic of a large counterion release. At this pH, hydrogen bonding may play the major role in peptide-heparin binding as this is associated with a negative enthalpy and entropy.[30] Also, NMR studies have shown that the immidazolium ring of histimine, which is the same as the histidine side chain, binds site-specifically, through hydrogen bonding, within a cleft of a heparin trisaccharide sequence. The cleft is formed by an IAI triad in which the I ring is 2-O-sulfo-α-L-iduronic acid, and the A ring is 2-deoxy-2-sulfamido-6-O-α-D-glucopyranosyl. [31]

As pH decreases, protonation of the histidine side chains of CPH4 increases and heparin affinity of CPH4 increases, as does the enthalpy and entropy. The increase in

enthalpy and entropy signify that counterion release from the binding interaction is becoming more intense and that electrostatic forces are becoming dominant.

It is often the case that the first and last several data points for the titration of heparin into the peptide solution, or vice versa, need to be deleted so an appropriate model can be fit to a sigmoidal set of data points. These data points are most likely associated with aggregation of peptide/heparin complexes.[26, 32, 33] At particular ratios of heparin and peptide, the peptide/heparin aggregate may fall out into solution making it possible to titrate free peptide or heparin, or aggregation may not appear until the end of the titration resulting in data points which can then be fit with a binding model resulting in thermodynamic parameters which can be used to describe the binding interaction. However, at times, some aggregate is left behind as can be seen as a white, cloudy precipitate in the titrated solution. It appears that aggregation is a consequence of using relatively high concentrations of heparin and peptides, with a high density of cationic residues, that are necessary for ITC measurements.[34] In this research, concentrations of both peptide and heparin were reduced to try to avoid aggregation, however, this served only to diminish the signal associated with the binding interaction.

3.4 Summary

The ITC and heparin affinity results indicate that as peptide length increases, so does binding affinity of the peptides to heparin. This increase in binding is most likely due to the increase in the number of cationic residues per peptide and therefore

stronger electrostatic interactions per peptide as indicated by the entropy and enthalpy values determined by ITC for CPK and CPR peptides at pH 7.4. For CPH4 binding is too weak to be measured by ITC at pH 7.4, due to lack of protonation of the histidine imidazole groups. However, ITC measurements taken at decreasing pH show an increase in entropy and an increase in enthalpy. This suggests that at higher (pH 6.5) site-specific hydrogen bonding is adding to a more favorable enthalpy driven process and is the dominant force in the binding interaction with heparin, but at lower pH (pH 5.0), entropy is positive and enthalpy, although still negative, has become more positive indicating that counterion release, as a result of binding the cationic imidazolium side chains, is a larger part of the driving force in the interaction with heparin. Also, heparin affinity chromatography confirms that increased protonation of the imidazolium ring of histidine correlates to an increase in heparin-binding affinity; as pH of the mobile phase decreases, retention time of CPH4 increases.

Although the peptides synthesized are too short to form a stable α-helix, secondary structure measurements indicate a locally ordered structure for these peptides that is similar to that of a polyproline II helix. A polyproline II helix is a left-handed helix of about 3 residues per turn, and consists of trans amide bonds. There is seen on the CD spectrum, of all peptides, a large minimum at about 200 nm and a weak maximum at about 220 nm, suggesting a transition state.

Taken together, the binding and structural characterization of these peptides allows for the rational design of heparin binding peptides. Cationic residues play the

primary role in binding affinity of peptides to heparin. Knowing the secondary structure of the peptide will help in the strategic placement of residues for optimal binding to heparin. For example, use of helix-forming residues, such as alanine and leucine, can be used to form a more stable and ideal polyproline II-type helix, and cationic residues can be placed in every third position to form an amphipathic face of cationic charge which may maximize electrostatic interaction to heparin.

The data show that histidine-only-containing peptides will probably not be useful in circumstances in which heparin binding is critical. Physiologic pH is 7.4 and at this pH the histidine side chains are about 10% protonated; as a consequence histidine-containing peptides exhibit weak electrostatic interactions with heparin at pH 7.4.

3.5 References

1. Wang, J.; Rabenstein, D. L., *Biochim. Biophys. Acta* **2009,** *1790*, 1689-1697.

2. Manning, G. S., *Acc. Chem. Res.* **1979,** *12*, 443-449.

3. Rabenstein, D. L.; Bratt, P.; Peng, J., *Biochemistry* **1998,** *37*, 14121-14127.

4. Conrad, H. E., *Heparin-Binding Proteins*. Academic Press: San Diego, 1998.

5. Cardin, A. D.; Weintraub, H. J. R., *Arteriosclerosis* **1989,** *9*, 21-32.

6. Cardin, A.; Demeter, D. A.; Weintraub, H. J. R.; Jackson, R. L., *Methods Enzymol.* **1991,** *203*, 556-583.

7. Verrecchio, A.; Germann, M. W.; Schick, B. P.; Kung, B.; Twardowski, T.; San Antonio, J. D., *J. Biol. Chem.* **2000,** *275*, 7701-7707.

8. Margalit, H.; Fischer, N.; Ben-Sasson, S. A., *J. Biol. Chem.* **1993,** *268*, 19228-19231.

9. Kelly, M. A.; Chellgren, B. W.; Rucker, A. L.; Troutman, J. M.; Fried, M. G.; Miller, A.; Creamer, T. P., *Biochemistry* **2001,** *40*, 14376-14383.

10. Marqusee, S.; Robbins, V. H.; Baldwin, R. L., *Proc. Nat. Acad. Sci. U.S.A.* **1989,** *86*, 5286-5290.

11. Petukhov, M.; Yumoto, N.; Murase, S.; Onmura, R.; Yoshikawa, S., *Biochemistry* **1996,** *35*, 387-397.

12. Shoemaker, K. R.; Kim, P. S.; York, E. J.; Stewart, J. M.; Baldwin, R. L., *Nature* **1987,** *326*, 563-567.

13. Sreerama, N.; Woody, R. W., *Proteins* **1999,** *36*, 400-406.

14. Gokce, I.; Woody, R. W.; Anderluh, G.; Lakey, J. H., *J. Am. Chem. Soc.* **2005,** *127*, 9700-9701.

15. Mezei, M.; Fleming, P. J.; Srinivasan, R.; Rose, G. D., *Proteins* **2004,** *55*, 502-507.

16. Rose, G. D.; Pappu, R. V., *Prot. Sci.* **2002,** *11*, 2437-2455.

17. Tiffany, M. L.; Krimm, S., *Biopolymers* **1969,** *8*, 347-359.

18. Krimm, S.; Tiffany, M. L., *Biopolymers* **1972,** *11*, 2309-2316.

19. Rucker, A. L.; Creamer, T. P., *Prot. Sci.* **2002,** *11*, 980-985.

20. Wu, C. W.; Jayaraman, G.; Chien, K. Y.; Liu, Y. J.; Lyu, P. C., *Peptides* **2003,** *24*, 1853-1861.

21. Jayaraman, G.; Wu, C. W.; Liu, Y. J.; Chien, K. Y.; Fang, P. C.; Lyu, P. C., *FEBS Lett.* **2000,** *482*, 154-158.

22. Ferran, D. S.; Sobel, M.; Harris, R. B., *Biochemistry* **1992,** *31*, 5010-5016.

23. Jackle, H.; Luisi, P. L., *Biopolymers* **1981,** *20*, 65-88.

24. Stapley, B. J.; Creamer, T. P., *Prot. Sci.* **1999,** *8*, 587-595.

25. Hileman, R. E.; Jennings, R. N.; Linhardt, R. J., *Biochemistry* **1998,** *37*, 15231-15237.

26. Goncalves, E.; Kitas, E.; Seelig, J., *Biochemistry* **2005,** *44*, 2692-2702.

27. Fromm, J. R.; Hileman, R. E.; Caldwell, E. E. O.; Weiler, J. M.; Linhardt, R. J., *Arch. Biochem. Biophys.* **1995,** *323*, 279-287.

28. Nelson, D. L.; Cox, M. M., *Principles of Biochemistry*. 4th ed.; W. H. Freeman and Company: New York, 2005.

29. Pichon, C.; Goncalves, C.; Midoux, P., *Adv. Drug Deliv. Rev.* **2001,** *53*, 75-94.

30. Liang, Y., *J. Iran. Chem. Soc.* **2006,** *3*, 209-219.

31. Chuang, W.; Christ, M. D.; Peng, J.; Rabenstein, D. L., *Biochemistry* **2000,** *39*, 3542-3555.

32. Seelig, J.; Ziegler, A., *Biophys. J.* **2004,** *86*, 254-263.

33. Seelig, J.; Kitas, E.; Goncalves, C., *Biochemistry* **2006,** *45*, 3086-3094.

34. Hernaiz, M. J.; LeBrun, L. A.; Wu, Y.; Sen, J. W.; Linhardt, R. J.; Heegaard, J. H. H., *Eur. J. Biochem.* **2002,** *269*, 2860-2867.

Chapter 4

Heparin-Binding Peptoids

4.1 Introduction

4.1.1 Peptoid Structure

Peptoids are a class of peptidomimetics which differ from peptides in that the functional side-chain is located on the backbone amide-nitrogen rather than the α-carbon. The consequence of this translocation is that the peptoid backbone is achiral and lacks amide protons, which precludes stabilization of peptoid secondary structure by the backbone-backbone hydrogen bonding that stabilizes peptide α-helices.[1]

Although peptoids lack stabilization of secondary structure by backbone-backbone hydrogen bonding, peptoids can be sterically forced into a stable secondary structure by using side chains derived from bulky α-chiral amines. Barron et al.[2] have developed a set of design rules for the formation of peptoid secondary structure. The minimal sequence rules for stabilization of secondary structure are: composition of at least 50% α-chiral aromatic monomers, with at least one on the C-terminus, and placement of aromatic monomers so that the aromatic rings can add stability by aromatic stacking. These rules work well for peptoids consisting of 6-12 residues, however, in peptoids with more than 12 residues, these rules are more flexible in terms of the placement of monomers. NMR[3] and X-ray crystal structures[4] show that peptoids in this secondary conformation form a polyproline I-type helix consisting of

approximately three residues per turn, with cis amide bonds, and having a pitch of 6.0 Å or 6.7 Å for all aromatic or all aliphatic α-chiral side-chains, respectively. The secondary structure is most likely stabilized by steric interactions between the bulky α-chiral side-chains, and electronic repulsions by aromatic π and carbonyl lone-pair electrons which is indicated by studies in which peptoids were exposed to extreme environments:[5] α-helical peptides normally lose their secondary structure in low ionic strength solutions, due to lack of screening of charged side-chains from counter ions. Peptoids in similar conditions, 5 mM sodium phosphate, were examined by CD and compared to the CD signal of a relatively high ionic strength, 150 mM sodium phosphate, peptoid solution. The results indicate that the CD signal of the 50 mM solution did not significantly change compared to the 150 mM solution in which counterion screening is expected to take place. In the presence of 8 M urea, a chaotropic agent, the peptoid solution still maintained a strong CD signature indicative of helical structure. Even at the high temperature of 75 ^{o}C, CD spectra indicated only small changes in secondary structure. With these results in mind, it is proposed that strong steric forces are primarily responsible for the polyproline type-I structure of peptoids.

Quantum mechanical calculations have also been used to determine low-energy, secondary conformations of peptoids by utilizing Ramachandran plots. These plots have revealed torsion angles (ϕ,Ψ), Fig. 4.1, of experimentally determined structures of short peptoids.[6, 7] When ω is in the cis conformation, peptoid torsion angles of (ϕ,Ψ) fall in the low energy minima of (±90^{o},180^{o}) with (-90^{o},180^{o}) approximating a polyproline I helix.

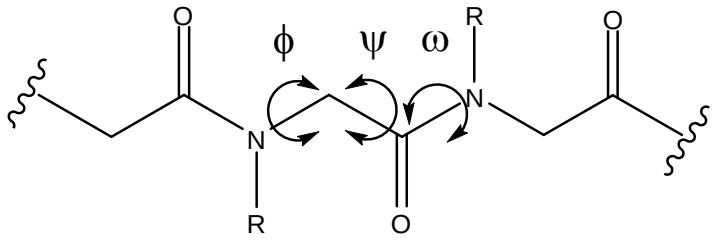

Fig. 4.1. Structural formula of a generic peptoid showing the location of the torsion angles: ϕ (between the C_α and amide nitrogen), Ψ (between the C_α and the carbonyl carbon , and ω (between the carbonyl carbon and the amide nitrogen).

When ω is in the trans conformation, torsion angles of ($\pm 90^o$, 180^o) are also prevalent with (-90^o, 180^o) approximating a polyproline II helix. The theoretically determined torsion angles correlate well with those attributed to peptoid structures determined experimentally.

Quantum mechanical simulations of two dipeptoid models, one containing an N-(methoxymethyl) glycine (Nme) linear side chain, and another containing an (S)-N-(phenylethyl) glycine (Nspe) branched side chain, Fig. 4.2, illustrate the effect of side chains on backbone torsion angles.[7] The theoretical calculations show that the dihedral angles of the Nme peptoid are equally distributed between ($\pm 90^o$, 180^o) while ω is in the cis or trans conformation. However, the peptoid with the Nspe side chain exhibits dihedral angles of, primarily, (-90^o, 180^o) with ω in either the cis or trans conformation. These calculations are in line with the empirical observations that bulky chiral side chains restrict the freedom of the peptoid backbone; moreover, by utilizing theoretical calculations, this restriction may be, in large part, attributed to a restriction on the ϕ dihedral angle by the chiral side chain.

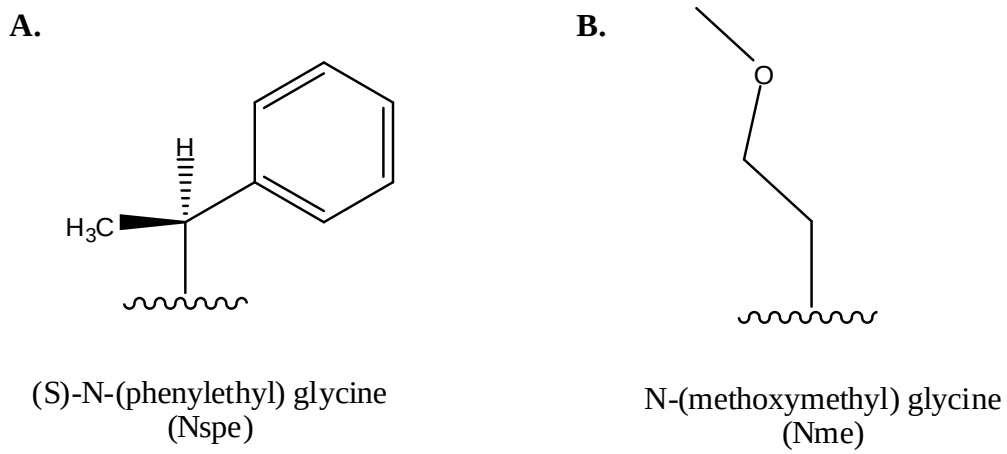

Fig. 4.2. Structures of **A.** Nspe and **B.** Nme monomers used in model dipeptoids to determine (ϕ, Ψ) torsion angles.

4.1.2 Peptoids as Biological Mimics.

Peptoids, as a class of peptidomimetics, are of interest as they have the potential to mimic biological compounds, such as peptides and proteins, in their activity.[8] There are several aspects which make peptoids attractive substitutes for peptides: they have been found to be biologically active,[9-11] are less prone to proteolysis,[12] are not immunogenic,[10] and offer ease of synthesis with the ability to incorporate a wide variety of functional side-chains.[13]

Barron et al. synthesized a peptoid to mimic a lung surfactant protein, located in the air-liquid interface in the lungs, critical for proper respiration. The peptoid was based on residues 13-28 of surfactant protein SP-C[14] which is α-helical in structure and exhibits extreme hydrophobicity. The peptoid, a 14-mer of all Nspe monomers and a hydrophobic tail of achiral residues at the N-terminus, was tested in a model lipid mixture emulating the surfactant mixture in the lungs. The surface activity of the

mixture plus peptoid was tested for surface tension, respreadability, and surface morphology. The results indicated that this particular peptoid performed comparably to SP-C peptide analogues already shown to have favorable surface activity in a biomimetic phospholipid mixture;[15, 16] although the peptoid consisted of all α-chiral aromatic monomers, it was superior to a similar peptoid tested consisting of all α-chiral aliphatic residues and more closely resembled the character of the SP-C protein. The conclusion was that the side-chain chemistry was less important for a viable replacement for a lung surfactant protein than the hydrophobic nature and helical stability, which was evidenced by CD, of the peptoid.

A tertiary peptoid structure has also been designed by Zuckermann et al.[17] to mimic the zinc cofactor-binding of proteins, which is necessary for enzyme catalysis.[18, 19] The structure consisted of Nspe (Fig. 2.7), Nsce [(S)-N-(carbonethyl)glycine], and Nae [N-(2-aminoethyl)glycine)] residues, Fig. 4.3, with histidine and cysteine residues to act as the zinc binding site. The design was accomplished by joining two helical peptoid segments with a Gly-Pro-Gly-Gly sequence which incorporated a turn between the two helix bundles. To test the binding of zinc, which would cause the helix bundles to come into closer proximity to each other, fluorescence resonance energy transfer (FRET) was utilized. A fluorophore and a quencher were added to the two ends of the peptoid structure, and FRET efficiency could be determined in the presence and absence of zinc. By adding zinc, the FRET efficiency did increase compared to the efficiency without zinc.

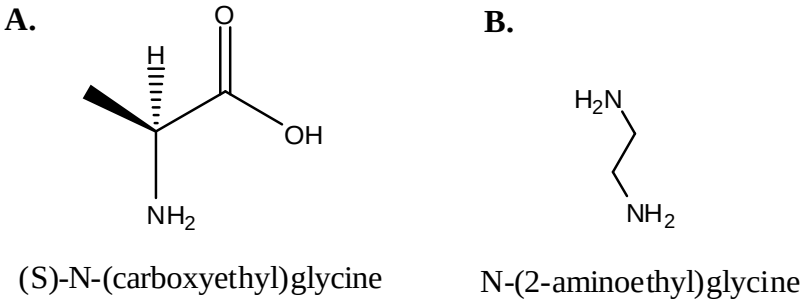

Fig. 4.3. Structural formulas of the amines used in the synthesis of a tertiary peptoid structure which mimics the zinc-cofactor binding of proteins.

After adding ethylenediaminetetraacetic acid (EDTA), a zinc chelating agent, the FRET efficiency decreased. The results of this study indicate that peptoids can be designed to form tertiary structures and therefore have the potential to mimic the activity of proteins with a more complex structure than that of just linear, helical peptides.

To this end, this chapter reports on the synthesis of a family of peptoids with a secondary structure similar to that of a polyproline I-type helix, stabilized by the addition of bulky α-chiral amines, and their binding interaction with heparin. As a polyproline I-type helix has about three residues per turn, the peptoids were designed with side chain cationic amine groups present at every third residue to form an amphipathic face of positive charge to facilitate electrostatic interactions with heparin, Fig. 4.4.

To test the effects that various monomers may have on helical structure or heparin-binding, enantiomers (S)-1-phenylethylamine and (R)-1-phenylethylamine were used to determine if chirality of the monomers or the screw-sense of the helix affects heparin-binding. Also, (S)-sec-buytlamine or (S)-1-phenylethylamine were used in place

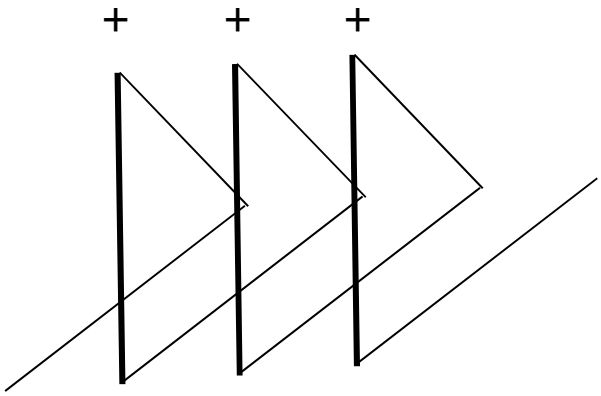

Fig. 4.4. A representation of an amphipathic, three-fold helix showing the face of positive charge of cationic side chains of residues incorporated at every third monomer position.

of n-butylamine to determine if their use could modulate helical stability and/or heparin-binding.

The binding interaction of these peptoids and heparin is characterized to determine their viability as a suitable replacement for protamine. Table 4.1 lists the peptoids synthesized in this work, and their structural formulas are shown in Fig. 4.5. (Nrpe-containing peptoids), Fig. 4.6 (Nspe-containing peptoids), and Fig. 4.7 (two peptoids which contain monomers in place of Nnb).

4.2 Results

4.2.1 Binding Constants

Figs. 4.8 and 4.9 show examples that are typical of $(NLys\text{-}Nnb\text{-}Nrpe)_n$ ITC binding data. The raw data in Fig. 4.8 shows an upward deflection of peaks indicating power is

Peptoid Sequence
$(NLys\text{-}Nnb\text{-}Nrpe)_n$ n = 1-4
$(NLys\text{-}Nnb\text{-}Nspe)_n$ n = 4-6
$(NLys\text{-}Nssb\text{-}Nspe)_4$
$(NLys\text{-}Nspe\text{-}Nspe)_4$

Table 4.1. List of peptoids synthesized in this work, where n is the number of repeat trimer sequences.

increased to the sample cell during each titration. The increase in power is necessary to maintain the temperature differential between the sample and reference cells of the calorimeter to compensate for the absorption of heat during the binding interaction. This is characteristic of an endothermic binding interaction which is similar to the lysine-containing peptides, discussed in Chapter 3.

The ITC results, as shown in Table 4.2, reveal that as peptoid length and number of cationic residues increase, so does heparin-binding affinity. For example, peptoid $(NLys\text{-}Nnb\text{-}Nrpe)_3$, and $(NLys\text{-}Nnb\text{-}Nrpe)_4$ show an increase in heparin-binding affinity with the addition of a trimer repeat sequence, resulting in an average K_b of $6.9X10^4\ M^{-1}$ and $2.3X10^5\ M^{-1}$, respectively. A heparin-binding constant could not be determined for $(NLys\text{-}Nnb\text{-}Nrpe)_1$ and $(NLys\text{-}Nnb\text{-}Nrpe)_2$, as their interaction with heparin was too weak to be measured accurately by ITC.

A.

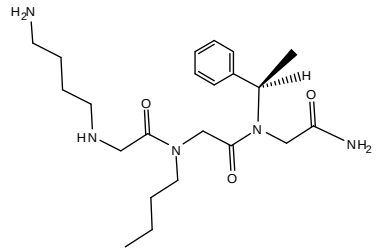

B.

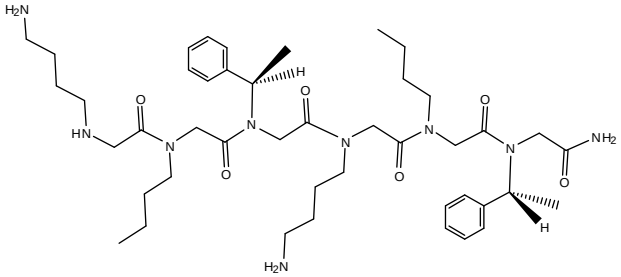

C.

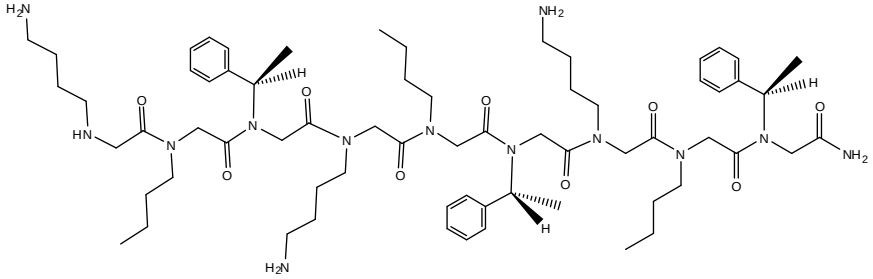

D.

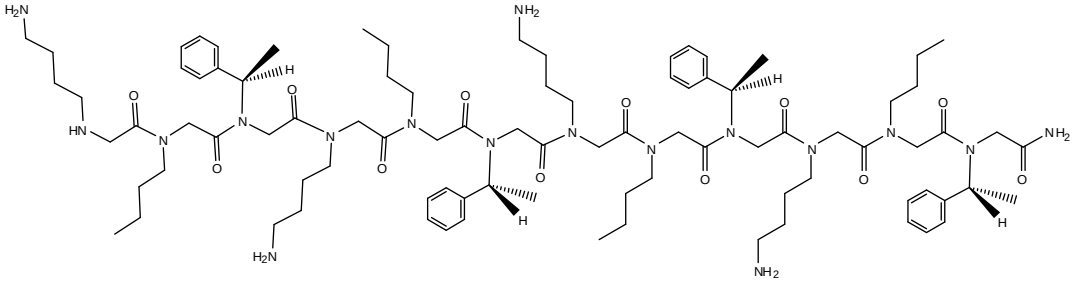

Fig.4.5. Structural formulas of Nrpe-containing peptoids: **A.** (NLys-Nnb-Nrpe)$_1$ **B.** (NLys-Nnb-Nrpe)$_2$ **C.** (NLys-Nnb-Nrpe)$_3$ **D.** (NLys-Nnb-Nrpe)$_4$. The placement of the Nrpe monomers in the peptoid sequence was chosen to drive the peptoids into a helical structure with the cationic ammonium groups on one side of the helix.

A.

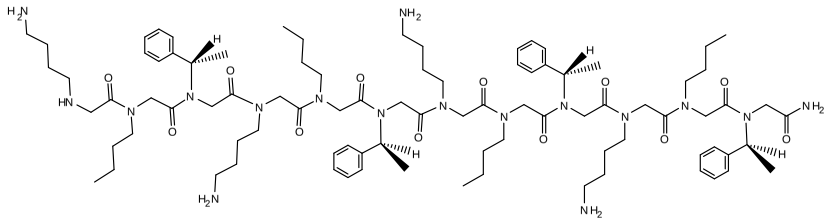

B.

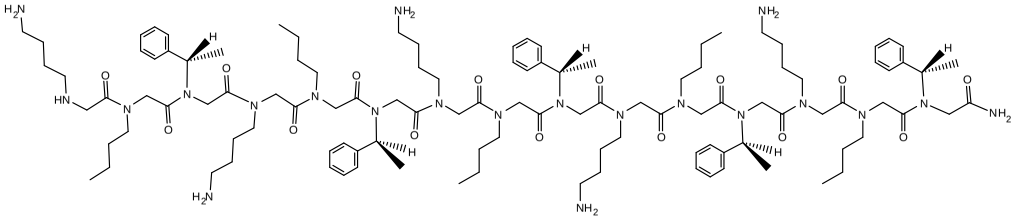

C.

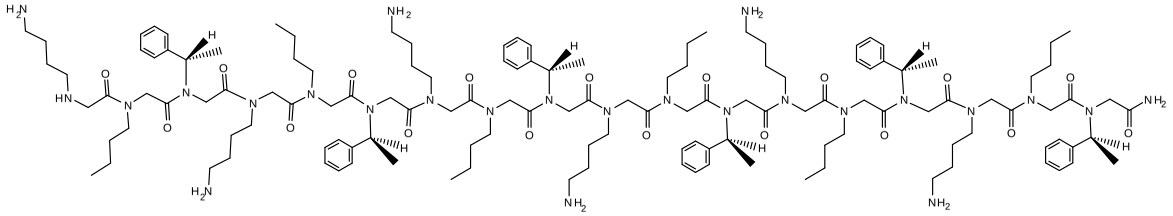

Fig.4.6. Structural formulas of Nspe-containing peptoids: **A.** $(NLys\text{-}Nnb\text{-}Nspe)_4$ **B.** $(NLys\text{-}Nnb\text{-}Nspe)_5$ **C.** $(NLys\text{-}Nnb\text{-}Nspe)_6$.

A.

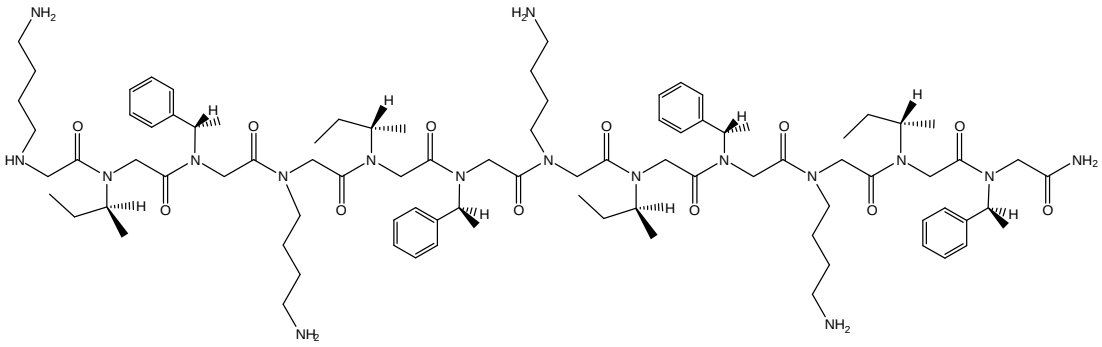

B.

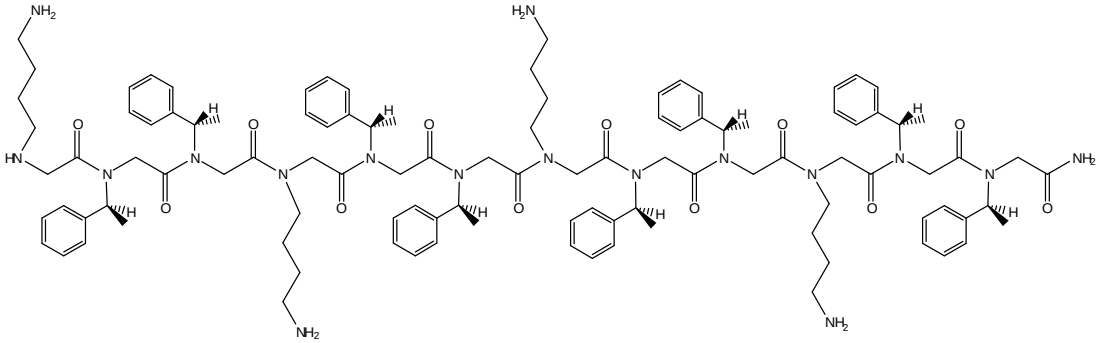

Fig. 4.7. Structural formulas of **A.** (NLys-Nssb-Nspe)$_4$ and **B.** (NLys-Nspe-Nspe)$_4$.

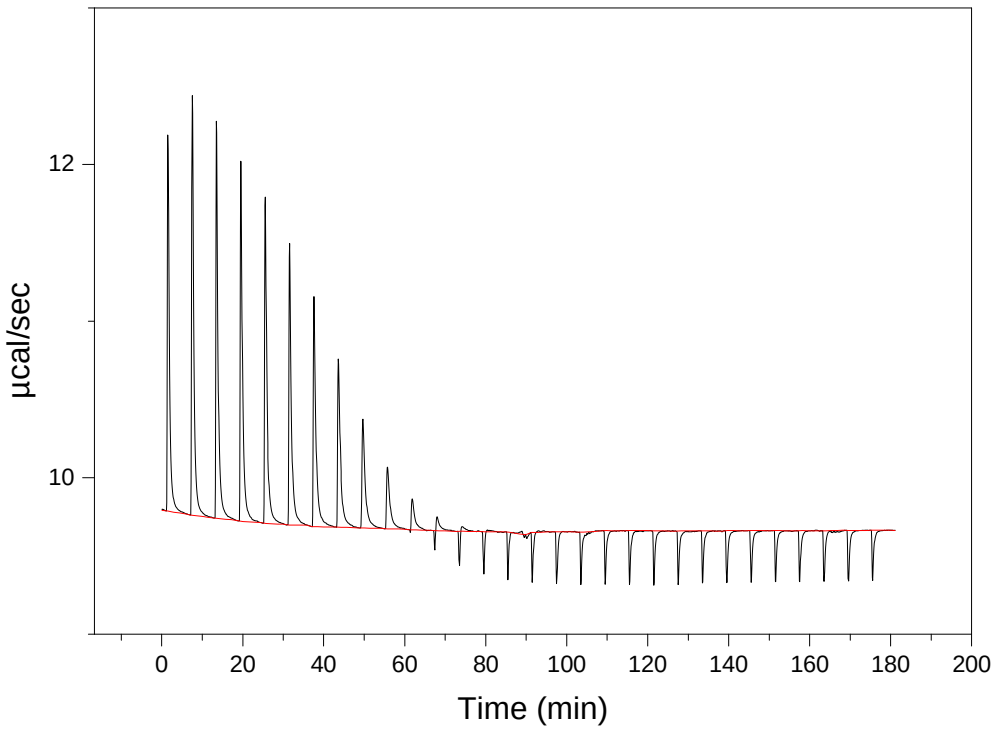

Fig. 4.8. Raw data for the titration of 0.4 mM $(NLysNnbNrpe)_3$ with 0.5 mM heparin. Parameters are: number of injections, 30; cell temperature,25 ^{o}C; injection volume, 6 µL, and spacing between injections is 360 sec. Upward deflecting peaks show an increase in power to the sample cell indicating that heat is being absorbed by the binding interaction.

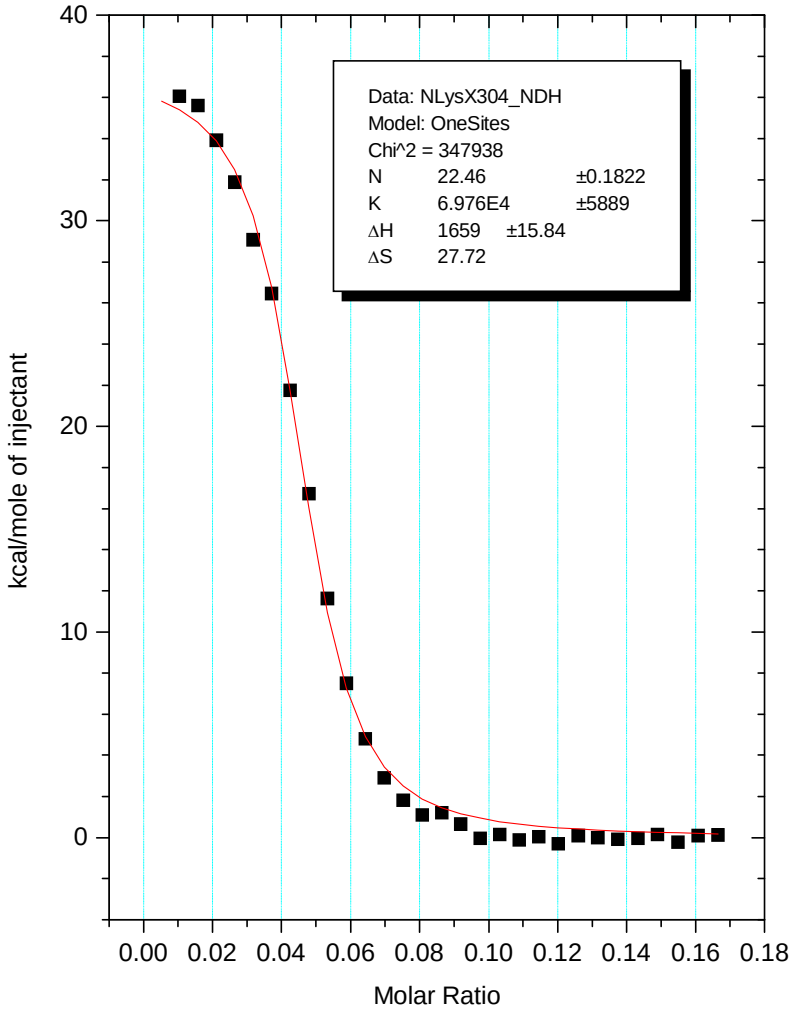

Fig. 4.9. Integrated data of Fig. 4.5 fit to a single-set-of sites model resulting in thermodynamic values given in the figure.

Peptoid Sequence	K_b (M^{-1})	N (binding sites)	ΔH (cal/mol)	ΔS (cal/mol·°C)
$(NLysNnbNrpe)_1$	N/D	N/D	N/D	N/D
$(NLysNnbNrpe)_2$	N/D	N/D	N/D	N/D
$(NLysNnbNrpe)_3$	$6.9X10^4 \pm 196.6$	22.6 ± .1	1650 ± 9	27.67 ± .05
$(NLysNnbNrpe)_4$	$(2.3 \pm .4)X10^5$	18.92 ± .02	2320 ± 48	32.3 ± .1
$(NLysNnbNspe)_4$	$(5.8 \pm .2)X10^5$	16.1 ± .1	2880 ± 23	36.04 ± .05
$(NLysNnbNspe)_5$	$(1.9 \pm .2)X10^6$	20.9 ± .4	2461 ± 51	37.0 ± .3
$(NLysNnbNspe)_6$	$(3.4 \pm .2)X10^6$	13.1 ± .4	4790 ± 32	45.9 ± .2
$(NLysNssbNspe)_4$	$(3.8 \pm .4)X10^5$	15.7 ± .1	3440 ± 92	37.0 ± .3
$(NLysNspeNspe)_4$	N/D	N/D	N/D	N/D

Table 4.2. List of peptoids and their corresponding thermodynamic values for heparin-peptoid binding as determined by ITC. The uncertainties are the standard deviations of the average of three replicates.

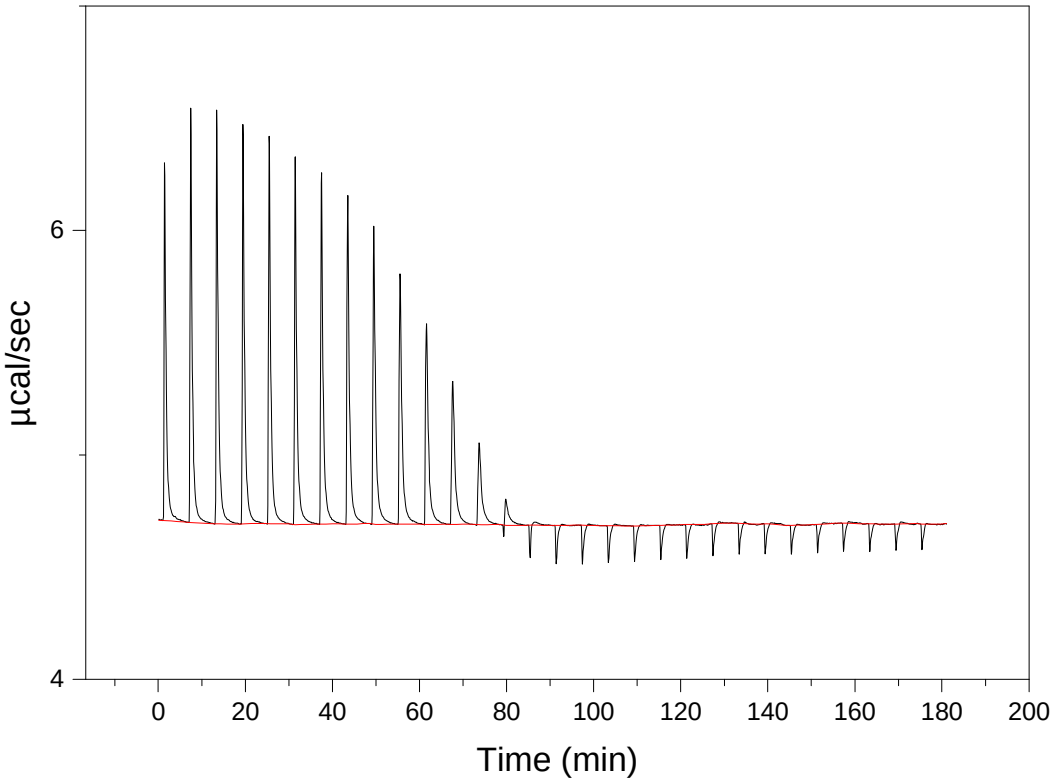

Fig. 4.10. Raw data for the titration of 0.2 mM $(NLysNnbNspe)_4$ with 0.25 mM heparin. Parameters are: number of injections, 30; cell temperature,25 ^{o}C; injection volume, 6 µL, and spacing between injections is 360 sec. Upward deflecting peaks show an increase in power to the sample cell indicating that heat is being absorbed by the binding interaction.

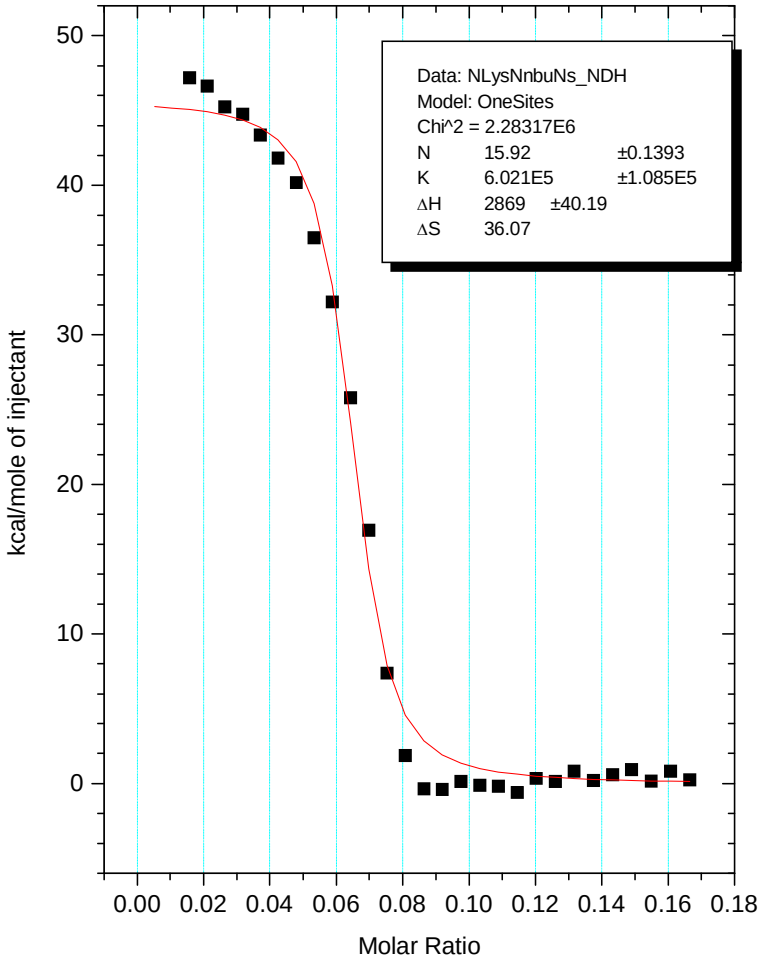

Fig. 4.11. Integrated data of Fig. 4.7 fit to a single-set-of sites model resulting in thermodynamic values given in the figure for the binding of $(NLys\text{-}Nnb\text{-}Nspe)_4$ by heparin.

As with the lysine-containing peptides discussed in Chapter 3, peptoids containing the lysine-like residue (NLys) exhibit an entropy-driven interaction as indicated by the favorable increase in entropy, from 28 to 32 cal/mol·^{o}C, and an unfavorable increase in enthalpy, from 1650 to 2320 cal/mol, upon binding to heparin.

Peptoids were also synthesized incorporating the Nspe residue instead of Nrpe to determine if chirality had any effect on peptoid-heparin binding. Figs. 4.10 and 4.11 present ITC binding data of (NLys-Nnb-Nspe)$_4$. The raw ITC binding data of Fig. 4.10, again, shows an endothermic binding interaction which is representative of the NLys-containing peptoids. Although the binding interaction is similar to that of (NLys-Nnb-Nrpe)$_4$, the K_b for (NLys-Nnb-Nspe)$_4$ is 5.8X10^5 M^{-1}, which is significantly greater than the K_b of (NLys-Nnb-Nrpe)$_4$ (2.3X10^5 M^{-1}).

To determine the effect on helicity and heparin-binding affinity of adding twice the number of bulky α-chiral amines, the peptoids (NLys-Nssb-Nspe)$_4$ and (NLys-Nspe-Nspe)$_4$ were synthesized. The addition of bulky α-chiral amines may influence the binding affinity of the peptoid to heparin by affecting the peptoid secondary structure, as discussed in Section 4.1.1. Stabilizing the peptoid-secondary structure may orient the cationic residues of the peptoid in a more linear orientation along the peptoid backbone. The alignment of the cationic residues may affect the heparin-binding affinity of the peptoid. The ITC binding data of (NLys-Nssb-Nspe)$_4$ (data not shown) indicates that it binds with slightly less affinity to heparin with a K_b of 3.76X10^5 M^{-1}, as compared to the K_b for (NLys-Nnb-Nspe)$_4$ (5.8X10^5 M^{-1}), Table 4.2. Unfortunately, (NLys-Nspe-

Nspe)$_4$ could not be evaluated by ITC as aggregation, upon titration with heparin, inhibited binding experiments.

4.2.2 Circular Dichroism

The circular dichroism (CD) spectra of the peptoids synthesized in this work show absorption bands at about 190, 200, and 220 nm. The absorption pattern of the spectra can be attributed to the CD signature of a regular repeating structure similar to that of a polyproline I-type helix, as described in Section 4.1.2. The CD spectra also reveal that the Nspe-containing peptoids produce CD spectra which are mirror images of the Nrpe-containing peptoids which can be ascribed to the handedness of a peptoid helix. The handedness of the peptoid helix is determined by the α-chiral amine that is utilized to stabilize the peptoid secondary structure. Peptoids containing all Nrpe residues, as the structure-inducing element, result in a left-handed helix and those containing Nspe residues result in a right-handed helix. The CD spectra in Fig. 4.9 are of peptoids containing Nrpe residues and therefore represent a helical structure with a left-handed screw-sense.[2] The positive absorption band at about 218 nm originates from the nπ* transition of the amide chromophore, while the positive band at about 208 nm and negative band around 190 nm originate from the exiton split of the ππ* transition.[20]

As shown in Fig. 4.12, the CD spectra of the peptoids indicate a correlation between the number of trimer repeats of (NLys-Nnb-Nrpe) and helicity. The increase in helicity is in line with the rules set by Barron and coworkers,[2] that as the chain length

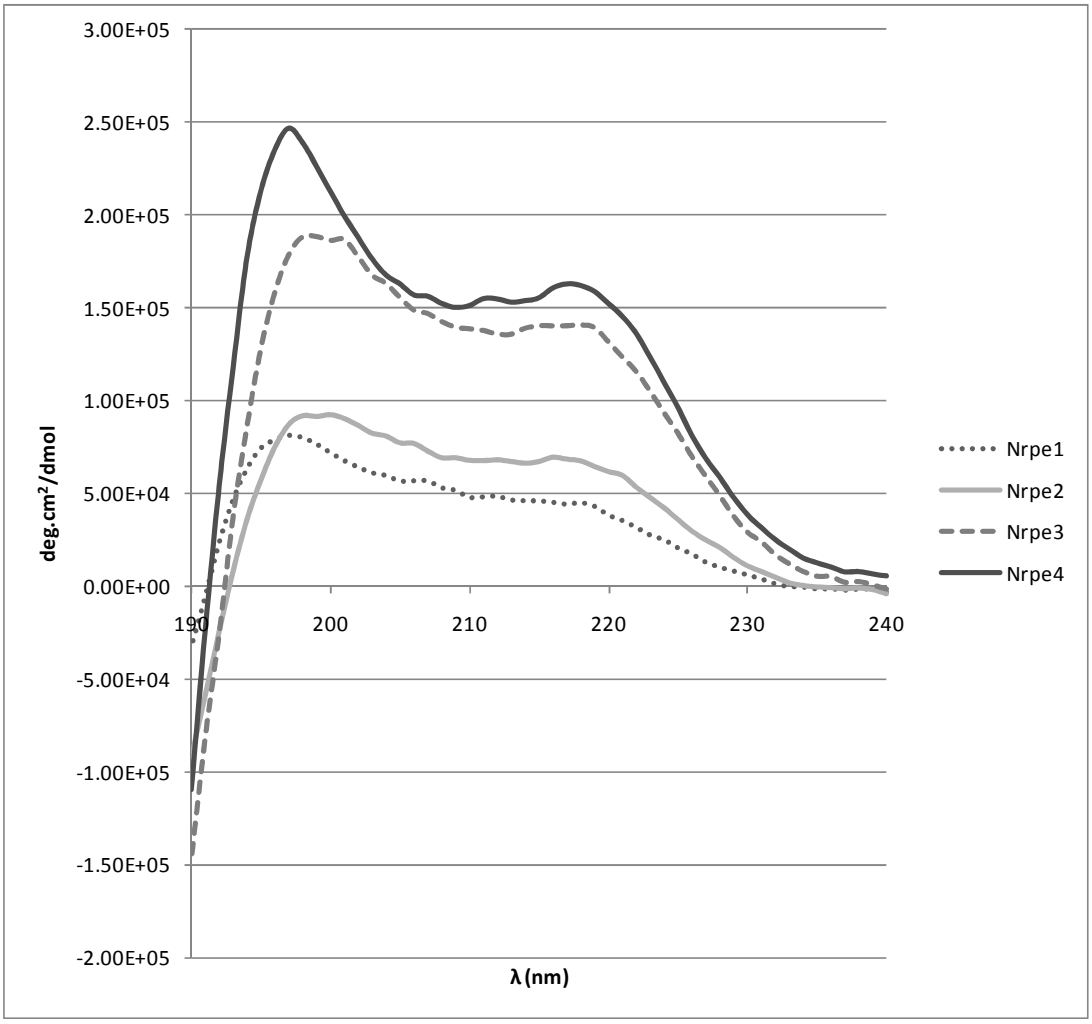

Fig. 4.12. CD spectra of the Nrpe-containing peptoids. Nrpe1 is the peptoid containing only one NLys-Nnb-Nrpe trimer repeat sequence, and so forth. Spectra show that peptoids increase in helix stability as they increase in trimer repeat sequences. The spectra were taken of 100 µM samples in the absence of heparin.

increases, so can helical stability. Although, as stated above, peptoids of this type form a polyproline I-type helix, the CD spectrum is similar to that of a peptide α-helix. One reason as to why these peptoids result in a CD spectrum similar to that of a peptide α-helix is that the aromatic moieties may absorb in the far UV region, thereby contributing to the CD spectrum.[4]

In contrast, the peptoids containing the Nspe residue show CD spectra that are opposite in ellipticity than those containing the Nrpe residue, Fig. 4.13. The spectrum of $(NLys\text{-}Nspe\text{-}Nspe)_4$ shows that by doubling the amount of Nspe residues, secondary structure becomes more stable, as indicated by an increase in intensity of the absorption bands. This shows that not only chain length, but also the number of α-chiral aromatic residues in the peptoid, plays an important role in the stabilization of secondary structure.

Interestingly, the CD spectra also show a decrease in helical character of $(NLys\text{-}Nnb\text{-}Nspe)_5$. This reduction in helical character may be due to the peptoid adopting more of an irregular trans configuration of the peptoid amide bond which is a minor, but significant, contribution of the overall population of configurational isomers due to the low energy barrier of the peptoid amide bond.[3] Barron et al. have hypothesized a chain length-dependent shift in the relative population of cis-amide isomers of Nrpe-containing peptoids.[21] In their study, the characteristic CD absorption bands decrease as the chain length increases from an Nrpe 5mer to an Nrpe 8mer. The CD intensity increases again as the chain is lengthened. This is similar to what is observed in the CD

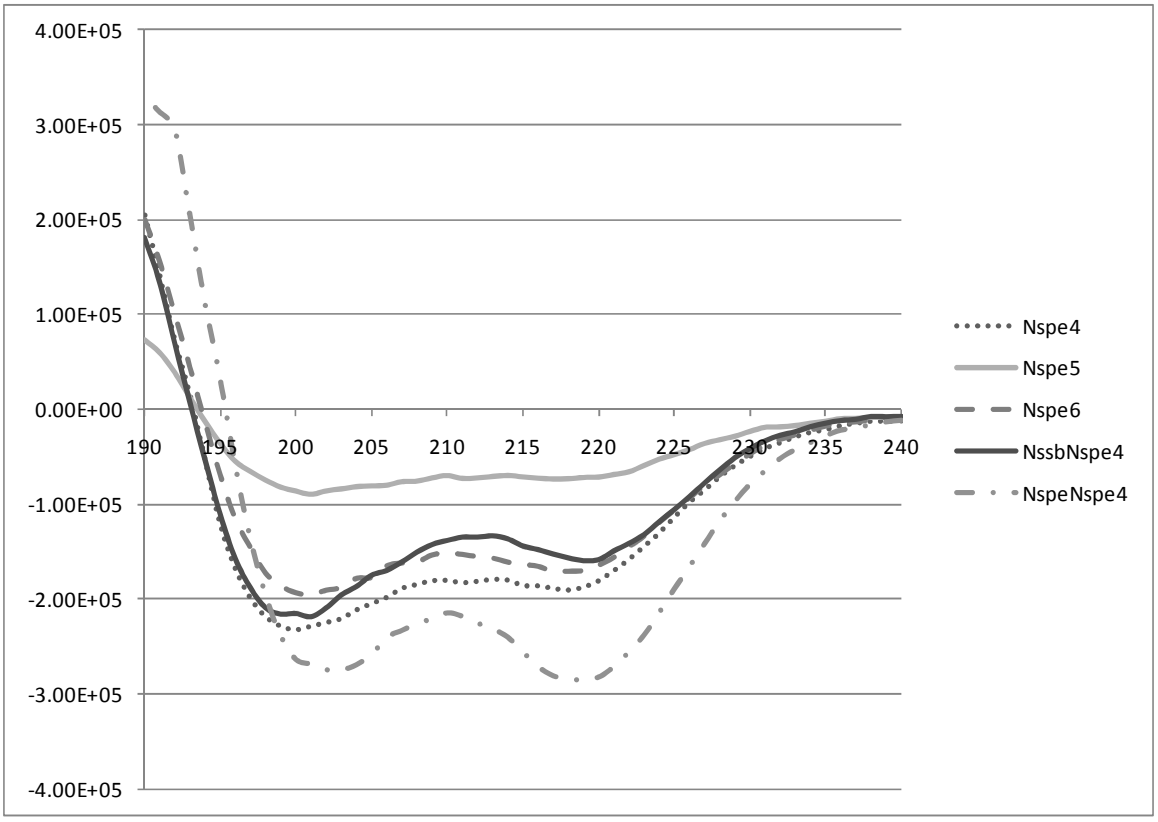

Fig. 4.13. CD spectra showing the helical stability of peptoids of various chain lengths and composition. Nspe4 is the peptoid containing four NLys-Nnb-Nspe trimer sequences, and so forth. Peptoid NssbNspe4 is the peptoid containing four NLys-Nssb-Nspe trimer sequences. The spectra were taken of 100 µM samples in the absence of heparin.

spectra of $(NLys\text{-}Nnb\text{-}Nspe)_4$ and $(NLys\text{-}Nnb\text{-}Nspe)_5$. The change in helical stability may then be attributed to a relative shift from cis to trans-amide configuration as the chain length is increased from a 12mer to a 15mer for the (NLys-Nnb-Nspe) trimer repeat sequence. As the peptoid is increased to an 18mer there is an increase in the CD absorption bands indicating another length-dependent shift to the cis-amide isomer as seen in the absorption spectrum of $(NLys\text{-}Nnb\text{-}Nspe)_6$. The shift to an alternate configurational isomer may also be reflected in the ITC data of $(NLys\text{-}Nnb\text{-}Nspe)_5$ in which the number of binding sites, N, is similar to that of the peptoids composed of only four trimer repeat sequences. As the peptoid becomes less structurally confined, it can adopt a more flexible and less extended conformation which may allow it to decrease its overall length. A consequence of this is that more of these peptoids can bind to a heparin oligosaccharide. However there is still an increase in heparin-binding affinity of the $(NLys\text{-}Nnb\text{-}Nspe)_5$ peptoid although it may be less helical in structure. This may indicate that for this particular sequence, addition of cationic residues play a more significant role in heparin-binding than overall helical conformation.

Peptoid $(NLys\text{-}Nssb\text{-}Nspe)_4$ contains, in addition to an α-chiral aromatic amine, an α-chiral aliphatic amine, so it may be expected to have a more stable secondary structure as compared to $(NLys\text{-}Nnb\text{-}Nspe)_4$. However, the CD spectra show that this peptoid has a weaker CD signature which may suggest a shift to an alternate conformation. $(NLys\text{-}Nssb\text{-}Nspe)_4$ also exhibits weaker binding compared to $(NLys\text{-}Nnb\text{-}Nspe)_4$, as measured by ITC. The decrease in helical stability of $(NLys\text{-}Nssb\text{-}Nspe)_4$ may

indicate that not only is a shift in cis-amide population length-dependent, but also sequence-dependent, as well.

For peptoids of similar length and number of cationic residues, it may be hypothesized that helicity is an important factor in heparin binding; as the peptoid conforms to a structure resulting in a pitch closer to 3 residues/turn, this allows the cationic residues to orient in a more linear fashion along the helical axis resulting in enhanced binding to the anionic groups aligned on the polysaccharide chain of heparin.

4.2.3 Heparin Affinity Chromatography

Heparin affinity chromatography was used to determine relative heparin-binding affinity between the peptoids synthesized in Table 4.1. Fig. 4.14 shows an example of a heparin affinity chromatogram of $(NLysNnbNspe)_4$.

As discussed in Section 3.2.3, peptides are eluted through the heparin affinity column via a cation exchange mechanism whereby peptides compete for the negative anionic groups of the heparin stationary phase with Na^+ ions from the mobile phase. The stronger the binding between heparin and peptide, the higher the Na^+ ion concentration must be to displace the peptide from the heparin stationary phase; therefore, the stronger the binding, the longer the retention time of the peptide by the column. As the peptoids in this work are highly cationic, it can be assumed that the binding mechanism between peptoids and the heparin stationary phase is similar.

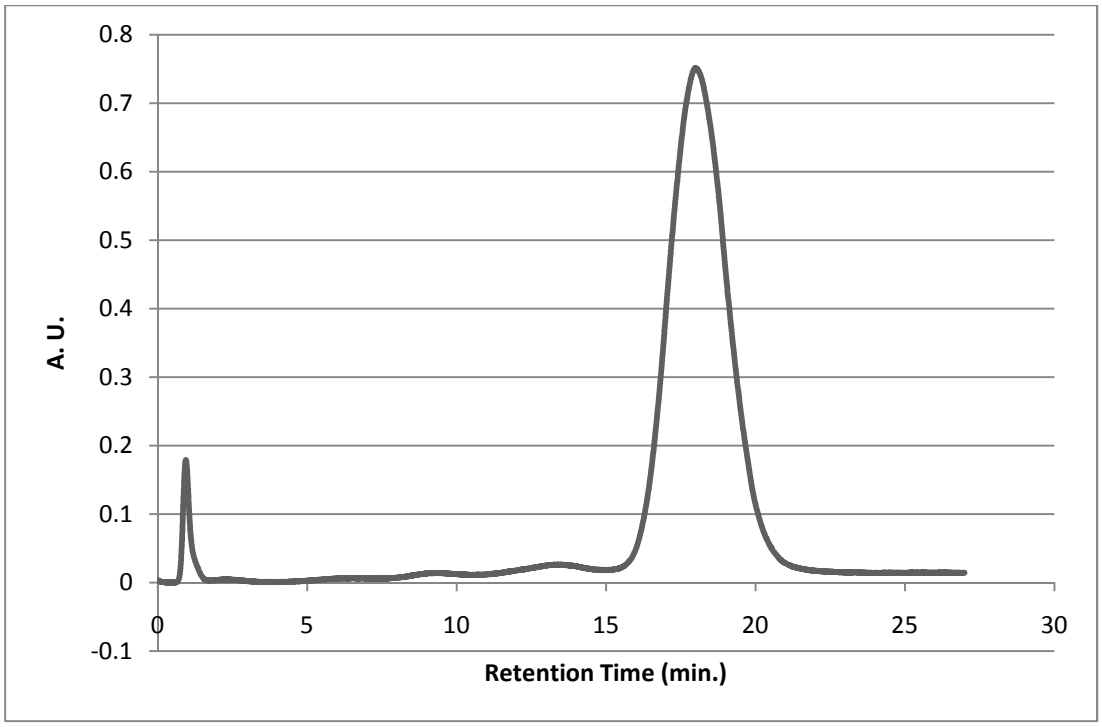

Fig. 4.14. Heparin affinity chromatogram of $(NLysNnbNspe)_4$ showing a retention time of 20.63 min. As calculated from the NaCl gradient and the elution time, $(NLysNnbNspe)_4$ elutes at a NaCl concentration of about 0.21 M.

As expected, Table 4.3 shows that peptoids with a greater number of cationic residues exhibit a longer retention time within the column. A binding constant for $(NLys\text{-}Nnb\text{-}Nrpe)_1$ and $(NLys\text{-}Nnb\text{-}Nrpe)_2$ could not determined by ITC, however, retention times of 4.24 and 10.09 min., respectively, were observed by heparin affinity chromatography. $(NLys\text{-}Nnb\text{-}Nspe)_6$ had the longest retention time of 30.18 min. A retention time for $(NLys\text{-}Nspe\text{-}Nspe)_4$ could not be measured as it had a tendency to aggregate within the column which resulted in the column becoming clogged. This is in line with binding constants determined by ITC.

There is a difference between the retention times of peptoids $(NLys\text{-}Nnb\text{-}Nrpe)_4$ and $(NLys\text{-}Nnb\text{-}Nspe)_4$, each containing either the (S) or (R) enantiomer of the phenylethyl amine monomer. $(NLys\text{-}Nnb\text{-}Nspe)_4$ has a retention time of 20.73 min., and $(NLys\text{-}Nnb\text{-}Nrpe)_4$ has a retention time of 20.01 min. As heparin is a helical polymer, this may explain the preference of heparin for Nspe-containing peptoids. The retention time of $(NLys\text{-}Nssb\text{-}Nspe)_4$ is 19.50 min.

As with the peptide binding data discussed in Section 3.2.3, a graph of $\log(K_b)$ versus the retention times of the peptoids was linear, Fig. 4.15. The equation obtained by a linear least squares fit of the data was used to estimate the binding constants of peptoids which had a heparin-binding interaction which was too weak to be measured accurately by ITC, Fig. 4.15. Binding constants of $3.2X10^3$ and $1.6X10^4$ M-1 were estimated for $(NLys\text{-}Nnb\text{-}Nrpe)_1$ and $(NLys\text{-}Nnb\text{-}Nrpe)_2$, respectively.

Peptoid	Avg. RT (min.)	Avg. K_b (M^{-1})
$(NLysNnbNrpe)_1$	4.24	$3.2X10^3$
$(NLysNnbNrpe)_2$	10.09	$1.6X10^4$
$(NLysNnbNrpe)_3$	15.95	$6.9X10^4$
$(NLysNnbNrpe)_4$	20.01	$2.3X10^5$
$(NLysNnbNspe)_4$	20.58	$5.8X10^5$
$(NLysNssbNspe)_4$	19.50	$3.8X10^5$
$(NLysNnbNspe)_5$	24.97	$1.9X10^6$
$(NLysNnbNspe)_6$	30.18	$3.4X10^6$
$(NLysNspeNspe)_4$	ND	ND

Table 4.3. The average retention time and K_b of each peptoid synthesized in this work, as determined by heparin affinity chromatography and isothermal titration calorimetry, respectively. The ITC values of $(NLysNnbNrpe)_1$ and $(NLysNnbNrpe)_2$ were calculated by the equation of the line in Fig. 4.5.

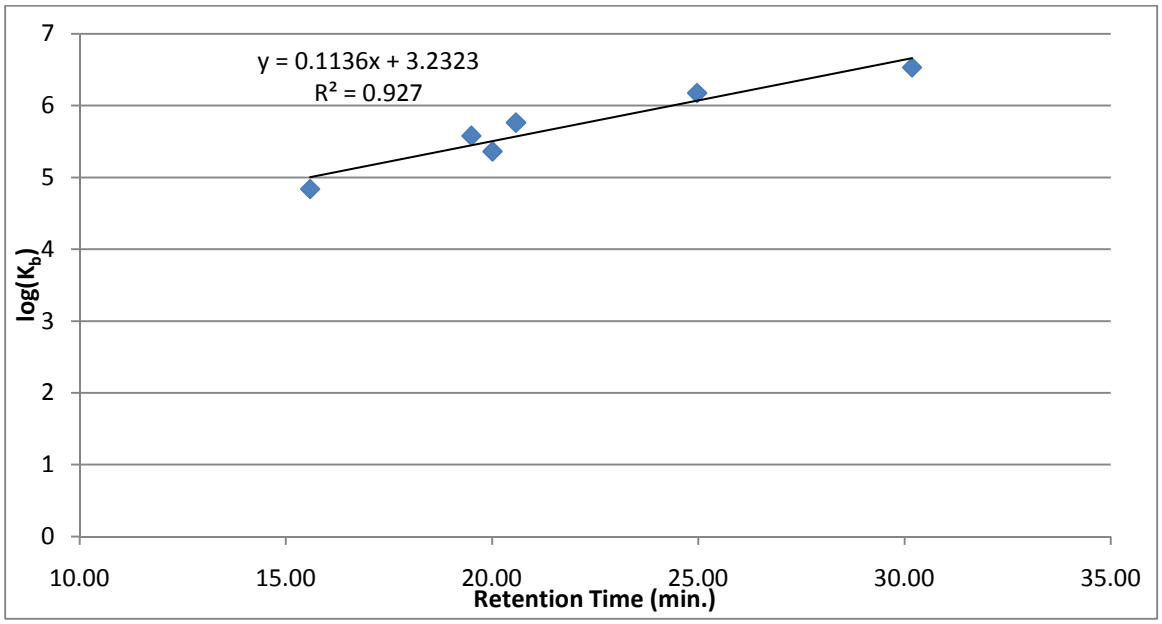

Fig. 4.15. Plot of log(K_b), determined by ITC vs the retention time as measured by heparin affinity chromatography for $(NLys\text{-}Nnb\text{-}Nrpe)_3$, $(NLys\text{-}Nnb\text{-}Nrpe)_4$, $(NLys\text{-}Nnb\text{-}Nspe)_4$, $(NLys\text{-}Nnb\text{-}Nspe)_5$ $(NLys\text{-}Nnb\text{-}Nspe)_6$ and $(NLys\text{-}Nssb\text{-}Nspe)_4$. A linear least squares fit of the data gives the equation: $\log K_b = 0.1206(\text{retention time}) + 2.9917$.

4.3 Discussion

The increases in entropy and enthalpy that are observed upon peptoid-heparin binding are consistent with electrostatic interactions. As discussed in Section 3.1.1, the binding interaction between a polyelectrolyte, such as heparin, and the cationic charges of peptides is accompanied by a counterion release of positively charged ions, such as Na^+, that are associated with the anionic charges of the polyelectrolyte. Although the binding of the ammonium side chain of lysine to the anionic groups of heparin would result in a favorable exothermic binding interaction, it is compensated by an unfavorable endothermic event from the release of counterions. However, the displacement of counterions from heparin drives the binding interaction by increasing the entropy of the system.

Interestingly, there is a significant difference in heparin-binding affinity between $(NLys\text{-}Nnb\text{-}Nspe)_4$ and $(NLys\text{-}Nnb\text{-}Nrpe)_4$. The difference in affinity may be due to the chiral selectivity of heparin, as the chirality of the aromatic residues, and therefore the handedness of the peptoid helix, is the only difference between the two peptoids. Accordingly, heparin has been successfully used for the separation of a variety of chiral drugs when used as a chiral mobile-phase additive, in capillary electrophoresis,[22-25] or as a stationary phase in high-performance liquid chromatography.[26] The chiral selectivity of heparin is thought to originate from the chirality of the carbohydrate subunits and its helical superstructure.[22, 24] This same phenomena most likely contributes to the difference in binding constants determined by ITC and in retention times observed in

heparin affinity chromatography of $(NLys\text{-}Nnb\text{-}Nspe)_4$ and $(NLys\text{-}Nnb\text{-}Nrpe)_4$. Moreover, work done by Stalcup et al.[26] showed that in the enantiomeric separation of chloroquine, the (-) enantiomer exhibited longer retention times when heparin was used as the chiral stationary phase in high-performance liquid chromatography. These results are parallel to the heparin-peptoid binding studies of this work in which the peptoid containing the (-) enantiomer (Nspe) exhibited stronger binding, not only in ITC, but also in heparin affinity chromatography, discussed below. These results are consistent with data acquired in heparin-hybrid binding studies discussed in Chapter 5.

The CD spectrum of $(NLys\text{-}Nssb\text{-}Nspe)_4$ shows that it has a slightly less stable helical structure than $(NLys\text{-}Nnb\text{-}Nspe)_4$ and $(NLys\text{-}Nnb\text{-}Nrpe)_4$. Although ITC data indicates that $(NLys\text{-}Nssb\text{-}Nspe)_4$ binds with slightly more affinity to heparin than $(NLys\text{-}Nnb\text{-}Nrpe)_4$, retention times suggest otherwise. The contradictory data for these peptoids is difficult to explain.

4.4 Summary

According to both the ITC and heparin affinity chromatography data, the most straightforward way to increase the heparin-binding affinity of a peptoid, is to increase its number of cationic residues. The chirality of the aromatic α-chiral amine also plays a part in heparin binding affinity, as peptoids, of a given length and sequence, containing the Nspe residue have a higher heparin-binding affinity than the peptoids containing the Nrpe residue.

According to this work, it is possible to design peptoids with a predictable secondary structure and relative heparin-binding affinity. This is a critical step in the design of drugs for which the modulation of heparin activity can influence the disease process, and in this case, serve as an antidote to heparin's anticoagulant activity. As peptoids have been shown to be bioactive, non-immunogenic, resistant to proteolysis, and easy to synthesize, it seems that peptoids may make a suitable replacement for the drug used to reverse the coagulation effects of heparin, which is currently, protamine.

4.5 References

1. Fowler, S. A.; Blackwell, H. E., *Org. Biomol. chem.* **2009,** *7*, 1508-1524.

2. Wu, C. W.; Sanborn, T. J.; Huang, K.; Zuckermann, R. N.; Barron, A. E., *J. Am. Chem. Soc.* **2001,** *123*, 6778-6784.

3. Armand, P.; Kirshenbaum, K.; Goldsmith, R. A.; Jones-Farr, S.; Barron, A. E.; Truong, K. T.; Dill, K. A.; Mierke, D. F.; Cohen, F. E.; Zuckermann, R. N.; Bradley, E. K., *Proc. Nat. Acad. Sci. U.S.A.* **1998,** *95*, 4309-4314.

4. Wu, C. W.; Kirshenbaum, K.; Sanborn, T. J.; Patch, J. A.; Huang, K.; Dill, K. A.; Zuckermann, R. N.; Barron, A. E., *J. Am. Chem. Soc.* **2003,** *125*, 13525-13530.

5. Sanborn, T. J.; Wu, C. W.; Zuckermann, R. N.; Barron, A. E., *Biopolymers* **2002,** *63*, 12-20.

6. Armand, P.; Kirshenbaum, K.; Falicov, A.; Dunbrack, R. L.; Dill, K. A.; Zuckermann, R. N.; Cohen, F. E., *Fold. Des.* **1997,** *2*, 369-375.

7. Butterfoss, G. L.; Renfrew, P. D.; Kuhlman, G.; Kirshenbaum, K.; Bonneau, R., *J. Am. Chem. Soc.* **2009,** *131*, 16798-16807.

8. Kirshenbaum, K.; Zuckermann, R. N.; Dill, K. A., *Curr. Opin. Struct. Biol.* **1999,** *9*, 530-535.

9. Chongsiriwatana, N. P.; Patch, J. A.; Czyewski, A. M.; Dohm, M. T.; Ivankin, A.; Gidalevitz, D.; Zuckermann, R. N.; Barron, A. E., *Proc. Nat. Acad. Sci. U.S.A.* **2008,** *105*, 2794-2799.

10. Astle, J. M.; Udugamasooriya, D. G.; Smallshaw, J. E.; Kodadek, T., *Int. J. Pept. Res. Ther.* **2008,** *14*, 223-227.

11. Lim, H.; Archer, C. T.; Kodadek, T., *J. Am. Chem. Soc.* **2009,** *129*, 7750-7751.

12. Miller, S. M.; Simon, R. J.; Ng, S.; Zuckermann, R. N.; Kerr, J. M.; Moos, W. H., *Drug Dev. Res.* **1995,** *35*, 20-32.

13. Zuckermann, R. N.; Kerr, J. M.; Kent, S. B. H.; Moos, W. H., *J. Am. Chem. Soc.* **1992,** *114*, 10646-10647.

14. Brown, N. J.; Wu, C. W.; Seurynck-Servoss, S. L.; Barron, A. E., *Biochem.* **2008,** *47*, 1808-1818.

15. Nilsson, G.; Gustafsson, M.; Vandenbussche, G.; Veldhuizen, E.; Griffiths, W. J.; Sjovall, J.; Haagsman, H. P.; Ruysschaert, J. M.; Robertson, B.; Curstedt, T. J., J., *Eur. J. Biochem.* **1998,** *255*, 116-124.

16. Ikegami, M.; Jobe, A. H., *Pediatr. Res.* **1998,** *44*, 860-864.

17. Lee, B.; Chu, T. K.; Dill, K. A.; Zuckermann, R. N., *J. Am. Chem. Soc.* **2008,** *130*, 8847-8855.

18. Berg, J. M.; Godwin, H. A., *Annu. Rev. Biophys. Biomol. Struct.* **1997,** *26*, 357-371.

19. Coleman, J. E., *Annu. Rev. Biochem.* **1992,** *61*, 897-946.

20. Kirshenbaum, K.; Barron, A. E.; Goldsmith, R. A.; Armand, P.; Bradley, E. K.; Truong, K. T.; Dill, K. A.; Cohen, F. E.; Zuckermann, R. N., *Proc. Nat. Acad. Sci. U.S.A.* **1998,** *95*, 4303-4308.

21. Wu, C. W.; Sanborn, T. J.; Zuckermann, R. N.; Barron, A. E., *J. Am. Chem. Soc.* **2001,** *123*, 2958-2963.

22. Stalcup, A. M.; Agyel, N. M., *Anal. Chem.* **1994,** *66*, 3054-3059.

23. Nishi, H.; Nakamura, K.; Nakai, H.; Sato, T., *Anal. Chem.* **1995,** *67*, 2334-2341.

24. Jin, Y.; Stalcup, A. M., *Electrophoresis* **1998,** *19*, 2119-2123.

25. Abushoffa, A. M.; Clark, B. J., *J. Chrom. A* **1995,** *700*, 51-58.

26. Stalcup, A. M.; Gahm, K. H.; Baldueza, *Anal. Chem.* **1996,** *68*, 2248-2250.

Chapter 5

Peptide-Peptoid Hybrid/Heparin Binding Studies

5.1 Introduction

5.1.1. Introduction to Hybrids

Peptide/peptoid hybrids, from here on referred to as hybrids, are a class of peptidomimetics that are similar to peptoids except that natural amino acid residues are incorporated into the backbone chain, Fig. 5.1. Previously, peptide/peptoid hybrids were referred to as peptomers, from *pep*tide-pep*to*id poly*mers*.[1] This, however, would be an incorrect usage of the term as it already had been used to describe cross-linked/polymerized peptide fragments.[2]

The synthesis of hybrids can be realized by a combination of the submonomer method of peptoid synthesis and standard Fmoc-peptide synthesis methodology.[3] The combination of these synthetic methods has been utilized in the creation of combinatorial hybrid libraries.[1, 4] By using a portioning-mixing procedure, a diverse library on a single bead composed of thousands of different hybrids can be generated. The hybrids composing this library can then be readily sequenced using standard Edman degradation chemistry. The portioning-mixing procedure facilitates ease of synthesis and analysis of the hybrid library. Consequently, this approach is considered to improve the drug discovery process by increasing the odds of identifying a lead compound.[1]

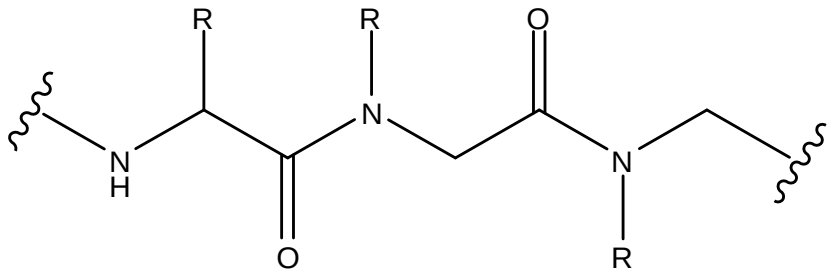

Fig. 5.1. Generic form of a hybrid structural formula. The side chains (R) are of the peptoid monomers if located on the amide nitrogen, and of the amino acid residue if located on the C_α.

Hybrid libraries can also be assembled on a continuous surface. Using a SPOT synthesis technique, which was originally developed for peptide synthesis, hybrids can be readily assembled on cellulose membranes. This method of synthesis was found to be effective in high-throughput parallel solid-phase synthesis of hybrids. After the synthesis is complete, dry-state cleavage of the hybrids can be performed by UV irradiation, made amenable by the use of a photo-labile linker.[4]

5.1.2. Biological Activity of Hybrids

Goodman et al. reported the first use of hybrids in the synthesis of a biomimetic structure.[5, 6] In this work, N-isobutylglycine (NLeu) was incorporated into trimer repeats of Gly-[(Gly-Pro-NLeu)$_6$-NH$_2$]$_3$ and Gly-[(Gly-Pro-NLeu)$_9$-NH$_2$]$_3$, which are similar to the triple-helical portions of collagen. Both sequences were synthesized on a Kemp triacid template. Molecular modeling and subsequent analysis by circular dichroism and ^{1}H-NMR confirm the assembling of these hybrids into collagen-like triple helices consisting

of archetypal polyproline II-like backbone conformations. The authors indicate that the stability of these structures provide the foundation for the design of collagen-like biomaterials.

The design of hybrids as antimicrobial agents is also important, as microbes are becoming increasingly resistant to traditional antibiotics, as reported by Hansen, et al.[7] In this study, Hansen and coworkers developed short, novel lysine-peptoid hybrids which were designed to have amphipathic features: cationic charges located on one face of the helical structure and hydrophobic residues comprising the other. The characteristics of the hybrid design mimic that of nearly all antimicrobial peptides. This type of motif is thought to be important in the antimicrobial agent's ability to distinguish between the negatively charged nature of bacterial cell membranes and the zwitterionic membrane of mammalian cells, resulting in low hemolytic activity. Several hybrids developed in this study show good antimicrobial activity against *S. aureus* and *E. coli,* and at the same time, demonstrating low hemolytic activity. In further studies, these same authors designed a series of lysine-peptoid hybrids to demonstrate their resistance to proteolytic degradation. [3] To allow for complete digestion, these hybrids were incubated with trypsin for 18 hrs. Analysis of digestion fragments indicated that six out of the nine hybrids were completely resistant to tryspin, Fig. 5.2. The results reveal that the lysine-peptoid amide bond imparts resistance against degradation by trypsin.

Biologically active hybrids have also been developed based on short peptide sequences occurring naturally within plants,[8] bacteria,[9] and animals.[10, 11] Two hybrids

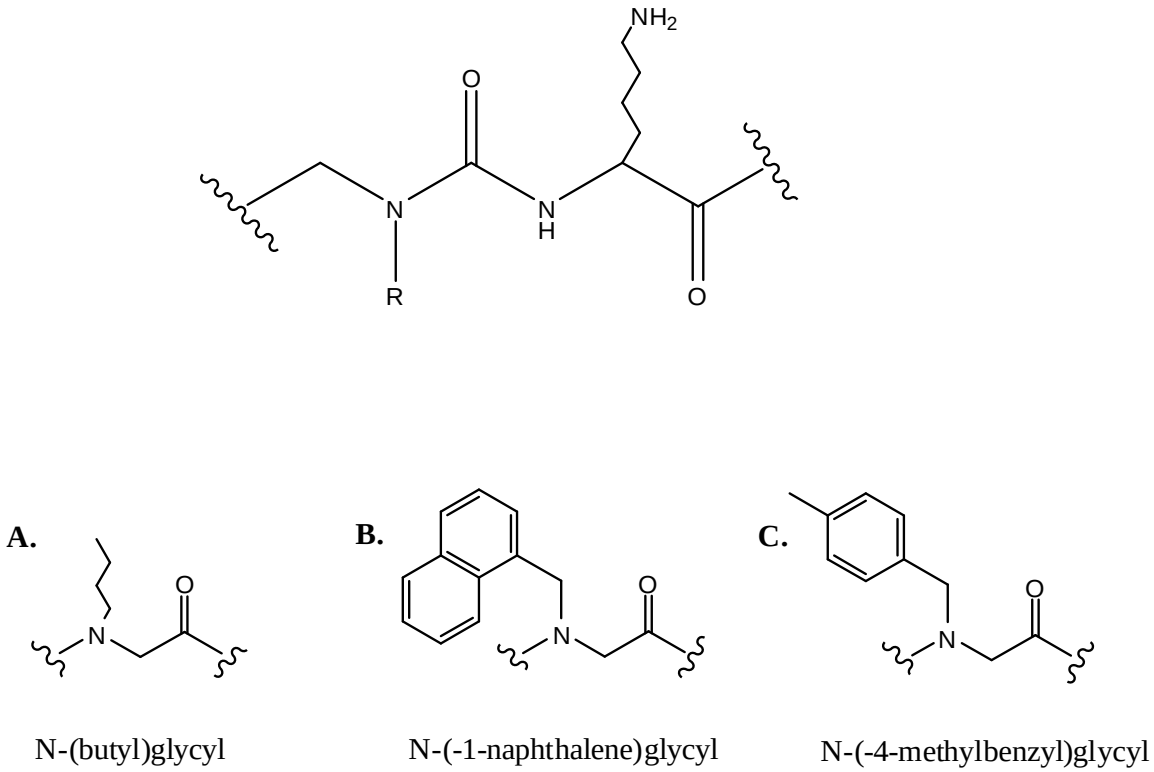

Fig. 5.2. Structural formula of the Lysine-peptoid amide bond of proteolytic resistant hybrids. R is either **A.** N-(butyl)glycyl, **B.** N-(-1-naphthalene)glycyl, or **C.** N-(-4-methylbenzyl)glycyl.

based on the short peptide, sunflower trypsin inhibitor-1 (SFTI-1), a member of the Bowman-Birk family of trypsin inhibitors, were designed so as to study their activity as serine protease inhibitors. Three analogues of SFTI-1 were evaluated: an acyclic version of the 14-residue peptide (which has equal activity as the native version), and two hybrids with the Lys5 residue replaced with either an NLys or an N-benzylglycine (Nphe) residue, Fig. 5.3. Residues Lys5 and Ser6 form the peptide bond which is thought to be the active site of the inhibitor. Enzymatic studies show that the hybrid with the NLys residue demonstrated potent inhibition of the trypsin protease. The analogue containing the Nphe residue was very effective in the inhibition of the chymotrypsin protease. Structural elucidation studies using NMR also showed no significant structural variation in the hybrids as compared to the acyclic version of the native peptide.

Proteolytic susceptibility assays demonstrated that the amide bond of the reactive site of both hybrids was completely protease resistant even after 72 hrs of incubation with catalytic amounts of the enzymes; the half-life of the reactive site-amide bond of the acyclic SFTI-1 version was only 2.7 hrs. The authors indicate that hybrids of this type may be useful as therapeutic agents, as research has revealed that Bowman-Birk type inhibitors exhibit anticarcinogenic activity.

Macrocyclic hybrids have also been designed to mimic autoinducing peptide-I (AIP-I) used in quorum sensing by *Staphylococcus aureus*.[9] AIP-I binds to a transmembrane receptor (AgrC-I) on *S. aureus*, which modulates virulence by intracellular signaling. One of the hybrid analogues, shown in Fig. 5.4, was found to

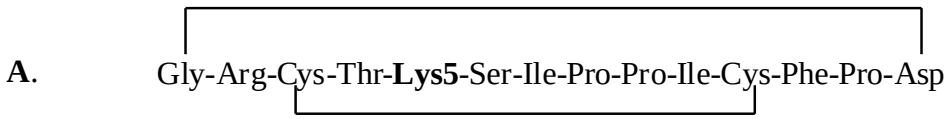

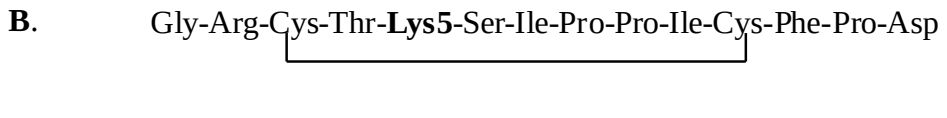

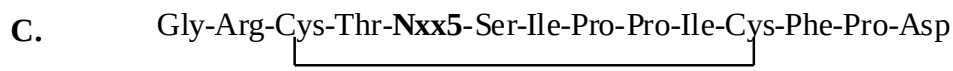

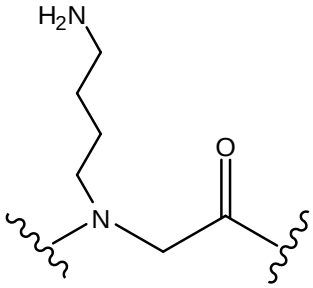

N-(4-aminobutyl)-glycine

(NLys)

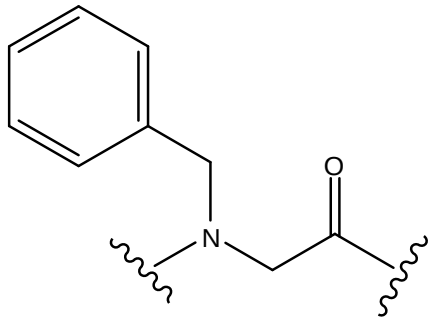

N-benzylglycine

(Nphe)

Fig. 5.3. Sequence of **A.** native SFTI-1, **B.** acyclic version of SFTI-1, and **C.** hybrid analogue of SFTI-1 containing either an N-(4-aminobutyl)-glycine (NLys) or an N-benzylglycine (Nphe) residue in the Lys5 position.

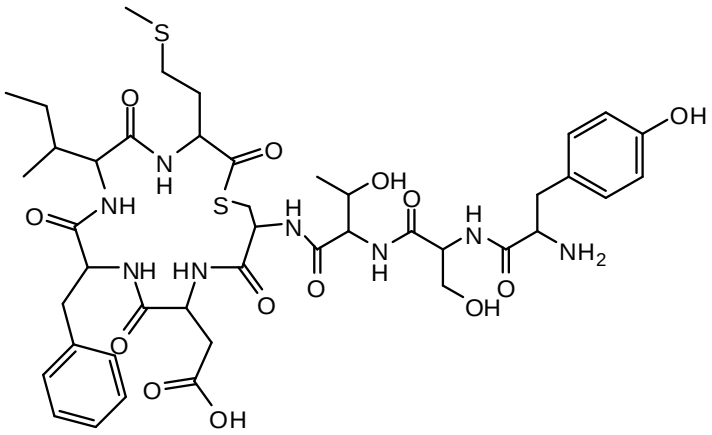

A. *S. aureus* AIP1

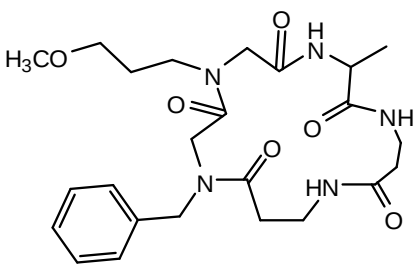

B. Simplified Hybrid

Fig. 5.4.A. Autoinducing peptide-I (AIP-I) used in quorum sensing by *Staphylococcus aureus*. **B.** Macrocyclic hybrid analogue which was shown to stimulate a phenotype associated with inhibition of virulence of *S. aureus* by binding to the transmembrane receptor, AgrC-I.

stimulate a phenotype associated with AgrC-I inhibition. The data shows the feasibility of hybrids as a new type of antibiotic.

Ovadia et al. designed a library of hybrids in which linear and, the first reported, backbone cyclic hybrids were synthesized. The hybrids were based on a peptide sequence that was found to specifically activate the melanocortin-4-receptor (MC4R), Fig. 5.5, which is important for the regulation of energy homeostasis and appetite.[12] The results indicate the potential of these hybrids as agonists of MC4R. Moreover, cyclic backbone hybrids demonstrated enhanced proteolytic resistance and intestinal permeability in *in vitro* studies as compared to their linear hybrid counterparts, and the parent peptide.

The authors state that the advantage of hybrids over peptoids is that converting peptides to hybrids reduces transformations in essential amino acids comprising the lead motif. The lesser degree of transformation may result in an analogue with improved pharmacologic properties.

A search of the literature has yet to reveal any studies on hybrid-heparin binding interactions. However, there are a multitude of studies, some mentioned above, on the capacity of hybrids to mimic peptides that can modulate biological activity. Hybrids have an advantage in that they are less susceptible to proteolytic degradation which may enhance their effectiveness as therapeutic agents. With this in mind, a series of hybrids have been synthesized. Their sequences are shown in Table 5.1, and their binding

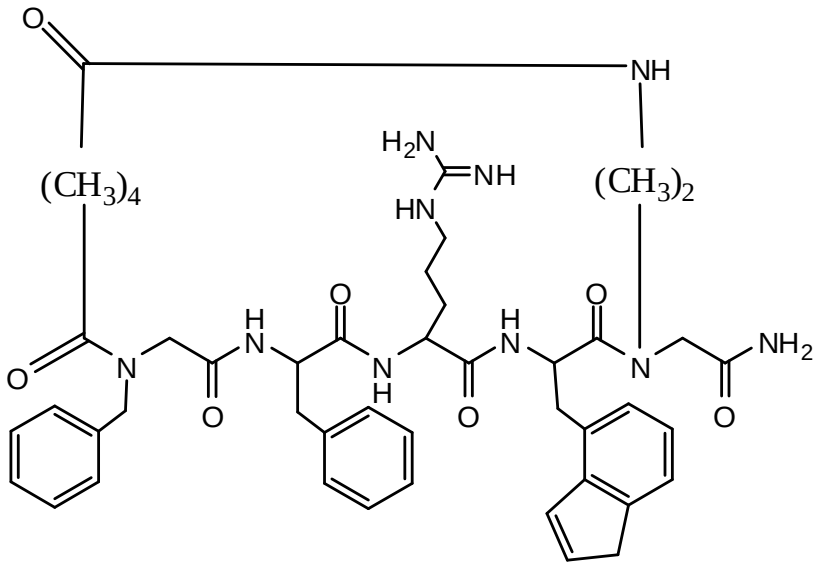

Fig. 5.5. Cyclic hybrid which was found to specifically stimulate the melanocortin-4-receptor (MC4R).

Hybrid Sequence
$(K\text{-}Nnb\text{-}Nrpe)_n\text{-}NH_2$ n = 1-4
$(K\text{-}Nnb\text{-}Nspe)_n\text{-}NH_2$ n = 4-6
$(R\text{-}Nnb\text{-}Nrpe)_n\text{-}NH_2$ n = 1-4
$(Orn\text{-}Nnb\text{-}Nspe)_4\text{-}NH_2$

Table 5.1. List of hybrids synthesized in this work, where n is the number of repeat trimer sequences, K is the amino acid lysine, R the amino acid arginine, Orn the non-natural amino acid orninthine and Nnb, Nspe and Nrpe are peptoid monomers, Fig. 2.7.

interaction with heparin has been characterized. Several examples of hybrid structures are shown in Fig.5.6.

The hybrids were designed based on the peptoid trimer repeat sequence in Chapter 4, $(NLys\text{-}Nnb\text{-}Nspe)_n\text{-}NH_2$, except that a lysine or arginine amino acid is incorporated in place of the NLys residue. The hybrid is therefore composed of a sequence with a chiral peptoid monomer at every third residue, in addition to the chiral Nspe side chain, which should impart to it a stable helical secondary structure. Cationic amino acids, either lysine or arginine, are included for every third residue. This should render the hybrid amphiphilic, with a face of cationic charge which would facilitate electrostatic binding with the anionic groups of heparin.

In chapter 3, it was found that arginine-containing peptides have a higher binding affinity to heparin than the corresponding lysine-containing peptides. As the guanidinium group of arginine is expected to bind more tightly to heparin, than the

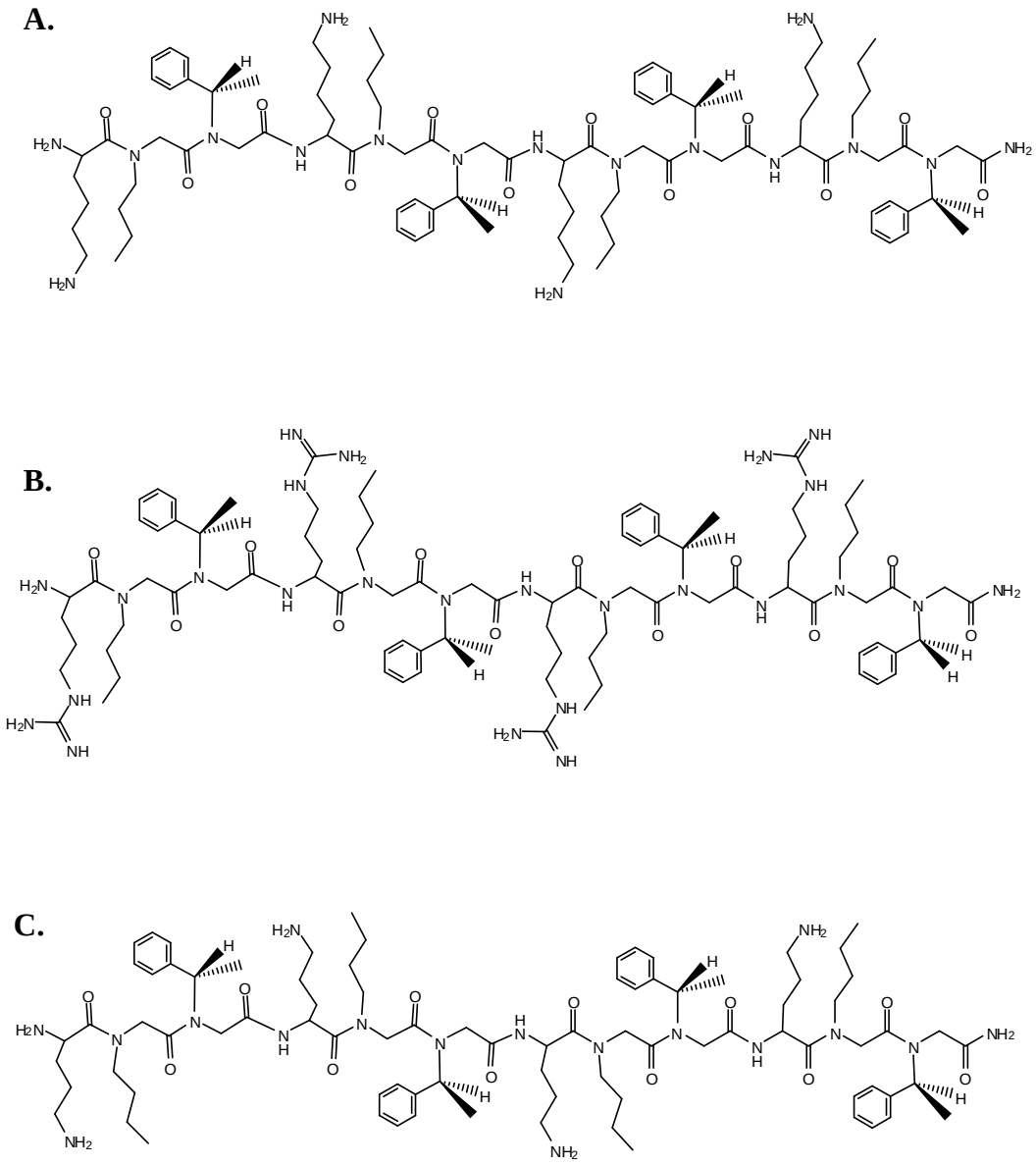

Fig. 5.6. Structural formulas of: **A.** (K-Nnb-Nspe)$_4$-NH$_2$, **B.** (R-Nnb-Nrpe)$_4$-NH$_2$, and **C.** (Orn-Nnb-Nspe)$_4$-NH$_2$.

ammonium group of lysine, Section 3.3, it is expected that by incorporating an arginine amino acid into the hybrid sequence, a higher heparin-binding affinity will result when compared to the heparin-binding affinity of hybrids containing lysine.

To determine if the chirality of peptoid monomers affects the heparin-binding of the hybrids, either Nspe or Nrpe, Fig. 2.7, were incorporated into the hybrid sequence. Ornithine was also included, in place of lysine, to determine the effect a shorter chain length of the cationic side chain would have on heparin-binding.

Heparin is universally used as an anticoagulant and, as discussed in Section 1.4.4.1, there is a need to develop a safer drug to reverse its anticoagulant activity. Currently, Protamine is the drug of choice used for the purpose of inactivating heparin's effects, as reported in Chapter 1. However, there are a number of deleterious side-effects associated with its use. The primary interacting force between heparin and Protamine is electrostatic, so the hybrids were designed so as to take advantage of this type of interaction. Hybrids, therefore, may have potential as a suitable replacement for Protamine.

5.2 Results

5.2.1 Hybrid Synthesis

The synthesis of the hybrids was accomplished by a combination of peptide and peptoid methodologies, as discussed in Section 2.3.2. To form the various peptoid monomers, two steps were taken, (i) the acylation of the resin or previous monomer

building block, (ii), the addition of the amino side chain via an S_N2 reaction. The addition of the side chain is an efficient process resulting in a practical yield after approximately 2 hrs of coupling time.

However, the coupling of the amino acids, lysine or arginine, to the secondary amine of a peptoid monomer during hybrid synthesis was found to be less efficient. This is probably due to steric interactions between the side chain of the peptoid monomer, and the bulky side chain and its protecting group (Fig. 2.4), and the amino acid activating agent of the incoming amino acid, Fig. 5.7. Therefore, coupling time of the amino acid to the secondary amine had to be extended to 24 hrs to result in a practical yield.

5.2.2 Binding Constants

5.2.2.1 Lysine-Containing and Ornithine-Containing Hybrids.

Isothermal titration calorimetry (ITC) shows that as with peptoids, there is an increase in heparin-binding affinity of hybrids as the chain length and number of cationic residues increase in the hybrids. Figs. 5.8 and 5.9 are an example of data acquired by ITC. Again, hybrids with lysine residues show positive entropy and enthalpy changes, i.e. endothermic, associated with an electrostatic interaction with heparin. Hybrids (K-Nnb-Nrpe)$_1$-NH_2 and (K-Nnb-Nrpe)$_2$-NH_2 were too weak in their binding interaction with heparin to quantitatively determine a binding constant by ITC. (K-Nnb-Nrpe)$_3$-NH_2 was the smallest lysine-containing hybrid whose binding constant was measurable by ITC

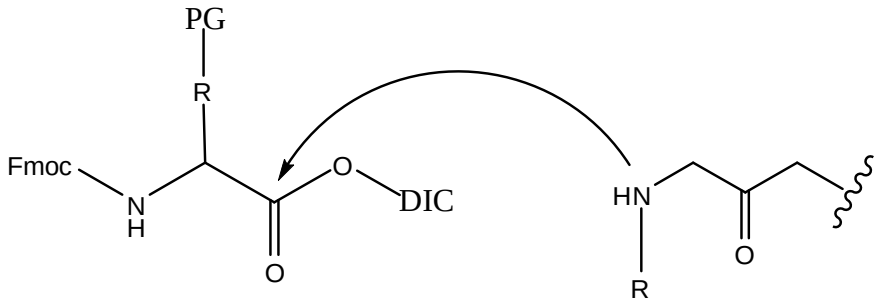

Fig. 5.7. Steric hinderance between the side chain (R) and side chain protecting group (PG), the activating agent (DIC) of the incoming amino acid, and the side chain (R) of the peptoid monomer

with a K_b of $2.5X10^4$ M^{-1}. Interestingly, there was a significant difference in binding between (K-Nnb-Nrpe)$_4$-NH_2 and (K-Nnb-Nspe)$_4$-NH_2 with a K_b of $1.7X10^5$ and $2.5X10^5$ M^{-1}, respectively. (K-Nnb-Nspe)$_6$-NH_2 has the largest binding constant with a K_b of $5.5X10^6$ M^{-1}.

To compare differences in binding with differences in length of the cationic side-chain, ornithine residues were used in place of lysine. The binding interaction of (Orn-Nnb-Nspe)$_4$-NH_2 with heparin resulted in a K_b of $3.5X10^5$ M^{-1} which is slightly higher than that of (K-Nnb-Nspe)$_4$-NH_2. The measured K_b of (Orn-Nnb-Nspe)$_4$-NH_2 may be unreliable (data not shown) as the binding affinity results from heparin affinity chromatography are contradictory, as will be discussed below. A summary of the ITC results of the lysine- and ornithine-containing hybrids is given in Table 5.2.

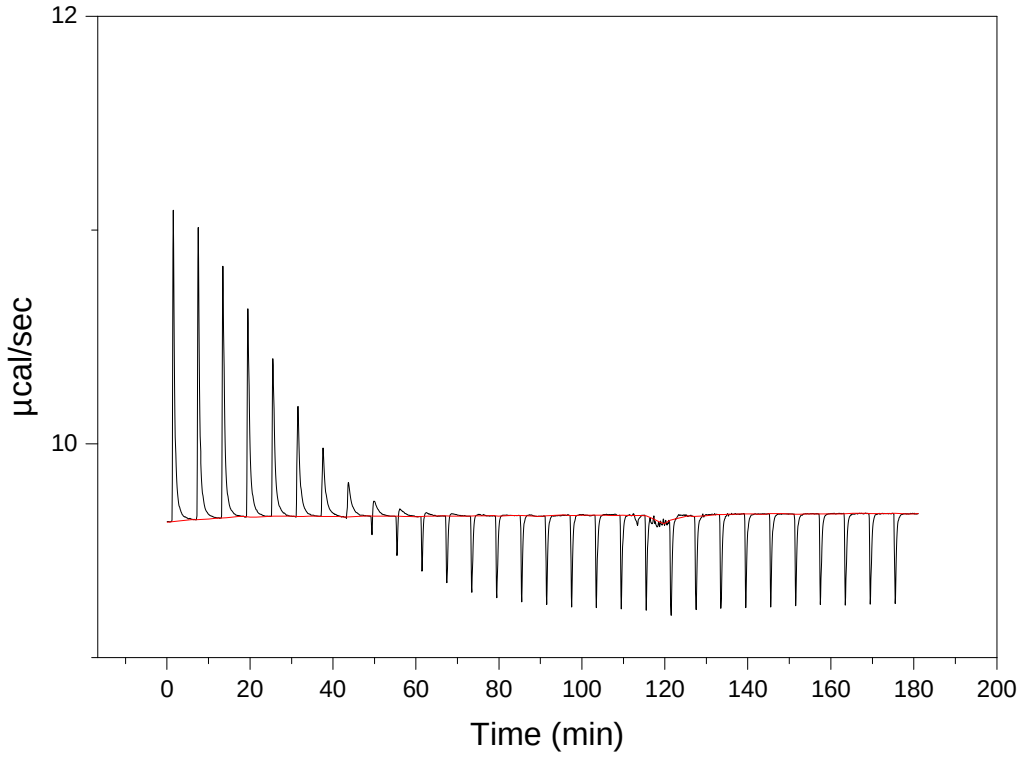

Fig. 5.8. Raw data for the titration of 0.4 mM (K-Nnb-Nrpe)$_3$-NH$_2$ with 0.5 mM heparin. Parameters are: number of injections, 30; cell temperature,25 ^{o}C; injection volume, 6 µL; and spacing between injections is 360 sec. Upward deflecting peaks show an increase in power to the sample cell indicating an endothermic binding interaction.

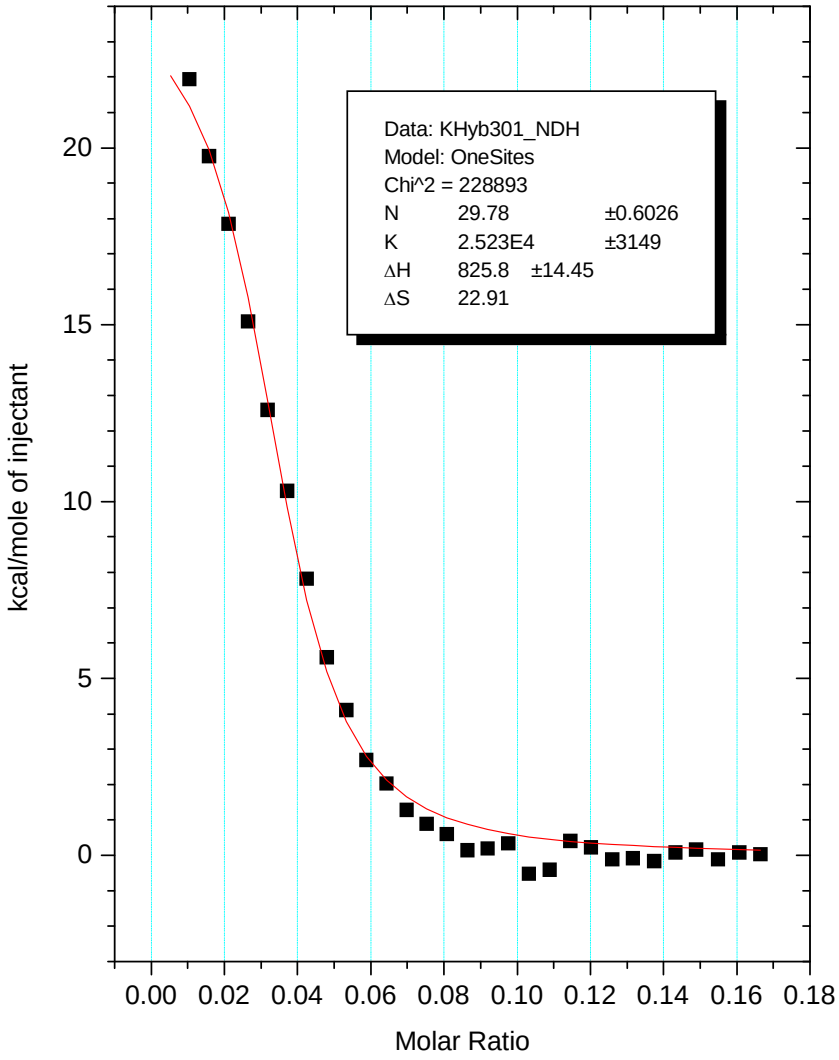

Fig. 5.9. Integrated data of Fig. 5.8 fit to a single-set-of sites model resulting in the thermodynamic values given in the figure.

Hybrid	$K_b(M^{-1})$	N	ΔH(cal/mol)	ΔS(cal/mol·°C)
$(K\text{-}Nnb\text{-}Nrpe)_1\text{-}NH_2$	ND	ND	ND	ND
$(K\text{-}Nnb\text{-}Nrpe)_2\text{-}NH_2$	ND	ND	ND	ND
$(K\text{-}Nnb\text{-}Nrpe)_3\text{-}NH_2$	$(2.5 \pm .1)X10^4$	30 ± .2	830 ± 21	23.91 ± .04
$(K\text{-}Nnb\text{-}Nrpe)_4\text{-}NH_2$	$(1.7 \pm .09)X10^5$	20.3 ± .1	1710 ± 20	32.3 ± .1
$(K\text{-}Nnb\text{-}Nspe)_4\text{-}NH_2$	$(2.5 \pm .08)X10^5$	18.7 ± .02	1670 ± 17	30.33 ± .03
$(K\text{-}Nnb\text{-}Nspe)_5\text{-}NH_2$	$(2.2\pm.3)X10^6$	13.4 ± .09	2200 ± 6	36.4 ± .3
$(K\text{-}Nnb\text{-}Nspe)_6\text{-}NH_2$	$(5.5 \pm .5)X10^6$	16.4 ± .2	1850 ± 56	37.1 ± .4
$(Orn\text{-}Nnb\text{-}Nspe)_4\text{-}NH_2$	$(3.5 \pm .8)X10^5$	22.4 ± .1	810 ± 221	28.2 ± .2

Table 5.2. Thermodynamic values for the binding of each of the lysine- and ornithine-containing hybrids by heparin, as determined by ITC. K_b is the measured binding constant, N is the number of binding sites that the hybrids can occupy on the heparin oligosaccharide, ΔH is the change in enthalpy and ΔS is the change in entropy, upon heparin binding. Values that could not be determined are labeled as (ND).

5.2.2.2 Arginine-Containing Hybrids.

The arginine-containing hybrids also exhibit an increase of binding affinity to heparin with a corresponding increase in chain length and number of cationic residues. ITC measurements show that, as with peptides, arginine-containing hybrids bind with a higher affinity to heparin than their lysine-containing counterparts. Figs. 5.10 and 5.11 show an example of typical ITC data of $(R\text{-}Nnb\text{-}Nrpe)_3\text{-}NH_2$. Similarly, as for $(K\text{-}Nnb\text{-}Nrpe)_1\text{-}NH_2$ and $(K\text{-}Nnb\text{-}Nrpe)_2\text{-}NH_2$, ITC results for $(R\text{-}Nnb\text{-}Nrpe)_1\text{-}NH_2$ and $(R\text{-}Nnb\text{-}Nrpe)_2\text{-}NH_2$ could not be obtained due to weak heparin-binding. $(R\text{-}Nnb\text{-}Nrpe)_4\text{-}NH_2$ gave the largest binding constant of the arginine-containing hybrids with a K_b of $8.5X10^5$ M^{-1}. A summary of the ITC results of the arginine-containing hybrids is given in Table 5.3.

5.2.2 Circular Dichroism

The CD spectra of hybrids containing the Nrpe residue show maximum absorbances at about 200 and 220 nm. This is indicative of a right-handed polyproline type-I helical structure similar to the Nrpe-containing peptoids discussed in Chapter 4. However, it appears that hybrids containing the L-amino acid, lysine, do not possess as stable a secondary structure as the corresponding peptoids as shown in Fig. 5.12. This is indicated by the lack of circular dichroism of the $(K\text{-}Nnb\text{-}Nrpe)_1\text{-}NH_2$ hybrid as compared to the CD spectra of $(NLys\text{-}Nnb\text{-}Nrpe)_1\text{-}NH_2$ which shows a nascent helical structure. However, as the chain length increases, the Nrpe-containing hybrids demonstrate

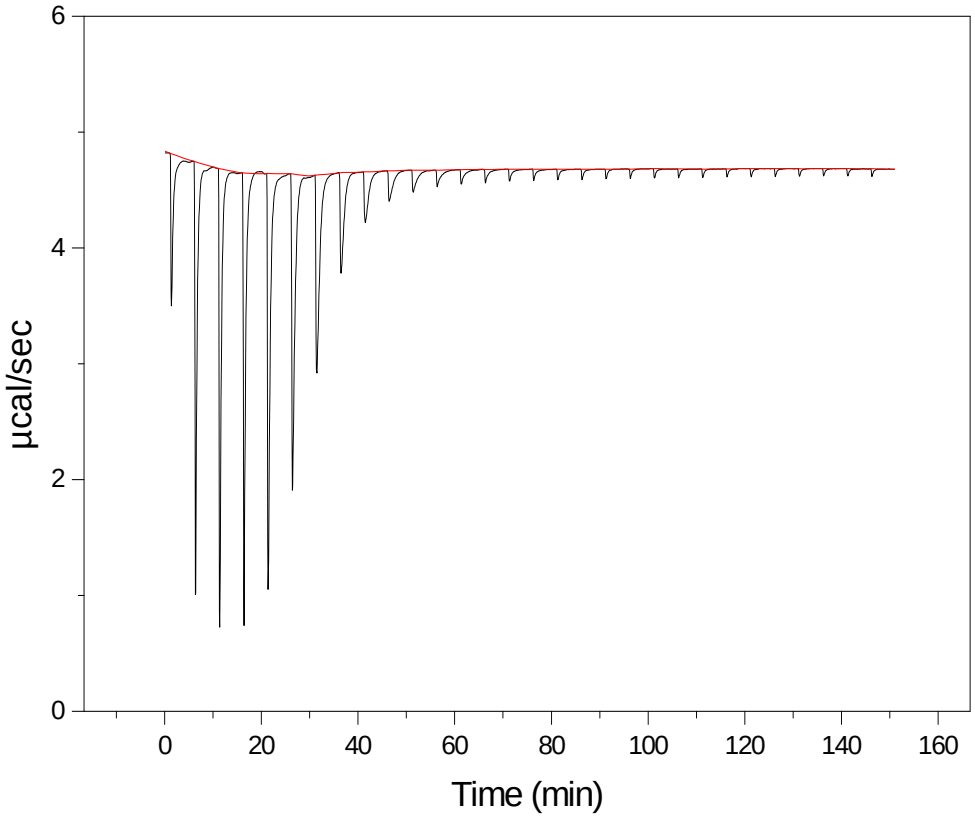

Fig. 5.10. Raw data for the titration of 0.4 mM (R-Nnb-Nrpe)$_3$-NH$_2$ with 1.4 mM heparin. Parameters are: number of injections, 30; cell temperature, 25 ^{o}C; injection volume, 10 µL; and spacing between injections is 300 sec. Downward deflecting peaks show a decrease in power to the sample cell indicating that heat is being evolved by the binding interaction.

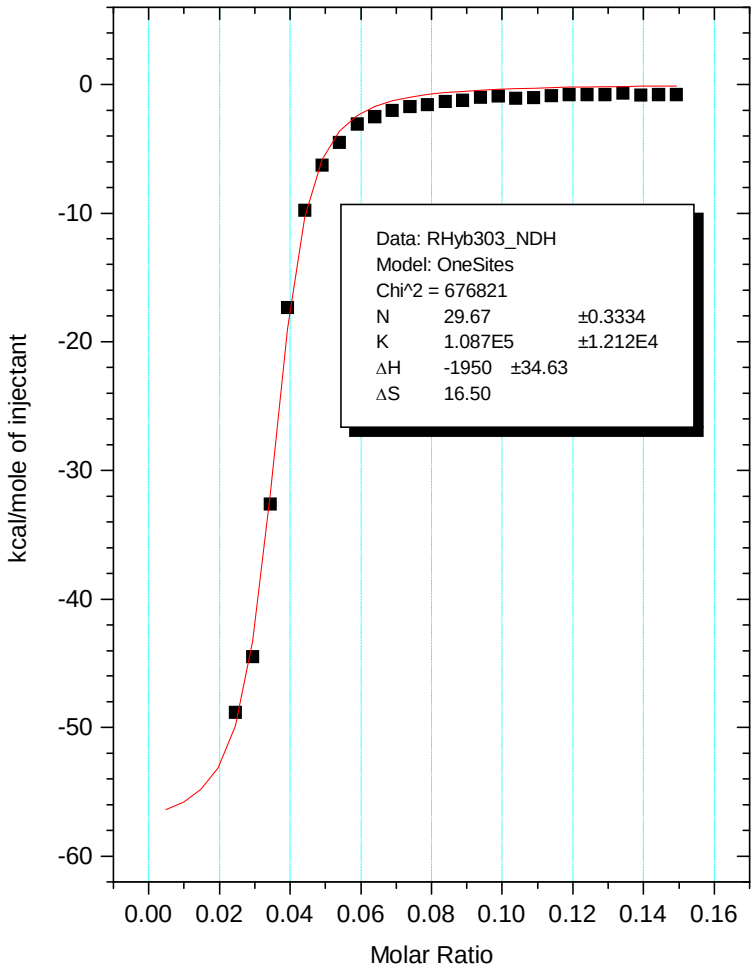

Fig. 5.11. Integrated data of Fig. 5.10 fit to a single-set-of sites model resulting in thermodynamic values given in the figure.

Hybrid	$K_b(M^{-1})$	N	ΔH(cal/mol)	ΔS(cal/mol·°C)
$(R\text{-}Nnb\text{-}Nrpe)_1\text{-}NH_2$	ND	ND	ND	ND
$(R\text{-}Nnb\text{-}Nrpe)_2\text{-}NH_2$	ND	ND	ND	ND
$(R\text{-}Nnb\text{-}Nrpe)_3\text{-}NH_2$	$(9.4 \pm 1.4)X10^4$	30.9 ± 1	-2030 ± 87	15.9 ± .6
$(R\text{-}Nnb\text{-}Nrpe)_4\text{-}NH_2$	$(8.5 \pm 2.0)X10^5$	18.1 ± .2	-3170 ± 140	16.3 ± .5

Table 5.3. Thermodynamic values for each of the arginine-containing hybrids, as determined by ITC. K_b is the measured binding constant, N is the number of binding sites that the hybrids can occupy on the heparin oligosaccharide, ΔH is the change in enthalpy and ΔS is the change in entropy, upon heparin binding. Values that could not be determined are labeled as (ND). $(R\text{-}Nnb\text{-}Nrpe)_3\text{-}NH_2$ values are the average of duplicate trails with the associated ranges. $(R\text{-}Nnb\text{-}Nrpe)_4\text{-}NH_2$ values are the average of triplicate trails with the associated standard deviation.

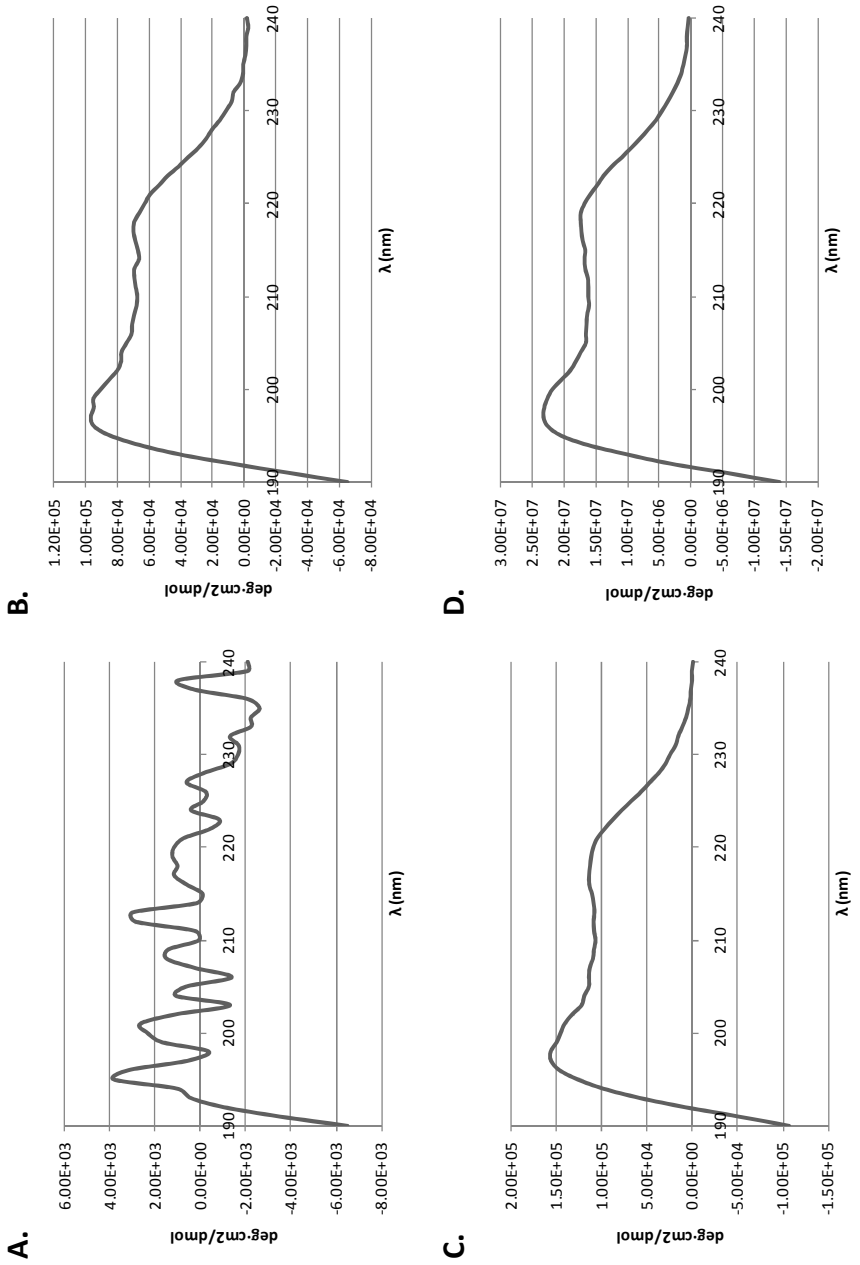

Fig. 5.12. CD spectra of **A.** (K-Nnb-Nrpe)$_1$-NH$_2$, for which no CD signature was observed, **B.** (K-Nnb-Nrpe)$_2$-NH$_2$, **C.** (K-Nnb-Nrpe)$_3$-NH$_2$, and **D.** (K-Nnb-Nrpe)$_4$-NH$_2$, which show maximum absorbances at about 200 and 220 nm, typical of polyproline I-type helices. CD samples were 100 µM hybrid.

increased helical stability as revealed by the increase in absorbance bands at about 200 and 220 nm. This is to be expected as stability of secondary structure can be a cooperative event.[13]

The CD spectra of the Nspe-containing hybrids, Fig. 5.13, also show a CD signature of a polyproline type-1 helix, but of opposite handedness. However, a comparison of the CD spectra of (K-Nnb-Nrpe)$_4$-NH$_2$ to that of (K-Nnb-Nspe)$_4$-NH$_2$ show that the intensities of the absorption bands are not equal. In fact, (K-Nnb-Nrpe)$_4$-NH$_2$ has a more intense CD spectrum indicating a more stable secondary structure. This may be due to the chirality of the L-lysine residue. The side chain on the α-carbon of the L-lysine residue may be in a position to sterically interact with the phenyl group of the adjacent Nrpe side chain. This may enhance the helical structure of Nrpe-containing hybrids by adding to the steric forces critical to forming a right-handed helix. This would be difficult to know since the actual positions of the lysine side chain and the phenyl groups of the peptoid monomers, relative to each other, is not known. The CD spectrum of (K-Nnb-Nrpe)$_4$-NH$_2$ is also significantly more intense than its peptoid counterpart, (NLys-Nnb-Nspe)$_4$-NH$_2$.

Arginine also appears to have a stabilizing effect on secondary structure. This is evident in the CD spectrum of (R-Nnb-Nrpe)$_1$-NH$_2$, Fig. 5.14, which shows that this hybrid conforms to a nascent polyproline type-I secondary structure. In contrast, (K-Nnb-Nrpe)$_1$-NH$_2$ shows no CD signature. This added stability may be due to increased steric interactions involving the slightly bulkier guanidinium group of the arginine side

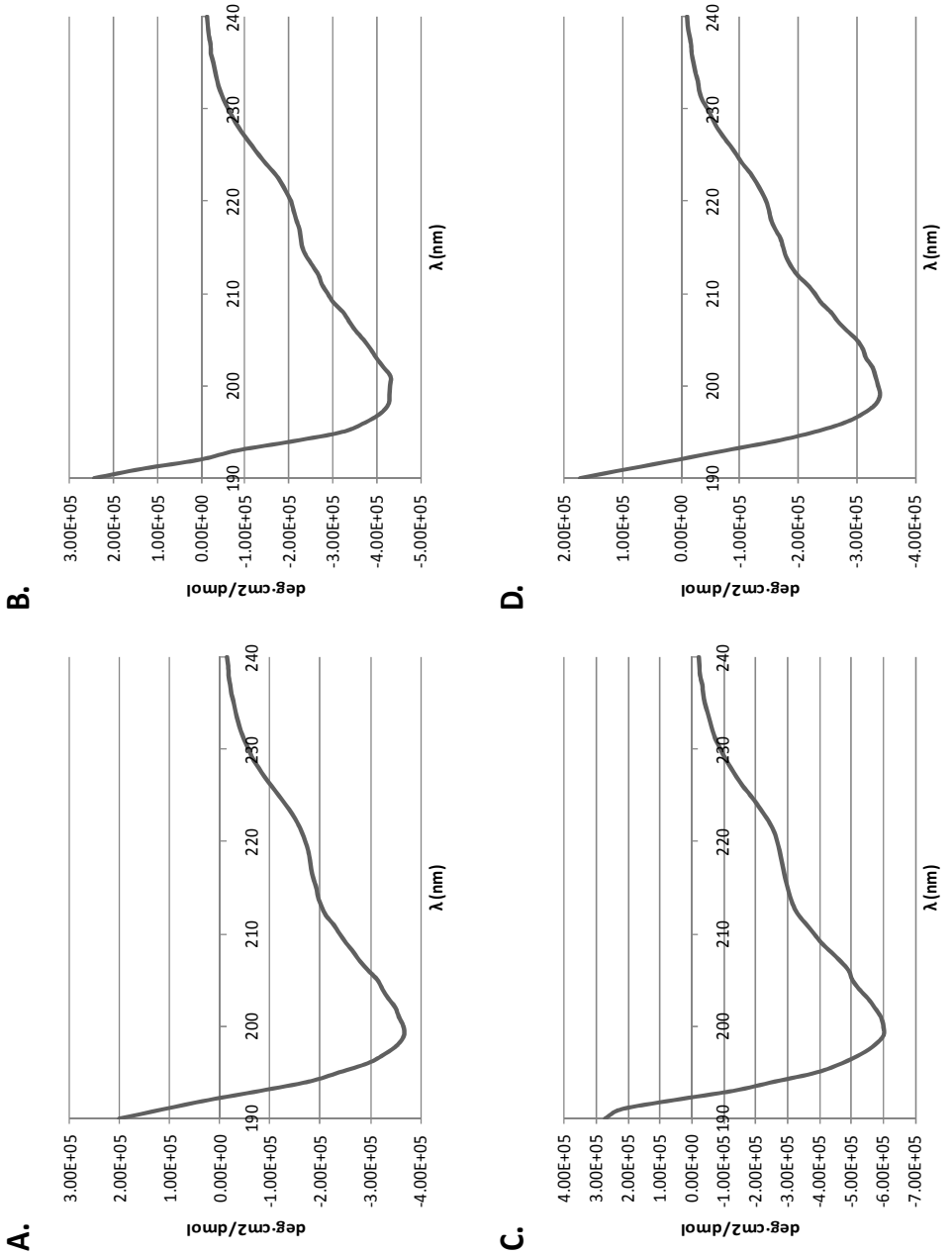

Fig. 5.13. CD spectra of **A.** (K-Nnb-Nspe)$_4$-NH$_2$, **B.** (K-Nnb-Nspe)$_5$-NH$_2$, **C.** (K-Nnb-Nspe)$_6$-NH$_2$, and **D.** (Orn-Nnb-Nspe)$_4$-NH$_2$, Which show maximum absorbances at about 200 and 220 nm, typical of polyproline I-type helices. CD samples were 100 µM hybrid.

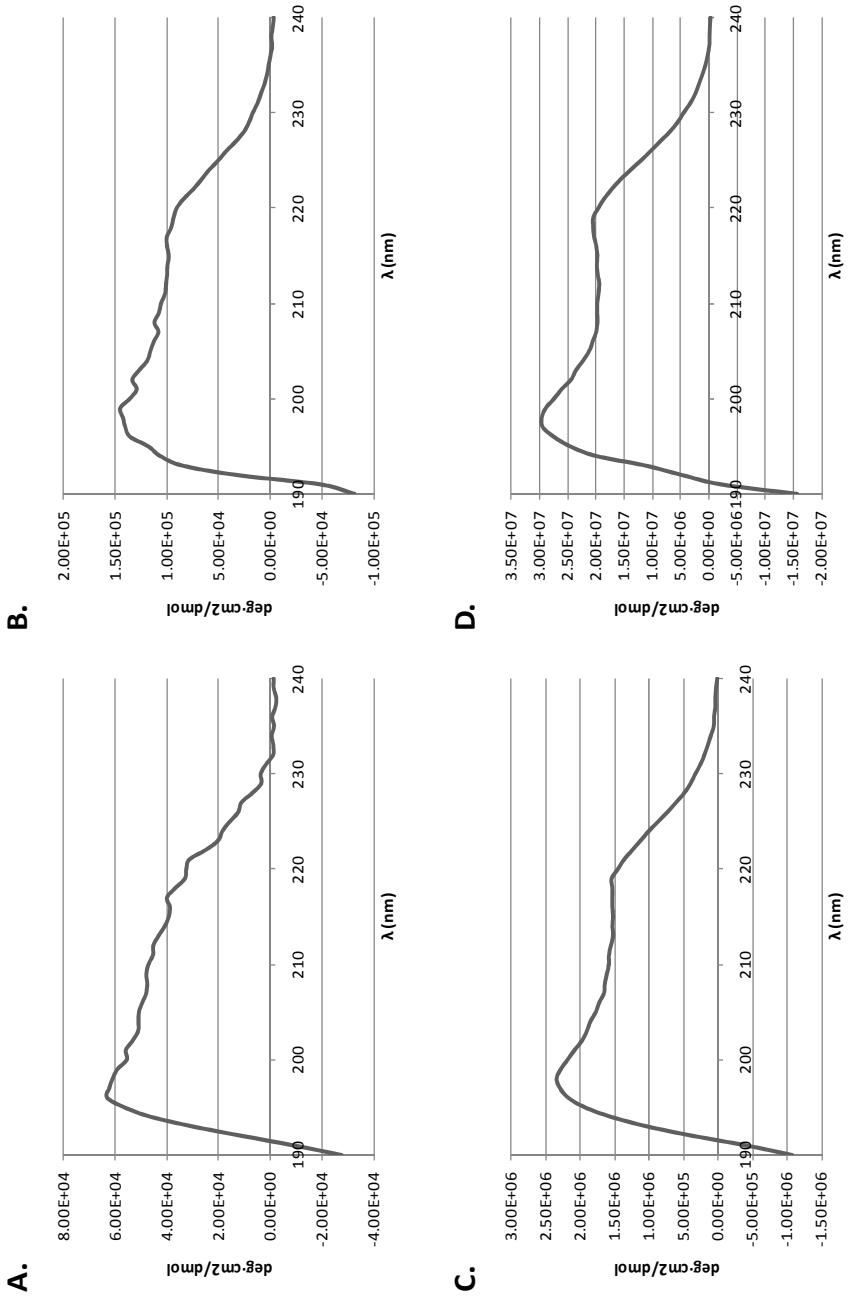

Fig. 5.14. CD spectra of **A.** (R-Nnb-Nrpe)$_1$-NH$_2$, **B.** (R-Nnb-Nrpe)$_2$-NH$_2$, **C.** (R-Nnb-Nrpe)$_3$-NH$_2$, and **D.** (R-Nnb-Nrpe)$_4$-NH$_2$, Which show maximum absorbances at about 200 and 220 nm, typical of polyproline I-type helices. CD samples were 100 µM hybrid.

chain. This enhanced stability may be due not only to its chrirality, but also to it being more bulky than the ammonium group of the lysine residue. CD spectra also show a slightly more intense CD signature of (R-Nnb-Nrpe)$_4$-NH_2 as compared to (K-Nnb-Nrpe)$_4$-NH_2.

5.2.3 Heparin Affinity Chromatography

As expected, hybrid-heparin binding data from heparin affinity chromatography show that as the chain length, and therefore, number of cationic residues, increases, so do the retention times of the hybrids in the column, Table 5.4. Fig. 5.15 shows an example of a heparin affinity chromatogram. Although a quantitative binding constant could not be determined for (K-Nnb-Nrpe)$_1$-NH_2 by ITC, its relative binding affinity for heparin could be estimated by heparin affinity chromatagraphy. As it has the smallest retention time, 13.86 min. of the hybrid studies, it also has the lowest heparin-binding affinity of the hybrid compounds.

Although hybrids (K-Nnb-Nrpe)$_4$-NH_2 and (K-Nnb-Nspe)$_4$-NH_2 are similar in sequence, there is a significant difference in heparin binding affinity between them, with retention times of 18.29 and 19.41 min. respectively. This difference, as discussed in Section 4.3, is thought to originate from the differences in interactions between the different chiral centers of the Nrpe and Nspe residues, and the chirality of the heparin subunits and its helical superstructure. Studies have shown that heparin is capable of

Hybrid	Avg. RT (min.)	Avg. K_b (M^{-1})
$(K\text{-}Nnb\text{-}Nrpe)_1\text{-}NH_2$	3.66	604
$(K\text{-}Nnb\text{-}Nrpe)_2\text{-}NH_2$	8.40	$3.8X10^3$
$(K\text{-}Nnb\text{-}Nrpe)_3\text{-}NH_2$	13.86	$2.5X10^4$
$(K\text{-}Nnb\text{-}Nrpe)_4\text{-}NH_2$	18.29	$1.7X10^5$
$(K\text{-}Nnb\text{-}Nspe)_4\text{-}NH_2$	19.41	$2.5X10^5$
$(K\text{-}Nnb\text{-}Nspe)_5\text{-}NH_2$	22.51	$2.2X10^6$
$(K\text{-}Nnb\text{-}Nspe)_6\text{-}NH_2$	27.25	$5.5X10^6$
$(R\text{-}Nnb\text{-}Nrpe)_1\text{-}NH_2$	4.12	723
$(R\text{-}Nnb\text{-}Nrpe)_2\text{-}NH_2$	10.75	$9.5X10^3$
$(R\text{-}Nnb\text{-}Nrpe)_3\text{-}NH_2$	17.48	$9.4X10^4$
$(R\text{-}Nnb\text{-}Nrpe)_4\text{-}NH_2$	23.57	$8.5X10^5$
$(Orn\text{-}Nnb\text{-}Nspe)_4\text{-}NH_2$	18.08	$1.6X10^5$

Table 5.4. Comparison of the retention times of the hybrids, as measured by heparin affinity chromatography, and their corresponding binding constants as determined by ITC. The K_b of $(K\text{-}Nnb\text{-}Nrpe)_1\text{-}NH_2$, $(K\text{-}Nnb\text{-}Nrpe)_2\text{-}NH_2$, $(R\text{-}Nnb\text{-}Nrpe)_1\text{-}NH_2$, $(R\text{-}Nnb\text{-}Nrpe)_2\text{-}NH_2$, and $(Orn\text{-}Nnb\text{-}Nspe)_4\text{-}NH_2$ were calculated from the equation of the best fit line in Fig.5.14: $\log K_b = 0.1689(\text{retention time}) + 2.1635$.

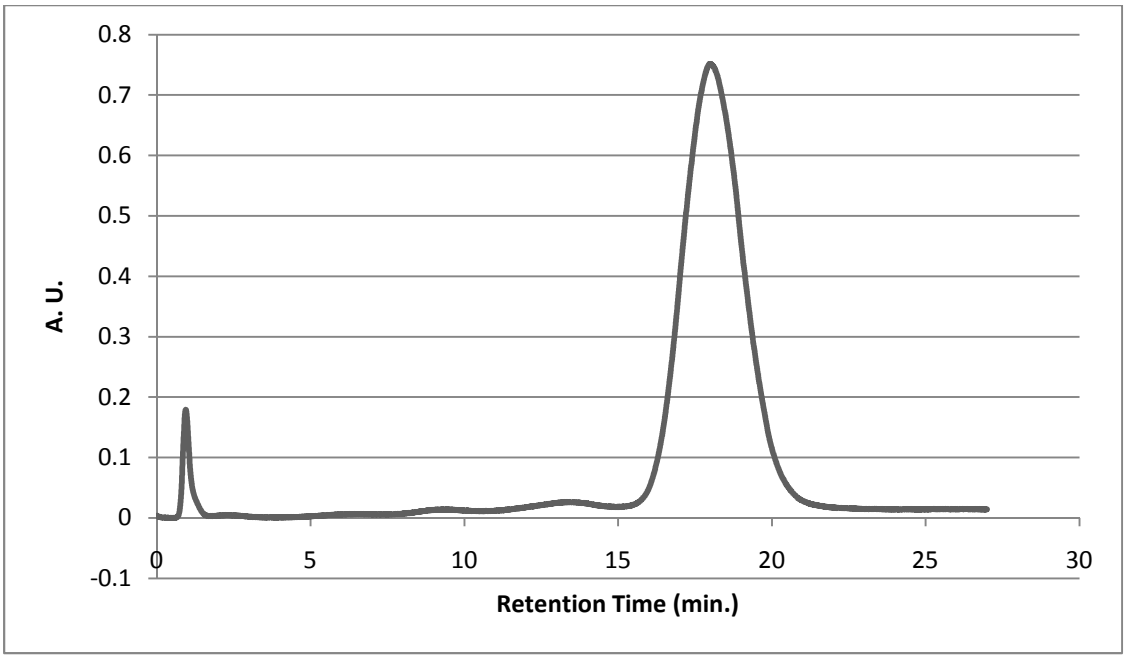

Fig. 5.15. Heparin affinity chromatogram of (Orn-Nnb-Nspe)$_4$-NH$_2$ showing a retention time of 17.98 min. As calculated from the retention time and the NaCl gradient, (Orn-Nnb-Nspe)$_4$-NH$_2$ elutes at a NaCl concentration of about 0.18 M.

separating chiral drugs when used as a chiral mobile-phase additive or as a stationary phase in high performance liquid chromatography. [14-16]

Although ITC data for $(Orn\text{-}Nnb\text{-}Nspe)_4\text{-}NH_2$ show that it has a K_b of $3.5X10^5$ M^{-1}, the integrated ITC data did not adhere as well to an appropriate binding model and so may not be as trustworthy. However, heparin affinity chromatography shows that this hybrid has a retention time of 18.08 min., which is smaller than $(K\text{-}Nnb\text{-}Nrpe)_4\text{-}NH_2$ and $(K\text{-}Nnb\text{-}Nspe)_4\text{-}NH_2$. Shortening the cationic side chains probably inhibits their interaction with the anionic groups of heparin. This may be due to the relatively longer side chains of adjacent hybrid residues preventing the ionic groups of both heparin and $(Orn\text{-}Nnb\text{-}Nspe)_4\text{-}NH_2$ from making as much contact.

Each of the arginine-containing hybrids exhibits a higher relative heparin-binding affinity than its lysine-containing counterpart. As an example, the retention times of $(R\text{-}Nnb\text{-}Nrpe)_4\text{-}NH_2$ and $(K\text{-}Nnb\text{-}Nrpe)_4\text{-}NH_2$ are 23.57 min. and 18.29 min., respectively. This is most likely due to the guanidinium group's higher capacity of forming hydrogen bonds as compared to the ammonium group on the lysine side chain, as discussed in Section 3.3.

As with the peptoid binding data discussed in Section 4.2.3, a graph of $\log(K_b)$ versus the retention times of the peptoids was utilized to determine the binding constants of hybrids which had a heparin-binding interaction which was too weak to be measured accurately by ITC, such as $(K\text{-}Nnb\text{-}Nrpe)_1\text{-}NH_2$, $(K\text{-}Nnb\text{-}Nrpe)_2\text{-}NH_2$, $(R\text{-}Nnb\text{-}Nrpe)_1\text{-}NH_2$, and $(R\text{-}Nnb\text{-}Nrpe)_2\text{-}NH_2$ or, as in the case of $(Orn\text{-}Nnb\text{-}Nspe)_4$, could not be

fit with an appropriate binding model, Fig.5.16. Based on the calculation from the equation of the line given in the plot, a K_b of 604, $3.8X10^3$, 723, $9.5X10^3$, and $1.6X10^5$ M^{-1} was calculated for each of the hybrids, respectively, Table 5.4.

5.3 Discussion

As seen in Chapter 4, ITC data show that for all the lysine-containing hybrid compounds, binding by heparin is an endothermic event with an increase in entropy providing the driving force for the reaction. There are multiple contributions to the enthalpy and entropy of the binding event. As heparin is a polyelectrolyte, it has associated with it a number of counterions, such as Na^+, to partially neutralize its high negative charge density. These counterions occupy a certain volume surrounding heparin. Upon binding to cationic groups on the side chains of hybrid residues, the cationic groups replace some of the counterions by an ion exchange process. Although the dissociation of counterions results in a positive enthalpy, it also results in positive entropy. The binding by the cationic side chains of the lysine residues to the anionic groups of heparin contribute to a negative enthalpy. Although the net change in enthalpy, according to the ITC data, of heparin-binding by lysine is positive, the net entropy is also positive. This may suggest that the binding between the lysine-containing hybrid and heparin is driven by the positive entropy created from the release of counterions upon hybrid-heparin binding.

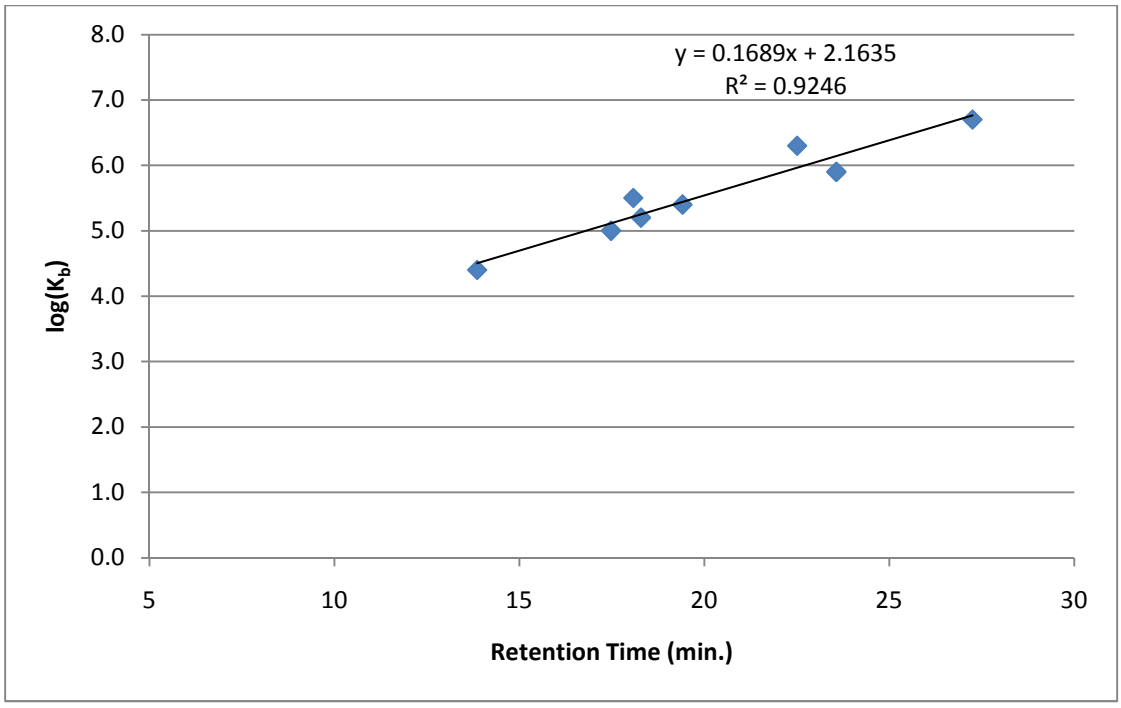

Fig. 5.16. Plot of log(K_b), determined by ITC vs the retention time as measured by heparin affinity chromatography. A linear least squares fit of the data gives the equation: logK_b = 0.1689(retention time) + 2.1635. Using this equation and retention time, binding constants were determined for: (K-Nnb-Nrpe)$_1$-NH_2, (K-Nnb-Nrpe)$_2$-NH_2, (R-Nnb-Nrpe)$_1$-NH_2, (R-Nnb-Nrpe)$_2$-NH_2, and (Orn-Nnb-Nspe)$_4$-NH_2, Table 5.4.

The binding of side chain-guanidinium groups to heparin is also accompanied by a counterion release, as indicated by the increase in entropy as determined by ITC. However, binding of hybrids containing arginine is also accompanied by a decrease in enthalpy, an exothermic reaction. This decrease in enthalpy most likely has to do with the higher capacity of the guanidinium groups of the arginine side chain to hydrogen bond to sulfate groups on heparin, as discussed in Chapter 3. The guanidinium group is able to form two hydrogen bonds to an anionic sulfate group with a close-to-ideal bond angle of 180^{o}; lysine can only form one, hence the higher binding affinity of arginine-containing hybrids.[17]

Overall, ITC data shows that as the chain length of the hybrid increases so does its heparin binding constant. The increased affinity is most likely attributable to the increased number of cationic residues that interact with heparin which is confirmed by heparin affinity chromatography. The binding takes place by a cation exchange process with the cationic residues of the hybrids competing with Na^{+} ions for heparin binding sites on the heparin stationary phase. As the number of cationic residues on the hybrid increases, so does the concentration of NaCl necessary to elute the hybrid.

Although there is a correlation between secondary structure, and heparin-binding affinity, as indicated by CD and ITC, the stability of the secondary structure, in this case, may not be that significant to heparin-binding affinity of the hybrid. This is difficult to tell since, although there is an increase in secondary structure and heparin-binding affinity with an increase in chain length, increase in secondary structure is a

cooperative effect and so will increase with chain length. Heparin-binding affinity is enhanced by the number of cationic residues incorporated into the hybrid. It may be that the difference in secondary structure is not significant enough between hybrids to counteract the increase in binding affinity by the addition of cationic side chains.

However, the difference in heparin-binding affinity between $(Orn\text{-}Nnb\text{-}Nspe)_4\text{-}NH_2$ and $(K\text{-}Nnb\text{-}Nspe)_4\text{-}NH_2$ demonstrates that stabilization of secondary structure does not play as much a part in heparin binding as does access to the cationic side chains, as shown by their very similar CD spectra. As the orinithine side chain is shorter than the lysine side chain, it may be possible that the, relatively longer, side chains adjacent to the ornithine residue are preventing the ammonium side chain from interacting with the anionic groups of heparin.

5.4 Summary

ITC and heparin affinity chromatography demonstrate that the heparin-binding capacity can be increased by the addition of cationic residues, which also must be accessible to the anionic groups on heparin. The ITC data show that lysine-containing hybrids bind to heparin by an entropy-driven interaction due to the release of counterions upon binding to heparin. As arginine can form more direct hydrogen bonds with the sulfate groups on heparin, the arginine-containing hybrids bind to heparin more strongly. The increase in hydrogen bonding contributes to a more enthalpy driven binding interaction.

CD studies show that the hybrids synthesized for this work can be designed to conform to a stable secondary structure, namely a polyproline I-type helix by the addition of bulky, α-chiral amines. Further addition of these groups can enhance the stability of this conformation. It has also been shown that the combination of an L-amino acid, such as L-lysine, with either an Nrpe or Nspe residue can either enhance or destabilize the polyproline I-type helix. This work shows that L-lysine appears to enhance the secondary conformation of hybrids consisting of Nrpe residues. The intensities of the 200 nm absorption bands of $(NLys\text{-}Nnb\text{-}Nspe)_4\text{-}NH_2$, $(NLys\text{-}Nnb\text{-}Nrpe)_4\text{-}NH_2$, and $(K\text{-}Nnb\text{-}Nspe)_4\text{-}NH_2$ are similar. As the same absorption band for $(K\text{-}Nnb\text{-}Nrpe)_4\text{-}NH_2$ is significantly more intense, it is possible that the side chain on the α-carbon of the L-lysine residue, is in a position to sterically interact with the phenyl group of the α-chrial side chain of the adjacent Nrpe residue.

The arginine residue also appears to have a stabilizing effect on the hybrid secondary structure, as shown by the CD signature for $(R\text{-}Nnb\text{-}Nrpe)_4\text{-}NH_2$, showing a nascent polyproline I-type helix, and the lack of a CD signature for $(K\text{-}Nnb\text{-}Nrpe)_4\text{-}NH_2$. This is possibly due to arginine having a slightly bulkier side chain than lysine's.

Together, the data indicate that it is possible to design hybrids with a particular structure and sequence that will bind heparin with relatively high affinity. As discussed above, hybrids have some advantages over peptides in their use as potential drugs. Therefore, it is important to elucidate criteria to be met for design of hybrids with particular characteristics which could facilitate their use as therapeutic agents. This

work has shown the potential of hybrids to bind heparin with relatively high affinity which may make them useful candidates as a replacement for Protamine in the reversal of heparin's anticoagulant activity.

5.5 References

1. Ostergaard, S.; Holm, A., *Mol. Diversity* **1997,** *3*, 17-27.

2. Olsen, C. A., *ChemBioChem* **2010,** *11*, 152-160.

3. *Peptides for Youth: The Proceedings of the 20th American Peptide Symposium*. Springer: New York, 2009; Vol. 611.

4. Ast, T.; Heine, N.; Germeroth, L.; Schneider-Mergener, J.; Wenshcuh, H., *Tetrahedron Lett.* **1999,** *40*, 4317-4218.

5. Giuseppe, M.; Feng, Y.; Goodman, M., *J. Am. Chem. Soc.* **1996,** *118*, 10725-10732.

6. Goodman, M.; Giuseppe, M.; Feng, Y., *J. Am. Chem. Soc.* **1996,** *118*, 10928-10929.

7. Ryge, T. S.; Hansen, P. R., *J. Peptide Sci.* **2005,** *11*, 727-734.

8. Stawikowski, M.; Stawikowska, R.; Jaskiewicz, A.; Zablotna, E.; Rolka, K., *ChemBioChem* **2005,** *6*, 1057-1061.

9. Fowler, S. A.; Blackwell, H. E., *Org. Lett.* **2008,** *10*, 2329-2332.

10. Zimmermann, J.; Kuhne, R.; Volkmer-Engert, R.; Jarchau, T.; Walter, U.; Oschkinat, H.; Ball, L. J., *J. Biol. Chem.* **2003,** *278*, 36810-36818.

11. Holder, J. R.; Bauzo, R. M.; Xiang, Z.; Scott, J.; Haskell-Luevano, C., *Bioorg. Med. Chem. Lett.* **2003,** *13*, 4505-4509.

12. Ovadia, O.; Linde, Y.; Luevano-Haskell, C.; Dirain, M. L.; Sheynis, T.; Jelinek, R.; Gilon, C.; Hoffman, A., *Bioorg. Med. Chem.* **2010,** *18*, 580-589.

13. Wu, C. W.; Sanborn, T. J.; Huang, K.; Zuckermann, R. N.; Barron, A. E., *J. Am. Chem. Soc.* **2001,** *123*, 6778-6784.

14. Stalcup, A. M.; Agyel, N. M., *Anal. Chem.* **1994,** *66*, 3054-3059.

15. Jin, Y.; Stalcup, A. M., *Electrophoresis* **1998,** *19*, 2119-2123.

16. Stalcup, A. M.; Gahm, K. H.; Baldueza, *Anal. Chem.* **1996,** *68*, 2248-2250.

17. Goncalves, E.; Kitas, E.; Seelig, J., *Biochemistry* **2005,** *44*, 2692-2702.

Chapter 6

Conclusions

The purpose of the work presented in this dissertation was to rationally design peptides, peptoids, and peptide/peptoid hybrids (hybrids) and determine their feasibility as substitutes for protamine. As discussed in Section 1.4.4.1, protamine is used to reverse heparin's anticoagulant activity when heparin is no longer necessary to prevent coagulation during certain medical procedures. Unfortunately, protamine can sometimes induce detrimental side-effects and so a safer alternative is deemed necessary.

To determine if these specially designed compounds will prove to be suitable replacements for protamine, a first step is to characterize their binding interaction with heparin. This was done by utilizing isothermal titration calorimetry (ITC) and heparin affinity chromatography (HAC) to establish quantitative and relative binding affinity to heparin, respectively. Circular dichroism spectroscopy (CD) was used to determine secondary structure of these compounds in the absence and presence of heparin.

The research in this study has suggested that binding of heparin by peptides, peptoids, or hybrids is primarily mediated by electrostatic interactions between the cationic side chains of the peptides, peptoids, and hybrids and the anionic groups of heparin. In each case, the binding of these compounds results in a net positive gain in entropy, which is suggestive of electrostatic interactions between cationic groups and

polyelectrolytes, such as heparin. This net gain in entropy is due to the release of counterions associated with heparin, which are displaced when peptides, peptoids, or hybrids bind to heparin electrostaticaly via their cationic side chains.

Although the net gain in entropy favorably drives the binding interaction, binding by the lysine-containing compounds results in an endothermic binding event and arginine-containing compounds, an exothermic binding event. This difference in the change in enthalpy upon heparin-binding can be attributed to the formation of hydrogen bonds formed between the guanidinium and ammonium groups of the amino acid and amine monomers, and the sulfate groups of heparin. The guanidinium group has been shown to form two hydrogen bonds with a sulfate group close to a 180^{o} bond angle, whereas an ammonium group will only form one. Because of this, the results from both ITC and HAC show that peptides and hybrids containing the arginine amino acid residue, bind to heparin with higher affinity than their corresponding lysine-containing counterparts.

The peptides designed in this work have sequences based on the consensus pattern of XBBBXXBX where B is a basic residue, such as lysine, arginine, or histidine, and X is any other residue, which in this work is: glycine, luecine, valine, and alanine, which, except for valine, have a helix-forming propensity. The secondary structure of these peptides, as demonstrated by CD, is consistent with a polyproline II-type helix. The helix is characterized by trans amide bonds, and a pitch of about 6 Å consisting of about three residues per turn, as discussed in Section 3.1.2, this pattern has been found in the

binding site of a number of heparin-binding proteins. ITC results show that these peptides can bind to heparin with high affinity when containing all lysine or all arginine residues. However, at pH 7.4, histidine-containing peptides bound weakly to heparin, as demonstrated by an undeterminable K_b by ITC.

Although some of the peptides designed in this work exhibit high binding affinity to heparin, which may make them reasonable substitutes for protamine, peptoids show several advantages which may make them more attractive alternatives to peptides, as discussed in Section 4.1.2. Not only are peptoids bioactive, but research has suggested that they are less susceptible to proteolysis and therefore more bioavailable, and less imminogenic than peptides.

Although the peptoid-backbone is incompatible with the formation of secondary structure, due to the lack of chirality and amide nitrogens, which negates intramolecular hydrogen bond formation, peptoids can be forced to form a secondary structure by incorporating bulky α-chiral amines. In this work (R)- and (S)-1-phenylethylamines were incorporated every third residue to force, by steric interactions, the peptoid backbone into a stable secondary structure. CD studies show that these peptoids form a polyproline I-type helix. Structural studies have determined that this helix is chacterized by cis amide bonds, and a pitch of approximately 6 Å consisting of about three residues per turn. By including an amine with a lysine-like moiety, every third residue, the peptoid was rendered amphipathic, with a face of cationic charge. This oriented the cationic side chains in a more linear fashion along the helix axis making them more

accessible to the anionic groups aligned along heparin's polysaccharide backbone. Indeed, ITC binding studies showed that peptoids with four lysine monomers bound more tightly to heparin than peptides containing four arginine residues. This suggests that the orientation of the side chains along the peptoid backbone is more advantageous for heparin-binding.

Chirality of the bulky α-chiral amine also affects heparin-binding. As was discussed in Section 4.3, peptoids containing the Nspe monomer exhibit greater heparin-binding than the corresponding Nrpe-containing peptoid.

Peptide/peptoid hybrids were of interest because not only do they show similar advantages over peptides, as peptoids do, but are less expensive to synthesize. Although the only difference between the hybrids and peptoids synthesized in this work is that the NLys residue of the peptoid was replaced by L-Lysine or L-arginine, and in one case, L-ornithine. However, one only has to peruse the chemical catalogues to notice that N-boc-1,4-diaminobutane (Fig. 2.7) is much more expensive than the equivalent amount of Fmoc-Lys(boc)-OH (Fig. 2.4). making hybrids, possibly, less expensive therapeutic agents.

Even though the hybrid backbone is comprised of an amino acid residue, every third monomer, the chirality and capacity to form hydrogen bonds has a negligible effect on its secondary structure. According to CD studies done in this research, the incorporation of bulky α-chiral amines (same as those included in the peptoid sequences), every third residue, also forces the hybrid into a polyproline I-type helix.

Therefore, with L-lysine residues placed every third residue in the hybrid sequence, hybrids will also form an amphipathic structure with cationic charges aligned along one face of the helix.

ITC binding studies show that hybrids containing the arginine amino acid bind heparin with a greater affinity than the corresponding lysine-containing hybrids. The lysine-containing hybrids did, however, bound heparin with a similar affinity as peptoids of similar length and sequence. It appears that monomers with shorter cationic side chains (such as ornithine), may be somewhat blocked by adjacent side chains from heparin's anionic groups, resulting in a lower heparin-binding affinity.

The Chirality of the L-lysine or L-arginine also appears to stabilize secondary structure. The position of the lysine or arginine side chain may be in a position to sterically interact with the phenyl group of the chiral Nrpe or Nspe monomer. This is evident as arginine-containing hybrids have a more stabile secondary structure than lysine-containing hybrids. Also, the Nspe monomer may sterically interact more with the L-lysine side chain than the Nrpe monomer as the hybrids containing Nspe appear to have a more stabile secondary structure, according to CD studies.

This work suggests that peptides, peptoids, and hybrids can be induced into a secondary structure by utilizing specific residues. This is important to the rational design of heparin-binding compounds, as predicting the orientation of side chains which may be critical to peptide, peptoid, or hybrid function can be predicted by the incorporation of certain monomers. By noting that a polyproline-type helices have a period of three

residues per turn, it seemed reasonable that incorporating cationic amine monomers into peptoids, every third residue, would create a face of cationic charge along one side of the peptoid. A face of cationic charge would be an ideal orientation of the cationic side chains so as to bind heparin's anionic groups which align themselves, linearly, along its polysaccharide backbone.

The binding studies done in this work also show that there are a variety of ways to enhance heparin-binding by peptides, peptoids, or hybrids. The most obvious way is the addition of cationic side chains. Other ways include: side chain length and chirality of aromatic side chains included in the sequence.

The work presented here has elucidated a variety of ways by which to tune heparin-binding affinity of peptides, peptoids, and hybrids. Rational design of peptides, peptoids, and hybrids, which modulate heparin/protein binding, may not only be important in the treatment of disease, but may be useful in the reversal of heparin's anticoagulant activity by their displacement of antithrombin from the heparin-antithrombin complex. The binding studies performed in this work have demonstrated the plausibility of these compounds to replace protamine for the use as an antidote to the anticoagulation effects of heparin.

Further work should be done to more fully demonstrate these compounds' ability to replace protamine. The anti-Xa chromogenic assay can be used to determine a compounds' capacity to displace heparin from antithrombin. If the results of this assay prove unsatisfactory, then increasing the length of the compound by the addition of

(NLys-Nnb-Nspe)$_n$ trimer repeats or adding more cationic charge to increase binding affinity to heparin may be necessary. As safety is the primary reason for doing this research *in vivo* testing should be done to test the compounds' immunogenicity and antigenicity. This can be examined by utilizing an enzyme-linked immunosorbent assay. If these can prove the efficacy and safety of any of these compounds in this research or future work, then maybe a replacement for protamine has been found.